**Title**
Modulation of TOR Complex 2 signaling and maintenance of plasma membrane homeostasis in Saccharomyces cerevisiae



**Author**
Leskoske, Kristin

**Publication Date**
2017

Peer reviewed|Thesis/dissertation

# Modulation of TOR Complex 2 signaling and maintenance of plasma membrane homeostasis in *Saccharomyces cerevisiae*

by

Kristin Leskoske

A dissertation submitted in partial satisfaction of the

requirements for the degree of

Doctor of Philosophy

in

Molecular and Cell Biology

in the

Graduate Division

of the

University of California, Berkeley

Committee in Charge:

Professor Jeremy W. Thorner, Chair
Professor David G. Drubin
Professor James H. Hurley
Professor John E. Dueber

Spring 2017

Abstract

Modulation of TOR Complex 2 signaling and maintenance of plasma membrane homeostasis in *Saccharomyces cerevisiae*

by

Kristin Leskoske

Doctor of Philosophy in Molecular and Cell Biology

University of California, Berkeley

Professor Jeremy W. Thorner, Chair

Target of Rapamycin (TOR) Complex 2 (TORC2) is a conserved multi-subunit protein kinase associated with the plasma membrane that is an essential regulator of growth. In *Saccharomyces cerevisiae*, TORC2 regulates the lipid composition and organization of the plasma membrane during normal cell growth and, in turn, responds to environmental insults (such as changes in osmotic conditions) that exert stress on the plasma membrane to maintain homeostasis. Ample genetic and biochemical evidence indicates that TORC2 exerts its effects solely via direct phosphorylation and stimulation of the activity of the downstream protein kinase Ypk1 (and its paralog Ypk2). Ypk1 action modulates plasma membrane lipid homeostasis in multiple ways, including up-regulation of sphingolipid synthesis and inhibition of aminoglycero-phospholipid flipping. Ypk1 also controls glycerol production and efflux, allowing cells to adapt to osmotic changes. Prior work demonstrated that TORC2 phosphorylates Ypk1 at two conserved sequence elements near its C-terminus, dubbed the "turn" and "hydrophobic" motifs. However, this study documents that TORC2 also phosphorylates Ypk1 at four additional C-terminal sites that are also critical for full TORC2-mediated stimulation of Ypk1 activity. Ala substitutions at the four new sites abrogated the ability of Ypk1 to rescue the phenotypes of Ypk1 deficiency, whereas Glu substitutions had no ill effect. Combining the Ala substitutions with an N-terminal mutation (D242A) that has been shown to bypass the need for TORC2 phosphorylation restored the ability to complement a Ypk1-deficient cell. These findings provide new insights about the molecular basis for TORC2-mediated activation of Ypk1. Moreover, TORC2 phosphorylation of Ypk1 changes differentially in response to different plasma membrane stresses; it is elevated in a sustained manner upon sphingolipid depletion, but rapidly and greatly diminished, although only transiently, upon hyperosmotic shock. In this work, new insights were also obtained about how hypertonic conditions influence TORC2. Results described here document that the plasma membrane osmosensor Sln1 is an upstream regulator of TORC2. Inactivation of Sln1, which causes activation of the Hog1 MAPK, leads to loss of TORC2 phosphorylation of Ypk1. This response requires the Hog1 MAPK itself and also the Slt2 MAPK. Upon Sln1 inactivation, Avo2 is hyperphosphorylated at its MAPK phosphoacceptor sites in a Hog1 and Slt2-dependent manner. These findings suggest that MAPK-mediated phosphorylation of Avo2 may provide a mechanism for exerting negative regulation on TORC2 function.

**Acknowledgements**

My six years in graduate school have been both the most challenging and the most rewarding years of my life, thus far. In this regard, I would like to acknowledge the following individuals who have supported me through this process:

My mentor Jeremy Thorner. Thank you for agreeing to take me on as your (next to) last graduate student and giving me the freedom to explore my scientific interests. I have grown astronomically as a scientist and I am grateful for the scientific training I received in your lab.

My thesis committee members David Drubin, Jim Hurley and John Dueber. Thank you for your guidance and support.

My "in-lab" mentor Françoise. Your guidance and friendship over the years has been invaluable. Talking and working with you makes lab work so much more enjoyable.

James and Joe. Living in a party house with six other people is not usually my first choice for housing. However, living with you guys in the Grizzly Peak house first year was the best decision I made. We had so much fun and, even though we are no longer roommates, I am glad we have remained friends.

My *seestar* Olivia. Even though we live on opposite sides of the country, we have grown closer over the years. I love you as both my sister and my friend.

My parents Julie and Steve or, as I like to call them, Mom and Dad. Thank you for your unconditional love and support and for your yearly visits.

And last, but certainly not least, Jeremiah. You are my rock. I love you and I am so excited to see what the future has in store for us.

**Table of Contents**

**List of Figures**

**List of Tables**

**List of Abbreviations**

| | |
|---|---|
| Aba | aureobasidin A |
| AID* | auxin-inducible degron |
| CIP | calf intestinal phosphatase |
| CRIM | conserved region in the middle |
| CWI | cell wall integrity |
| ER | endoplasmic reticulum |
| FRB | FKBP12-rapamycin binding |
| GAP | GTPase-activating protein |
| GEF | guanine exchange factor |
| HOG | high osmolarity glycerol |
| IPC | inositolphosphoryl-ceramide |
| LCB | long-chain base |
| mAb | monoclonal antibody |
| MAPK | mitogen-activated protein kinase |
| MAPKK | mitogen-activated protein kinase kinase |
| MAPKKK | mitogen-activated protein kinase kinase kinase |
| MS | mass spectrometry |
| MCC | membrane compartment containing Can1 |
| MCP | membrane compartment containing Pma1 |
| MCT | membrane compartment containing Tor2 |
| MIPC | mannosyl-inositolphosphoryl-ceramide |
| $M(IP)_2C$ | inositolphosphoryl-mannosyl-inositolphosphoryl-ceramide |
| mTORC2 | mammalian TORC2 |
| Myr | myriocin / ISP-1 |
| 1-NAA | 1-naphthalene-acetic acid |
| P3C | human rhinovirus 3C protease [EC 3.4.22.28] |
| PAGE | polyacrylamide gel electrophoresis |
| PBS | phosphate-buffered saline |
| PH | pleckstrin homology |
| PM | plasma membrane |
| PPP | pentose phosphate pathway |
| PtdCho | phosphatidylcholine |
| PtdEth | phosphatidylethanolamine |
| PtdGlo | phosphatidylglycerol |
| PdtIns | phosphatidylinositol |
| $PtdIns4,5P_2$ | phosphatidylinositol-4,5-*bis*phosphate |
| PtdSer | phosphatidylserine |
| RBD | Ras binding domain |
| ROS | reactive oxygen species |
| *Sc*TORC2 | *Saccharomyces cerevisiae* TORC2 |
| SDS | sodium dodecyl sulfate |
| SPT | L-serine:palmitoyl-CoA C-palmitoyltransferase (decarboxylating) [EC 2.3.1.50] |

| | |
|---|---|
| *Sp*TORC2 | *Schizosaccharomyces pombe* TORC2 |
| TBS | Tris-buffered saline |
| TOR | target of rapamycin |
| TORC1 | TOR complex 1 |
| TORC2 | TOR complex 2 |
| UPR | unfolded protein response |

## Chapter 1. Introduction

The ability to maintain a stable internal environment despite fluctuations in external environment is essential for life. Homeostasis, as it occurs at the cellular level, requires careful coordination of metabolic growth processes and adaptive stress responses. Two fundamental principles govern homeostatic maintenance. The first is effective boundaries between the cell and its environment. Cells cannot exist in isolation and rely on nutrients supplied by their environment. However, the exchange of metabolites between the cell and its environment leaves the cell vulnerable to environmental fluctuations that can cause physiological imbalances. Thus, cells are surrounded by a selectively permeable barrier that allows them to interact with their environment but still maintain a stable internal environment. Thus, ensuring the integrity of cellular barriers is crucial for maintaining homeostasis. The second fundamental feature of homeostasis is the need for signal transduction pathways that detect changes in both the internal and external environments and evoke the appropriate cellular responses. Elaborate signaling networks sense a wide variety of external and internal stimuli and transmit this information to the proper effectors. These signals are integrated and cellular metabolism is adjusted in order to maintain homeostasis. The TOR Complex 2 (TORC2) signaling network is an essential regulator of cellular homeostasis. TORC2 monitors signals that report on the condition of the cell envelope and controls the activity of downstream effectors to ensure that the integrity of these vital barriers is maintained.

### Cellular boundaries

All cells are separated from their environment by a dynamic, yet highly organized, lipid and protein bilayer called the plasma membrane (PM) (Simons and Sampaio, 2011). In eukaryotic cells, the PM mediates the exchange of metabolites between the cell and its environment through passive diffusion, active transporters, and gated channels, as well as by vesicle-mediated exocytosis and endocytosis. Additionally, eukaryotic cells also contain internal membrane-bound compartments, termed organelles, that segregate different metabolic processes within the cell. Eukaryotic membranes are composed of three major classes of lipids. Glycerophospholipids are the most abundant membrane lipid and consist of a hydrophobic diacylglycerol backbone with the third hydroxyl of glycerol esterified to phosphate, which can, in turn, be esterified to either glycerol (to form phosphatidylglycerol, PtdGlo), choline (to form phosphatidylcholine, PtdCho), ethanolamine (forming phosphatidylethanolamine, PtdEth), serine (forming phosphatidylserine, PtdSer) or inositol (forming phosphatidylinositol, PtdIns) (van Meer et al., 2008). Sphingolipids are the second most abundant class of membrane lipids. The fundamental sphingolipid unit is a ceramide in which a fatty acid is connected via an amide linkage to the amino group near the polar end of a long-chain sphingoid base (LCB). In yeast *(Saccharomyces cerevisiae*), the LCB is mainly phytosphingosine, and an inositol-phosphate group is esterified to the hydroxyl at the polar end of the LCB, generating inositol phosphoryl-ceramide (IPC). IPC can be decorated further by attachment of mannose in glycosidic linkage to a hydroxyl of the inositol ring, producing mannosyl-inositolphosphoryl-ceramide (MIPC), and an additional inositolphosphoryl moiety can be esterified to a hydroxyl in the mannopyranoside ring, yielding inositolphosphoryl-mannosyl-inositolphosphoryl-ceramide, also known as mannosyl-diinositolphosphoryl-ceramide [$M(IP)_2C$]. Thus, the major complex sphingolipids in yeast are IPC, MIPC, and $M(IP)_2C$ (Olson et al., 2016). The third class of membrane lipids is sterols, planar molecules consisting of four cyclic carbon rings, an acyl side chain and a hydrophilic

**FIGURE 1.1**

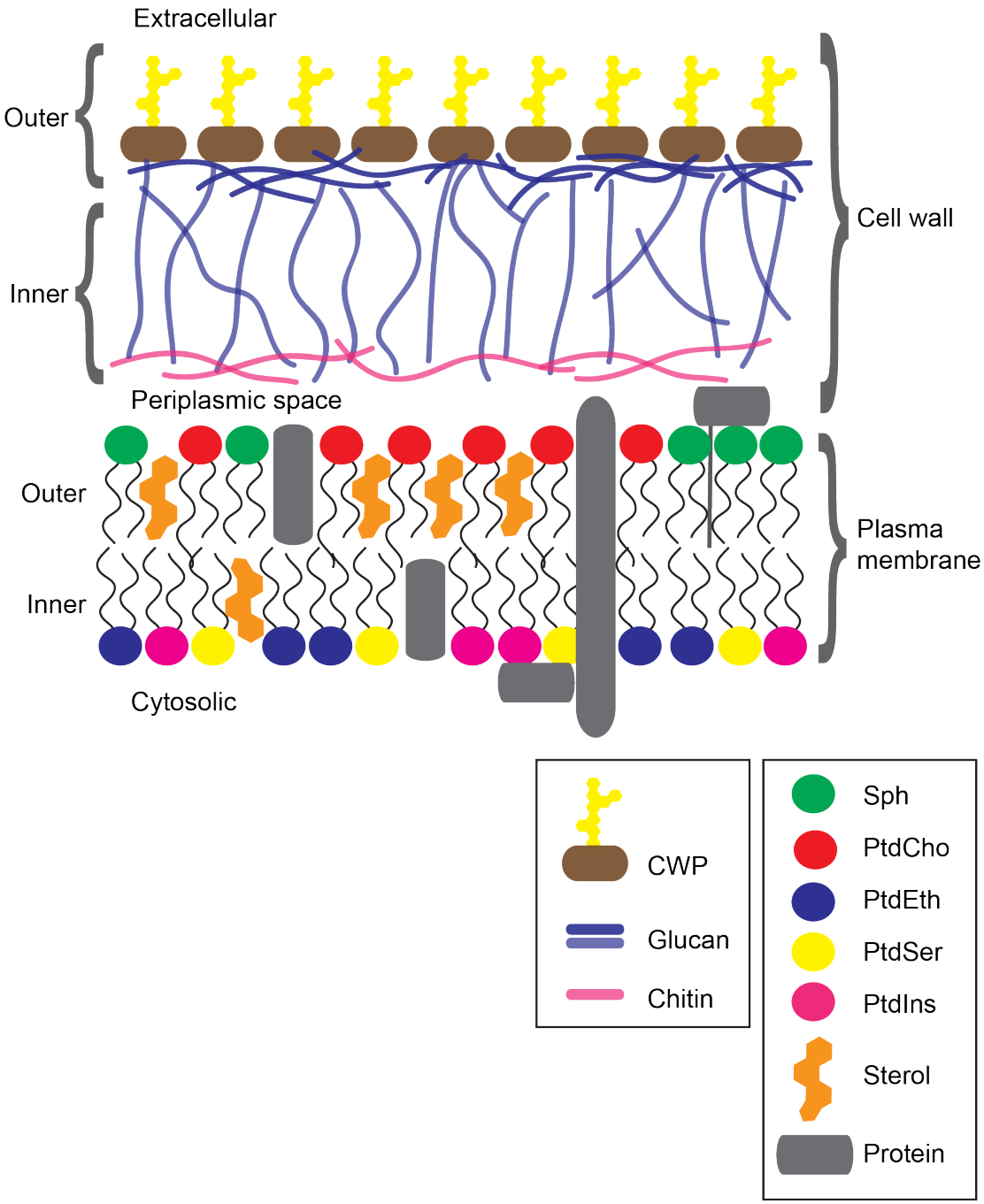


**Figure 1.1. Schematic depiction of the yeast cell envelope**. The outer cell wall (CW) layer is composed of mannose-rich glycoproteins (mannan) whereas the inner CW layer is composed primarily of chains of β-(1→3)-linked glucose with β-(1→6)-linked branches (glucan) and, at sites of cell division, long chains of β-(1→4)-linked N-acetylglucosamine (chitin). The outer plasma membrane (PM) leaflet is enriched in PtdCho and sphingolipids (Sph), whereas the inner PM leaflet contains primarily glycerophospholipids (PtdEth, PtdSer, PtdIns and its phosphorylated derivatives, mainly PtdIns4,5$P_2$). Sphingolipids and sterols cluster into microdomains.

hydroxyl group. In yeast, ergosterol is the major sterol.

Each eukaryotic membrane has a distinct lipid composition and preferred lipid organization. In *S. cerevisiae*, the PM displays an asymmetrical distribution of lipids between the bilayer. The outer leaflet of the PM is enriched for sphingolipids and PtdCho, whereas the inner leaflet contains predominantly glycerophospholipids (van Meer et al., 2008) (Figure 1.1).

The *S. cerevisiae* PM also displays lateral organization within the bilayer. Three lateral microdomains have been described, each named for a protein commonly found in that compartment: the membrane compartment containing the $H^+$-translocating ATPase Pma1 (MCP); the membrane compartment containing arginine permease Can1 (MCC); and, the membrane compartment containing the large protein kinase Tor2 (MCT) (Bartlett and Kim, 2014).

The distribution of lipids in the PM is the result of both the natural propensity for certain types of lipids, such as sphingolipids and sterols, to self-associate, as well as the result of cellular processes that move lipids between different cellular membranes and between leaflets of the same membrane. Additionally, PM-associated proteins also influence PM organization. One example of this interplay are PM-associated structures known as eisosomes. Two BAR (Bin/amphiphysin/Rvs) domain-containing proteins, Pil1 and Lsp1, assemble into large clusters on the cytoplasmic face of MCCs (Walther et al., 2006). Recruitment of Pil1 and Lsp1 requires their binding to PtdIns4,5$P_2$ and, their PM association deforms the membrane, producing furrow-like invaginations (Karotki et al., 2011).

The lipid composition and organization of the PM determine many of its physical properties, such as fluidity, permeability and curvature and, therefore, affect many different PM associated processes, such as endocytosis (Platta and Stenmark, 2011), solute transport (Divito and Amara, 2009), and signal transduction (Groves and Kuriyan, 2010). Additionally, lipids can also function as signaling molecules in two ways. Membrane lipids can mediate the recruitment and assembly of signaling complexes at the membrane, and the hydrolysis and modification of membrane lipid head groups can generate secondary messengers (Fernandis and Wenk, 2007).

In addition to the PM, fungi have an extra barrier that separates the cell from its environment: a 120nm thick cell wall (Figure 1.1). The cell wall acts as a sieve in which small molecules freely diffuse across, but large molecules, such as secreted enzymes are retained in the periplasmic space (Francois, 2016). The outer layer of the cell wall is electron-dense and consists of an extensive network of glycoproteins that act as a barrier and protective shield (Levin, 2011). The inner layer of the cell wall is composed primarily of beta-1,3-glucan chains branched through beta-1,6-glucan linkages as well as small amounts of chitin. The mechanical strength and elasticity of the cell wall can be attributed to the helix-like structure of the beta-1,3-glucan polymers in the inner layer. In addition to its barrier function, the cell wall also determines the shape, or morphology, of the cell.

**TOR Complex 2**

The PM and cell wall are highly dynamic structures that are continuously remodeled as the cell grows and divides. Elaborate signaling networks coordinate expansion at the cellular boundaries with the accumulation of intracellular volume and progression through the cell cycle. These signaling networks also play key roles in responding to environmental fluctuations that compromise the integrity of the cellular boundaries. The target of rapamycin (TOR), which is conserved from yeast to humans, plays a central role in this regulation (Brown et al., 1994a; Chiu

et al., 1994; Sabatini et al., 1994; Sabers et al., 1995). The TOR signaling network is comprised of two spatially, compositionally and functionally distinct TOR protein complexes: the rapamycin-sensitive TOR complex 1 (TORC1) and the rapamycin-insensitive TOR complex 2 (TORC2) (Hara et al., 2002; Jacinto et al., 2004; Kim et al., 2002; Loewith et al., 2002; Sarbassov et al., 2004; Loewith and Hall, 2011; Saxton and Sabatini, 2017). TORC1 localizes to the vacuolar/lysosomal membrane and regulates the rate of anabolic and catabolic processes according to nutrient availability. TORC2 localizes to the PM and responds to both internal and external fluctuations to maintain the integrity of this vital barrier. TORC1 and TORC2 play essential roles in maintaining cellular homeostasis and are both required for cell viability. My research focused on the TORC2 signaling network in *S. cerevisiae*.

In budding yeast, TORC2 is a large (~2 MDa) dimeric structure composed of two copies of a complex comprising Tor2, Lst8, Avo1, Avo2, Avo3 and two paralogous proteins Bit2 or Bit61 (Wullschleger et al., 2005) (Figure 1.2). The *S. cerevisiae* genome encodes two highly homologous TOR polypeptides, Tor1 and Tor2 (Heitman et al., 1991). TORC1 can assemble with either Tor1 or Tor2; however, TORC2 obligatorily contains only Tor2 (Loewith et al., 2002). The only other protein common to both complexes is the small *beta*-propeller protein Lst8 (Loewith et al., 2002). Lst8 binds to the kinase domain of Tor and is necessary for the catalytic activity of the complex as well as for cell viability (Wullschleger et al., 2005; Yang et al., 2013; Aylett et al., 2016; Baretić et al., 2016). The large Avo1 (131 kDa) and Avo3 (164 kDa) subunits are also essential for TORC2 function. The C-terminus of Avo1 contains a pleckstrin homology (PH) domain that binds PtdIns4,5$P_2$ and is necessary for efficient targeting of TORC2 to the PM (Berchtold and Walther, 2009). Avo1 also contains a conserved region in the middle (CRIM) domain that is necessary for substrate recognition and binding in both fungal and mammalian orthologs (Cameron et al., 2011; Liao and Chen, 2012; Tatebe et al., 2017). Sandwiched between the CRIM and PH domains of Avo1 is a putative, yet conserved, Ras-binding domain (RBD). Interestingly, Sin1, the human ortholog of Avo1, was first identified in a screen for suppressors of Ras function in yeast (Colicelli et al., 1991). The Dictyostelium ortholog of Avo1, RIP3, was also identified as a Ras-interacting protein by a two-hybrid screen (Lee et al., 1999). The Avo3 subunit contains a RasGEFN domain which shows weak homology to the region N-terminal to the catalytic domain of RAS guanine nucleotide exchange factors (GEF). Although it has not yet been demonstrated for *S. cerevisiae* TORC2, GTPases have been shown to regulate TORC2 in other species (Lee et al., 2005; Schroder et al., 2007; Hatano et al., 2015). Avo3 primarily functions as a scaffold and is essential for the structural integrity of the complex (Wullschleger et al., 2005). Avo3 is also responsible for the rapamycin insensitivity of TORC2. The C-terminus of Avo3 blocks the Fpr1-rapamycin binding (FRB) domain in Tor2 and an Avo3$^{\Delta C}$ mutant renders TORC2 sensitive to inhibition by rapamycin (Heitman et al., 1991; Gaubitz et al., 2015). Although Avo1 and Avo3 are essential for cell viability, Avo2, Bit61 and Bit2 are not. The function of these proteins in TORC2 is not well defined. Avo2 is only found in fungi and contains ankyrin repeats, which are known to mediate protein-protein interactions (Gaubitz et al., 2016). Bit61 and Bit2 are considered, by some, to be the equivalent of mammalian Protor-1 and Protor-2 (Loewith & Hall, 2011); however, there is little detectable sequence similarity between these yeast and mammalian proteins. It has been reported that Protor-1 is necessary for efficient activation and phosphorylation of the mTORC2 substrate SGK1 in the kidney (Pearce et al., 2011) and prior work from our laboratory has shown that the yeast TORC2 target Ypk1 (see below) is the functional ortholog of mammalian SGK1 (Casamayor et al., 1999).

**FIGURE 1.2**

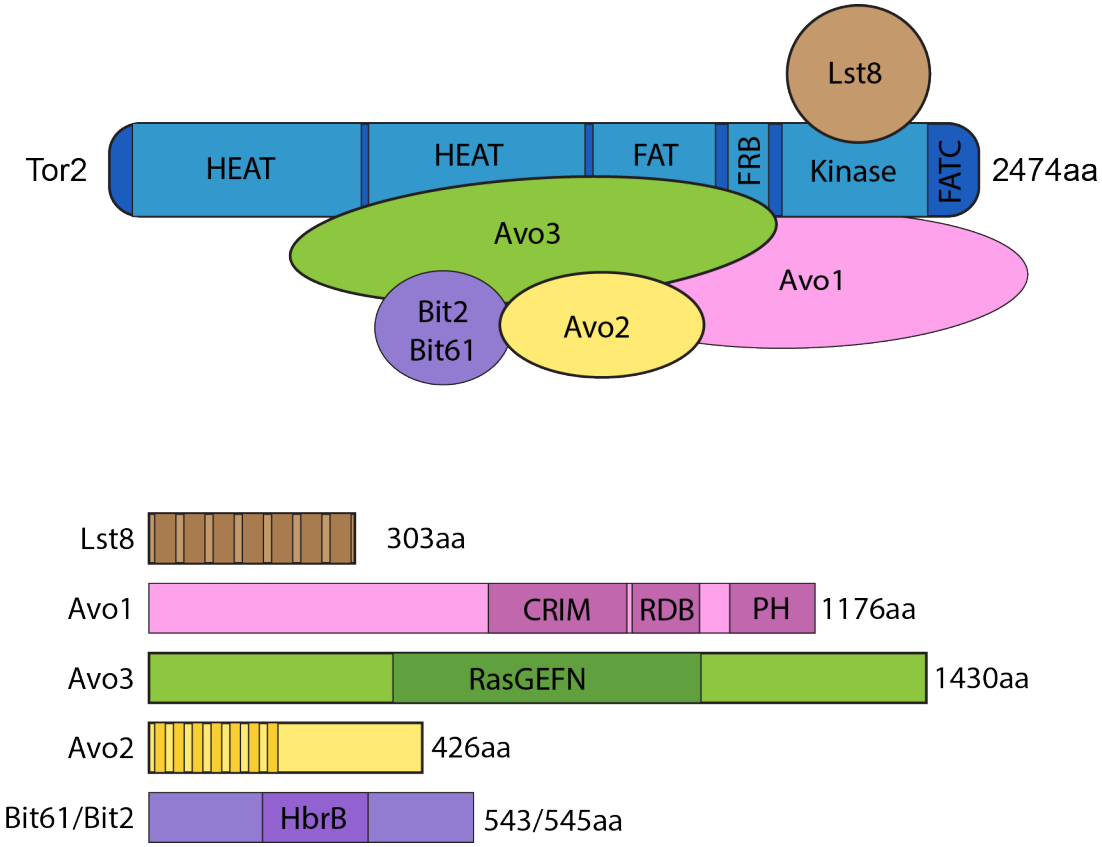


**Figure 1.2. Target of Rapamycin Complex 2.** TORC2 comprises essential proteins Tor2, Lst8, Avo1 and Avo3, and non-essential proteins Avo2 and Bit61 (and its paralog Bit2). The catalytic subunit is the large (2474-residue) protein kinase Tor2, which acts as a scaffold for complex assembly. Tor2 contains HEAT (Huntington, Elongation Factor 3, PR65/A, TOR) repeats followed by FAT (FRAP-ATM-TRRAP), FRB (FKBP12-rapamycin binding), kinase and FATC domains. Lst8 is necessary for catalytic activity and consists entirely of WD40 repeats that form a seven-bladed beta-propeller structure. Avo1 contains a conserved region in the middle (CRIM) that mediates substrate binding, as well as an apparent Ras-binding domain (RBD) and pleckstrin homology (PH) domain which binds PtdIns4,5$P_2$ and localizes TORC2 to the PM. Avo3 contains a region with weak homology to the N-terminal portion of Ras guanine exchange factors (GEFN). The C-terminus of Avo3 occludes the FRB domain of Tor2, rendering TORC2 insensitive to inhibition by rapamycin (Gaubitz et al., 2015). Avo2 contains ankyrin repeats and may bind to the TORC2 regulators Slm1 and Slm2. Bit61 and Bit2 share a conserved domain found in the *Aspergillus nidulans* protein HbrB, which is involved in filamentous growth. The function of Bit61/Bit2 in TORC2 is unknown.

**TORC2 signaling network**

Although complete loss of TORC2 function is lethal, the use of temperature-sensitive alleles and, later, alleles of TORC2 that can be inhibited by small molecules, has provided great insight into the cellular processes regulated by TORC2. These include sphingolipid biosynthesis (Beeler et al., 1998), polarization of the actin cytoskeleton (Schmidt et al., 1996; Kamada et al., 2005), endocytosis (deHart et al., 2002; deHart et al., 2003; Rispal et al., 2015), G2/M cell cycle progression (Helliwell et al., 1998a; Gaubitz et al., 2015), repression of calcineurin (Mulet et al., 2006), regulation of ribosome biogenesis via the pentose phosphate pathway (Kliegman et al., 2013), and maintenance of genome stability (Shimada et al., 2013).

The mechanisms by which TORC2 regulates these processes have been illuminated by studying the downstream targets of the TORC2 substrates and effectors Ypk1 and Ypk2. The essential processes that require TORC2 are executed via the paralogous Ypk kinases because expression of certain Ypk alleles ($Ypk1^{D242A}$ or $Ypk2^{D239A}$), which do not need to be phosphorylated by TORC2 in order to be fully functional, rescues the lethality of TORC2-deficient cells (Kamada et al., 2005; Roelants et al., 2011). Additionally, *ypk1Δ ypk2Δ* cells are inviable indicating that both Ypk1 and Ypk2 mediate the essential functions of TORC2 (Casamayor et al., 1999). Although *ypk2Δ* cells have no obvious deficiencies, *ypk1Δ* cells display numerous deleterious phenotypes, including slow growth, endocytic defects, decreased cold tolerance and altered sensitivity to various chemical compounds. Thus, Ypk1 is the primary TORC2 effector.

The best characterized functions of TORC2-Ypk1 signaling are regulating PM lipid and protein homeostasis and responding to hyperosmotic stress (Figure 1.3). Ypk1 stimulates sphingolipid biosynthesis in two ways: first, by phosphorylating and thereby alleviating the inhibition exerted by two ER-localized tetraspanins, Orm1 and Orm2, that are negative regulators of the enzyme (L-serine:palmitoyl-CoA acyltransferase; SPT) that catalyzes the first committed step in sphingolipid biosynthesis acyltransferase; SPT), thus upregulating flux into sphingolipid synthesis (Roelants et al., 2011); and, second, by phosphorylating and enhancing the activity of the catalytic subunits (Lac1 and Lag1) of the ceramide synthase complex, thereby directing sphingolipid flux toward the production of ceramides and complex sphingolipids (Muir et al., 2014). Ypk1 also regulates PM lipid organization by modulating flippase activity. Flippases are P-type ATPases that translocate aminoglycerophospholipids from the outer leaflet to the inner leaflet of the membrane. Ypk1 regulates flippase function by phosphorylating and inhibiting the flippase activating kinases Fpk1 and Fpk2 (Roelants et al., 2010). In addition to regulating flippase activity, Fpk1 also modulates actin-patch mediated endocytosis via the phosphorylation and inhibition of the protein kinase Akl1 (Roelants et al., 2017). Ypk1 also participates directly in the regulation of endocytosis by phosphorylating and inhibiting the activity of the alpha-arrestin Rod1 which mediates the ubiquitin-dependent endocytosis of specific PM proteins (Alvaro et al., 2016).

**FIGURE 1.3**

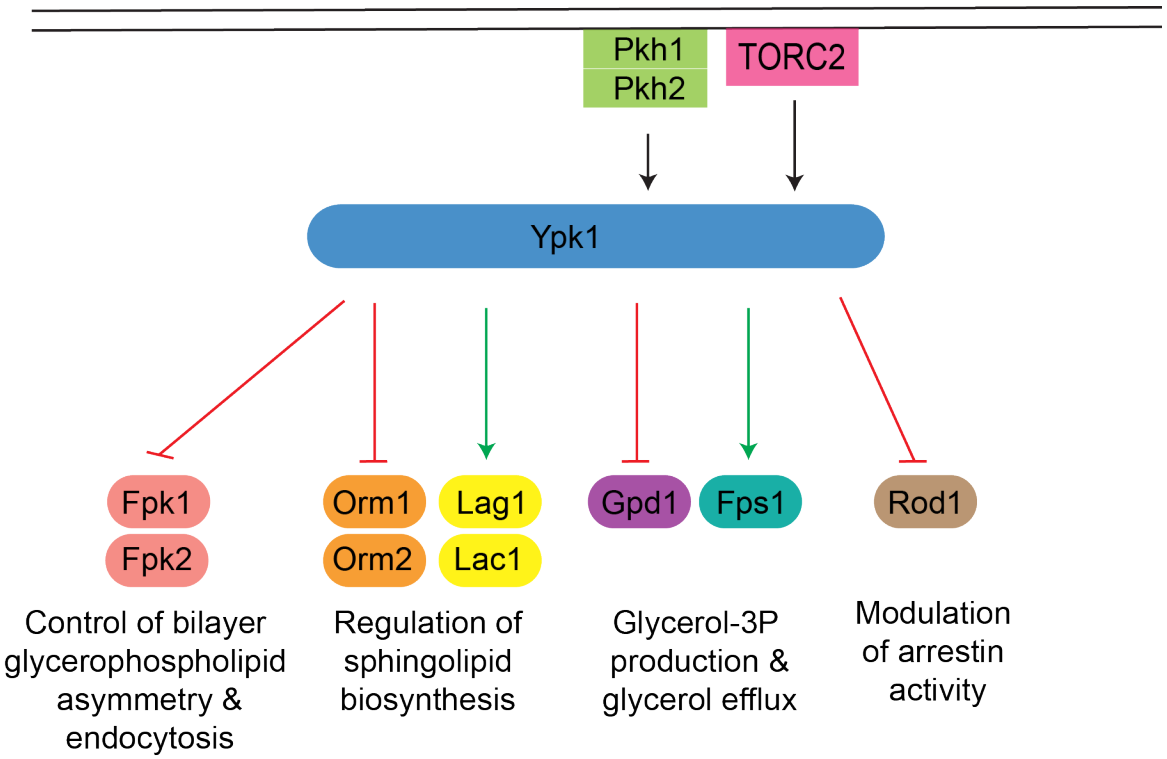


**Figure 1.3. The TORC2-Ypk1 signaling network.** Basal Ypk1 function requires phosphorylation of its activation loop by Pkh1 (or its paralog Pkh2) and further activation is elicited by TORC2-mediated phosphorylation of Ypk1. Ypk1, in turn, phosphorylates and thereby modulates the activities of proteins involved in bilayer glycerophospholipid asymmetry and endocytosis (Fpk1/Fpk2), sphingolipid biosynthesis (Orm1/Orm2, Lag1/Lac1), glycerol-3-phosphate production (Gpd1), glycerol efflux (Fps1) and ubiquitin-mediated endocytosis (Rod1).

Many of the phenotypes associated with TORC2-deficiency can be attributed to the loss of lipid homeostasis. For example, *orm1Δ orm2Δ tor2Δ* cells are viable (Rispal et al., 2015), suggesting that an essential function of TORC2-Ypk1 signaling is to maintain sufficient levels of sphingolipids. Sphingolipids are key structural components of the PM, as well as important signaling molecules. Characteristics of cells deficient in TORC2-Ypk1 signaling include defects in endocytosis, elevated levels of reactive oxygen species (ROS), depolarization of the actin cytoskeleton, high levels of calcineurin activity, increased sensitivity to inhibitors of sphingolipid biosynthesis, and decreased autophagy flux during amino acid starvation. Nearly all of these phenotypes can be attributed, at least in part, to insufficient sphingolipid levels. Diminished sphingolipid levels as well as excessive flippase activity cause defects in oxidative stress responses as well as vacuolar acidification resulting in increased ROS production from both vacuolar and mitochondrial sources (Niles et al., 2014). One purported mechanism by which deficiencies in TORC2-Ypk1 signaling result in elevated levels of ROS is through the misregulation of Pkc1 and cell wall integrity pathway (CWI). Although Pkc1, like Ypk1, is phosphorylated in a TORC2-dependent manner (Nomura and Inoue, 2015), Ypk1 activity also regulates Pkc1 activity through effects on the PM localization of Rom2, a Rho1 GEF, and of Rho1 itself (Schmidt et al., 1997; Niles and Powers, 2014; Hatakeyama et al., 2017). Rho1 activates Pkc1 (Kamada et al., 1996) and subsequently the CWI MAPK pathway [for a detailed overview of the CWI pathway, see Figure 4.1]. In addition to promoting cell wall remodeling, the CWI pathway also regulates oxidative stress response by stimulating the turnover of the transcriptional repressor Cyclin C (Krasley et al., 2006). Thus, decreased Pkc1/CWI pathway activation results in increased levels of ROS. ROS function as secondary messengers and play an important role in regulating actin cytoskeleton dynamics through the direct oxidation of actin. Hence, it is possible that the actin cytoskeleton defects observed in cells deficient in TORC2-Ypk1 signaling, could be attributable to elevated levels of ROS (Niles and Powers, 2014). Overexpression of a constitutively-active allele of Pkc1 ($Pkc1^{R398P}$) rescues the actin polarization defects and lethality of cells defective for TORC2-Ypk1 signaling (Helliwell et al., 1998b; Roelants et al., 2002; Schmelzle et al., 2002). Interestingly, overexpression of Rom2 or deletion of the Rho1 GAP SAC7 also rescues the lethality of a *tor2* temperature-sensitive allele at the restrictive temperature (Schmidt et al., 1997). Thus, available evidence indicates that TORC2-Ypk1 signaling is coordinated with the Pkc1/CWI pathway and affects cellular ROS levels.

In addition to disrupting proper polarization of the actin cytoskeleton, elevated levels of ROS also alter the function of the ER/PM-localized calcium channel Mid1, apparently resulting in increased cytosolic [$Ca^{2+}$], as judged by elevation of the activity of the $Ca^{2+}$-activated phosphatase calcineurin. Moreover, it has been reported that *ypk1Δ* cells have elevated levels of calcineurin activity and that deletion of Mid1 ameliorates the observed increase in calcineurin activity (Vlahakis et al., 2016). Calcineurin is activated under various environmental conditions that also cause PM stress (Cyert, 2003). Reciprocal regulation of TORC2 and calcineurin signaling (Mulet et al., 2006) balances cell growth and proliferation with survival-focused adaptive stress responses. It has been reported that TORC2-dependent repression of calcineurin activity is important for stimulating autophagy flux during amino acid starvation as calcineurin inhibits the general amino acid control (GAAC) response (Vlahakis et al., 2014). Additionally, calcineurin has been demonstrated to directly oppose TORC2 signaling by promoting the dephosphorylation of several downstream TORC2-Ypk1 substrates (Roelants et al., 2011; Muir et al., 2014).

TORC2-Ypk1 signaling also plays a critical role in responding to various stresses. Heat shock

upregulates TORC2-Ypk1 signaling transiently (Sun et al., 2011). TORC2-Ypk1 signaling is also modulated by both hypotonic and hypertonic stress. Under hypo-osmotic conditions, TORC2-mediated phosphorylation of Ypk1 is elevated (Berchtold et al., 2012). During hyper-osmotic stress, TORC2-mediated phosphorylation of Ypk1 is rapidly and markedly decreased, which promotes production and retention of the intracellular osmolyte glycerol in two ways. First, under normal osmotic conditions, Ypk1 retards the rate of glycerol-3-phosphate production from dihydroxyacetone-P by phosphorylating and inhibiting the glycerol-3P dehydrogenase Gpd1. Upon hypertonic stress, the deactivation of Ypk1 alleviates Gpd1 inhibition, allowing for a higher rate of production of glycerol-3P, which is dephosphorylated to produce glycerol (Lee et al., 2012). Second, under normal osmotic conditions, Ypk1-mediated phosphorylation maintains the aquaglyceroporin channel Fps1 in the open state, permitting glycerol efflux; upon hypertonic stress, deactivation of Ypk1 causes the channel to close, thereby promoting glycerol retention and minimizing water loss (Muir et al., 2015). How TORC2-Ypk1 signaling is down-regulated in response to hyperosmotic shock is not well understood, although this response does not require calcineurin function (Muir et al., 2015).

**Regulation of TORC2**

TORC2-Ypk1 signaling is modulated according to different PM stresses (Figure 1.4). In addition to heat shock and hypotonic conditions, TORC2-dependent phosphorylation of Ypk1 is markedly stimulated by sphingolipid depletion and weak acid stress (Roelants et al., 2011; Guerreiro et al., 2016; Omnus et al., 2016). Conversely, hypertonic stress rapidly and transiently downregulates TORC2 signaling (Muir et al., 2015). How, at the mechanistic level, TORC2 senses these different stresses is still a topic of current investigation. Regulation of TORC2 is mediated, at least in part, by dynamic changes in the localization of two, essential PH domain-containing PtdIns4,5$P_2$-binding proteins Slm1 and Slm2 (Audhya et al., 2004; Gallego et al., 2010). The essential functions of Slm1/Slm2 are confined to TORC2 signaling because the inviability of *slm1Δ slm2Δ* cells is rescued by the Ypk2$^{D239A}$ or Ypk1$^{D242A}$ alleles (Berchtold et al., 2012). Slm1/Slm2 are required for efficient phosphorylation of Ypk1 by TORC2 and this requirement for Slm1/Slm2 can be bypassed by artificially tethering Ypk1 to the PM (Niles et al., 2012). Ypk1 itself contains no recognizable membrane targeting domain, and it has been proposed that direct binding of Ypk1 to Slm1/Slm2 is the mechanism by which Ypk1 is delivered to TORC2 at the PM (Niles et al., 2012). By contrast, in both animal cells (Yang et al., 2006; Lu et al., 2011) and fission yeast (Ikeda et al., 2008; Shiozaki et al., 2013), there is compelling evidence that the Avo1 orthologs (mSin1 and Sin1, respectively) in the TORC2 complex bind and are required for phosphorylation of the Ypk1 orthologs in these organisms (Sgk1 and Gad8, respectively). Likewise, others have shown, in *S. cerevisiae*, that Ypk2 also seems to interact with the TORC2 complex via binding to Avo1 (Liao & Chen, 2012). Indeed, very recent biochemical and structural work has shown the CRIM domain of Sin1 (*S. pombe* Avo1) adopts a ubiquitin-like fold that is both necessary and sufficient for binding Gad8 (*S. pombe* Ypk1) and for TORC2-dependent Gad8 phosphorylation (Tatebe et al., 2017).

TORC2 localizes to distinct PM compartments termed MCTs (for membrane compartment containing Tor2) (Berchtold and Walther, 2009). Slm1/Slm2, on the other hand, are localized primarily to the eisosomes, which are distinct from MCTs. Increased PM tension, as occurs during sphingolipid depletion and hypotonic stress, triggers the release of Slm1/Slm2 from the eisosomes and their enhanced association with TORC2 (Berchtold et al., 2012). TORC2, in turn,

**FIGURE 1.4**

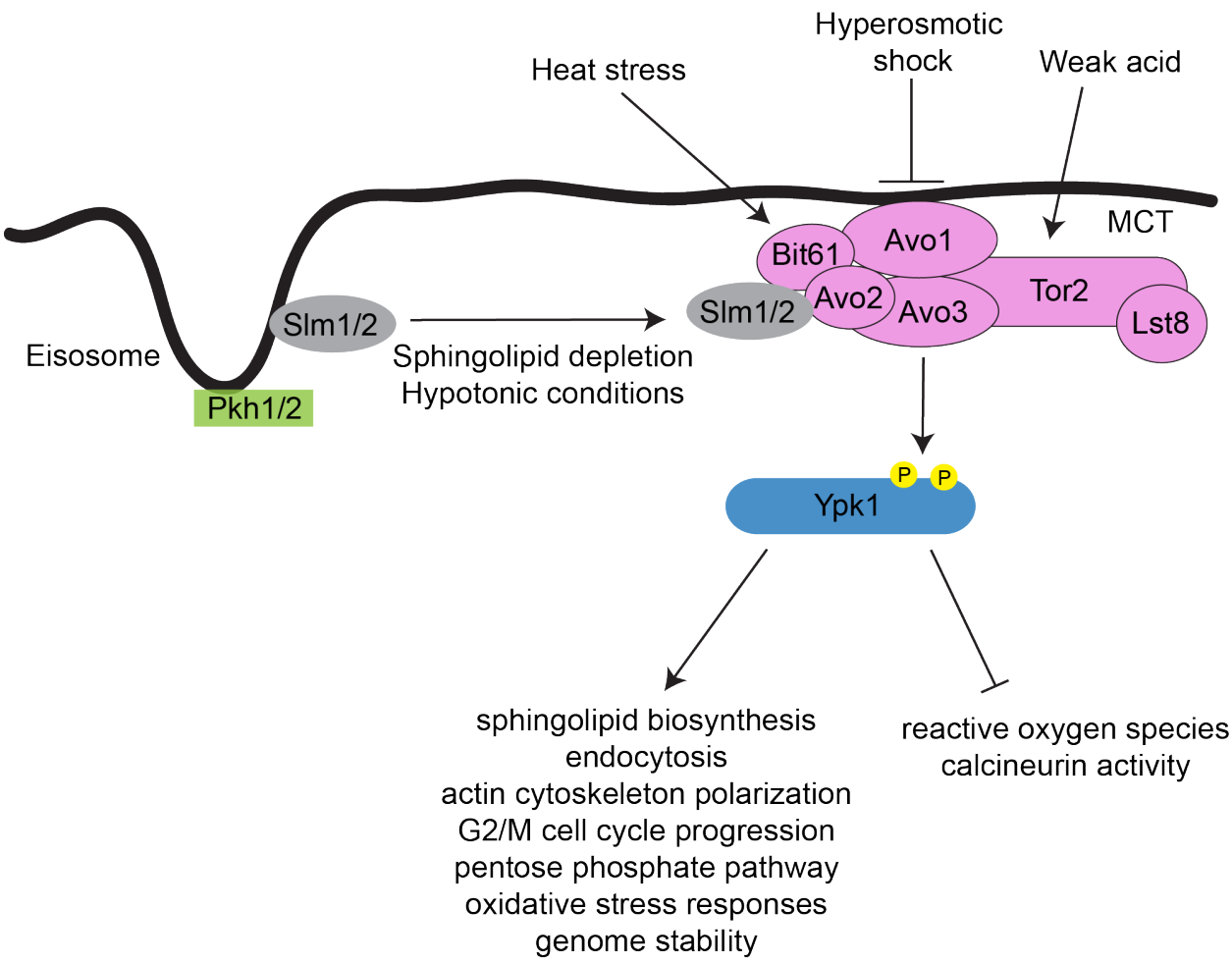


**Figure 1.4 Modulation of TORC2 signaling.** TORC2 senses the status of the PM and modulates the activity of its downstream effector Ypk1 to regulate many cellular processes. Increased PM tension triggers the release of Slm1 and Slm2 from eisosomes and enhanced association of Slm1/Slm2 with TORC2 stimulates TORC2-dependent phosphorylation of Ypk1.

stimulates the production of sphingolipids which relieves the increased PM tension.

How Slm1/Slm2 sense changes in the PM is still obscure. Although it was initially proposed that Slm1/Slm2 may respond to PM tension directly, increased ROS levels may also play a role in triggering the release of Slm1/Slm2 from the eisosomes because treating cells with a ROS scavenger, N-acetyl cysteine, prevents the dissociation of Slm1/Slm2 from the eisosomes after sphingolipid depletion (Niles et al., 2014). These observations still shed no light, however, on how ROS might act at the molecular level to promote Slm1/Slm2 dissociation from eisosomes. Interestingly, Slm1/Slm2 have been shown to cooperatively bind to both PtdIns4,5$P_2$ and IPC, raising the possibility that robust PM association of Slm1/Slm2 might require direct binding to IPC before it is further modified or transported to the outer leaflet (Gallego et al., 2010). Because Slm1 (and Slm2) have PtdIns4,5$P_2$-binding PH domains (Yu et al., 2004; Daquinag et al., 2007) and because recent evidence suggests that one role of eisosomes is to sequester and control the level of PM PtdIns4,5$P_2$ (Karotki et al., 2011; Kabeche et al., 2014; Kabeche et al., 2015), Slm1 and Slm2 may serve as a bridge to anchor the TORC2 complex in juxtaposition to eisosome-bound Pkh1 (and Pkh2) (Roelants et al., 2002), the required upstream activators of Ypk1 (and Ypk2). Moreover, because Slm1 and Slm2 also have docking sites (PIxIxT motifs) for, and have been demonstrated to associate with and be substrates for, calcineurin (Bultynck et al., 2006), changes in PtdIns4,5$P_2$ level could also modulate Ypk1 activity by affecting not only its rate of activation loop phosphorylation by Pkh1 and Pkh2, but also the rate of its calcineurin-mediated dephosphorylation. Interestingly, Slm1 has been shown to be phosphorylated in a TORC2-dependent manner (Audhya et al., 2004). However, the functional significance of this phosphorylation is unknown. In this regard, and considering that Slm1 and Slm2 are themselves dephosphorylated in a calcineurin-dependent manner, it has been reported that inhibition of calcineurin enhances Slm1 association with TORC2 (Mulet et al., 2006). On the other hand, although calcineurin antagonizes TORC2 signaling, calcineurin is not required for the down-regulation of TORC2 in response to hyperosmotic shock (Muir et al., 2015) or for TORC2 activation in response to sphingolipid depletion (Roelants et al., 2011).

In summary, Slm1/Slm2 clearly contribute to coupling TORC2 activity to changes in PM status. However, how they do so, is still unclear. Moreover, given the diversity of signals to which TORC2 responds, it is highly likely that other inputs also regulate TORC2 signaling.

**Thesis Overview**

The TORC2-Ypk1 signaling network plays a vital role in the maintenance of cellular homeostasis. The work I carried out and describe in this dissertation provided additional insight into the modulation of TORC2-Ypk1 signaling. Chapter 3 focuses on how TORC2 phosphorylation of Ypk1 regulates Ypk1 function. Briefly, TORC2 stimulates Ypk1 activation by phosphorylating Ypk1 at its conserved turn and hydrophobic motifs; however, I found that TORC2 also phosphorylates four additional sites in the C-terminus. I further discovered that these C-terminal phosphorylations of Ypk1 are necessary for efficient hydrophobic motif phosphorylation and for full Ypk1 activation. Thus, the extent of TORC2 phosphorylation of Ypk1 acts as a rheostat to fine-tune Ypk1 activity according to the needs of the cell and ensure that homeostasis is maintained. Chapter 4 introduces a novel mechanism by which TORC2 senses hyperosmotic stress and is coordinated with known stress-sensing pathways to ensure the integrity of the PM and cell wall during hypertonic conditions. Specifically, I discovered that the mitogen-activated protein kinases (MAPKs) Hog1 and Slt2, which are activated in response to hyperosmotic and cell wall stress, down-modulate TORC2 activity by mediating phosphorylation of the TORC2 subunit Avo2. MAPK-dependent phospho-regulation of TORC2 is a previously uncharacterized and exciting new area for further study. Finally, Chapter 5 integrates my new findings with our existing knowledge about TORC2-Ypk1 signaling. In this context, I also discuss future areas of study on the basis of some additional data I acquired during the course of my explorations of hypotheses about how different stresses modulate TORC2 function.

## Chapter 2. Materials and Methods

**Construction of yeast strains and growth conditions.** *S. cerevisiae* strains used in this work are described in Table 2.1. Unless stated otherwise, yeast cultures were grown in standard rich (YP) medium or in defined minimal (SC) medium containing 2% glucose/dextrose and were supplemented with the appropriate nutrients to permit growth of auxotrophs and/or to select for plasmids (Sherman, 2002). All cells were grown at 30°C unless indicated otherwise. For galactose induction, strains were grown in the appropriate SC medium containing 2% raffinose- 0.2% sucrose and genes under the control of galactose-inducible promoters were induced by the addition of 2% galactose for 3 h. Strains containing an auxin-inducible degron were cultured in YPD or the appropriate minimal dropout medium supplemented with 50 mM potassium phosphate buffer pH 6.2. Degradation was induced by the addition of the synthetic auxin 1-naphthaleneacetic acid (1-NAA; Sigma-Aldrich, St. Louis, MO) to the medium for the stated amount of time. For yeast growth assays on plates, overnight cultures were diluted in sterile water such that $A_{600\ nm}$ = 1 and spotted in 10-fold serial dilutions onto the appropriate plates. Alternatively, for some experiments, cells were plated as a lawn on YPD plates and 10 µL of the indicated drug were spotted onto sterile filter paper disks and immediately placed onto the lawn.

**Plasmids and recombinant DNA methods.** Plasmids used in this work (Table 2.2) were constructed using standard procedures in *E. coli* strain DH5α (Green & Sambrook, 2012). All PCR reactions were performed with Phusion™ High-Fidelity DNA Polymerase (New England Biolabs Inc.). Site-directed mutagenesis was performed by using appropriate mismatch oligonucleotide primers with the QuikChange™ method (Agilent Technologies, Inc., Santa Clara, CA), according to the manufacturer's instructions. The fidelity of all constructs was verified by nucleotide sequence analysis.

**Cell extract preparation and immunoblotting.** Samples of exponentially-growing cells were harvested by brief centrifugation and stored at -80°C. Cell pellets were thawed on ice and lysed in 150 µl 1.85 M NaOH, 7.4% β-mercaptoethanol. Proteins were precipitated by the addition of 150 µl 50% trichloroacetic acid on ice for 10 min. Precipitated proteins were pelleted by centrifugation and washed twice with ice cold acetone. Proteins were solubilized in 0.1 M Tris, 5% SDS to a final concentration of 0.025 $A_{600\ nm}$/µl and 5x SDS sample buffer was added to a final concentration of 1x. For samples subjected to phosphatase treatment, the precipitated proteins were resolubilized in 100 µl solubilization buffer (125 mM sorbitol, 180 mM Tris base, 42 mM NaCl, 10.5 mM $MgCl_2$, 420 µM EDTA, 4% SDS, 2% β-mercaptoethanol) and then diluted with 900 µl 50 mM Tris-HCl pH 8.5. Calf intestinal alkaline phosphatase (45 U; New England Biolabs Inc., Ipswich, MA) was added and the samples were incubated at 37°C for 2 hr. Proteins were recollected by TCA precipitation and resuspended in 0.1 M Tris, 5% SDS, as described above. Samples were boiled for 10 min and then resolved by SDS-PAGE. Standard 29:1 acrylamide:*bis*-acrylamide gels were used with the following exceptions: phosphorylated Ypk1-myc and FLAG-Lac1 were resolved by Phos-tag™ SDS-PAGE (Kinoshita et al., 2015) in 8% acrylamide, 35 µM Phos-tag™ affinity reagent [Wako Chemicals USA, Inc., Richmond, VA], 70 µM $MnCl_2$; 3xFLAG-Orm1 was resolved using 10% 75:1 acrylamide:*bis*-acrylamide gels run at 70V; and phosphorylated Avo2-3xFLAG was resolved in 8% acrylamide gels containing 17.5 µM Phos-tag™ reagent, 35 µM $MnCl_2$. Proteins were transferred to nitrocellulose membrane and blocked

with Odyssey™ buffer (Li-Cor Biosciences, Inc., Lincoln, NE) diluted 1:1 with PBS or TBS. Membranes were then probed with the appropriate primary antibody: mouse anti-myc mAb 9E10 (Monoclonal Antibody Facility, Cancer Research Laboratory, Univ. of California, Berkeley; 1:100); mouse anti-FLAG M2 mAb (Sigma-Aldrich; 1:10,000); rabbit polyclonal anti-Ypk1 phospho-Thr662 (gift of Ted Powers, Univ. of California, Davis; 1:20,000); mouse anti-HA.11 mAb (BioLegend, San Diego, CA; 1:1,000); rabbit polyclonal anti-Pgk1 (this lab, prepared as described in (Baum et al., 1978); 1:30,000); rabbit polyclonal anti-Avo3 (gift of Dr. Maria Nieves Martinez Marshall, this lab; 1:100) or goat anti-Tor2 (Santa Cruz Biotechnology, Dallas, TX; 1:1,000). Ypk1 Thr504 phosphorylation was detected using rabbit anti-SGK1 phospho-Thr256 (Santa Cruz Biotechnology; 1:1,000), dually phosphorylated Hog1 was detected using rabbit anti-p38 MAPK phospho-Thr180/phospho-Tyr182 mAb (Cell Signaling Technology, Danvers, MA; 1:1,000) and dually phosphorylated Slt2 was detected using anti-p44/42 (Erk1/2) MAPK phospho-Thr202/phospho-Tyr204 mAb (Cell Signaling Technology; 1:1000). After washing, the appropriate secondary antibody— CF770-conjugated goat anti-mouse IgG (Biotium, Fremont, CA), IRDye800CW-conjugated goat anti-rabbit IgG (Li-Cor), or IRDye680RD-conjugated goat anti-mouse IgG (Li-Cor) —was used for detection. Secondary antibodies were diluted 1:10,000 in 1:1 Odyssey™ buffer and PBS or TBS with 0.1% Tween-20 and 0.02% SDS. Immunoblots were visualized using an Odyssey™ infrared imaging system (Li-Cor).

**Identification of phosphorylation sites by mass spectrometry.** Ypk1 was immuno-precipitated from yeast and samples were prepared for and analyzed by mass spectrometry (MS), as described previously (Breslow et al., 2010).

**Immunoenrichment of TORC2.** A culture (1 L) of yeast cells expressing Avo3-3C-3xFLAG (yNM695) was grown in YPD to mid-exponential phase and harvested by centrifugation. The cells were washed once in 2x TNEGT buffer [100 mM Tris pH 7.6, 300 mM NaCl, 20% glycerol, 0.24% Tergitol™, 2 mM EDTA, 2 mM $NaVO_4$, 10 mM NaF, 10 mM Na-PPi, 10 mM β-glycerol phosphate, 0.1 mM PMSF plus 1x Roche complete protease inhibitor tablet (Roche, Basel, Switzerland)], then resuspended in 4 mL of 2x TNEGT buffer and frozen in droplets in liquid nitrogen. The cells were lysed cryogenically using Mixer Mill MM301 (Retsch, Düsseldorf, Germany). After the lysate was thawed on ice, 8 mL 1x TNEGT buffer [50 mM Tris pH 7.6, 150 mM NaCl, 10% glycerol, 0.12% Tergitol™, 1 mM EDTA, 1 mM $NaVO_4$, 5 mM NaF, 5 mM Na-PPi, 5 mM β-glycerol phosphate, 50 mM PMSF plus 1x Roche complete protease inhibitor tablet (Roche)] was added and the lysate was clarified by centrifugation at 2,000*xg* for 15 min. Avo3-3C-3xFLAG was then immunoprecipitated with 60 µl mouse anti-FLAG M2 mAb coupled-agarose resin (Sigma-Aldrich) equilibrated in 1x TNEGT buffer for 2 hr at 4°C. The resin was washed 4x in 1x TNEGT buffer without protease inhibitors and 2x in buffer for cleavage by human rhinovirus 3C protease (P3C) (50 mM Tris pH 7.6, 150 mM NaCl, 1 mM EDTA, 10% glycerol, 0.12% Tergitol™, 1 mM DTT, 2 mM $NaVO_4$, 10 mM NaF, 10 mM Na-PPi, 10 mM β-glycerol phosphate). Avo3-3C-3xFLAG was eluted in P3C buffer by cleavage with 12 U of commercial human rhinovirus 3C protease (PreScission™ protease; GE Healthcare, Little Chalfont, UK) at 4°C for 4 h.

***In vitro* TORC2 kinase assay**. Immunoprecipitated TORC2 was incubated with analog-sensitive $Ypk1^{as}$-TAP, purified as described in detail previously (Muir et al., 2014), in 1x kinase assay

buffer (20 mM Tris pH 7.6, 50 mM NaCl, 5 mM $MgCl_2$, 1 mM PMSF, 1 mM DTT, 20 mM 3-MB-PP1) with or without pan-TOR inhibitor NVP-BEZ235 (250 μM). Reactions were initiated by addition of 200 μM ATP and 5 μCi [γ-$^{32}$P]ATP, incubated at 30°C for 30 min, and terminated by addition of 5x SDS-PAGE sample buffer to 1x final concentration followed by boiling for 10 min. Labeled proteins were resolved by SDS-PAGE and analyzed by Coomassie blue staining and autoradiography on a Typhoon™ imaging system (GE Healthcare).

**Table 2.1**. *S. cerevisiae* strains used in this study

| Strain | Genotype | Source or Reference |
|---|---|---|
| BY4741 | *MAT***a** *his3Δ1 leu2Δ0 met15Δ0 ura3Δ0* | Research Genetics, Inc. |
| BY4742 | *MATα his3Δ1 leu2Δ0 lys2Δ0 ura3Δ0* | Research Genetics, Inc. |
| *akl1Δ* | BY4742 *akl1Δ::KanMX* | Research Genetics, Inc |
| *atg1Δ* | BY4742 *atg1Δ::KanMX* | Research Genetics, Inc |
| *ark1Δ* | BY4742 *ark1Δ::KanMX* | Research Genetics, Inc |
| *bck1Δ* | BY4742 *bck1Δ::KanMX* | Research Genetics, Inc |
| *bub1Δ* | BY4742 *bub1Δ::KanMX* | Research Genetics, Inc |
| *chk1Δ* | BY4742 *chk1Δ::KanMX* | Research Genetics, Inc |
| *cka1Δ* | BY4742 *cka1Δ::KanMX* | Research Genetics, Inc |
| *cka2Δ* | BY4742 *cka2Δ::KanMX* | Research Genetics, Inc |
| *cmk1Δ* | BY4742 *cmk1Δ::KanMX* | Research Genetics, Inc |
| *cmk2Δ* | BY4742 *cmk2Δ::KanMX* | Research Genetics, Inc |
| *ctk2Δ* | BY4742 *ctk2Δ::KanMX* | Research Genetics, Inc |
| *ctk3Δ* | BY4742 *ctk3Δ::KanMX* | Research Genetics, Inc |
| *dbf2Δ* | BY4742 *dbf2Δ::KanMX* | Research Genetics, Inc |
| *dbf20Δ* | BY4742 *dbf20Δ::KanMX* | Research Genetics, Inc |
| *dun1Δ* | BY4742 *dun1Δ::KanMX* | Research Genetics, Inc |
| *fmp48Δ* | BY4742 *fmp48Δ::KanMX* | Research Genetics, Inc |
| *hrk1Δ* | BY4742 *hrk1Δ::KanMX* | Research Genetics, Inc |
| *ime2Δ* | BY4742 *ime2Δ::KanMX* | Research Genetics, Inc |
| *ire1Δ* | BY4742 *ire1Δ::KanMX* | Research Genetics, Inc |
| *isr1Δ* | BY4742 *isr1Δ::KanMX* | Research Genetics, Inc |
| *kcc4Δ* | BY4742 *kcc4Δ::KanMX* | Research Genetics, Inc |
| *kin1Δ* | BY4742 *kin1Δ::KanMX* | Research Genetics, Inc |
| *hsl1Δ* | BY4742 *hsl1Δ::KanMX* | Research Genetics, Inc |
| *mck1Δ* | BY4742 *mck1Δ::KanMX* | Research Genetics, Inc |
| *mrk1Δ* | BY4742 *mrk1Δ::KanMX* | Research Genetics, Inc |
| *mkk2Δ* | BY4742 *mkk2Δ::KanMX* | Research Genetics, Inc |
| *kns1Δ* | BY4742 *kns1Δ::KanMX* | Research Genetics, Inc |
| *kss1Δ* | BY4742 *kss1Δ::KanMX* | Research Genetics, Inc |
| *mek1Δ* | BY4742 *mek1Δ::KanMX* | Research Genetics, Inc |
| *ptk2Δ* | BY4742 *ptk2Δ::KanMX* | Research Genetics, Inc |
| *rck1Δ* | BY4742 *rck1Δ::KanMX* | Research Genetics, Inc |
| *rim11Δ* | BY4742 *rim11Δ::KanMX* | Research Genetics, Inc |
| *ptk1Δ* | BY4742 *ptk1Δ::KanMX* | Research Genetics, Inc |
| *mkk1Δ* | BY4742 *mkk1Δ::KanMX* | Research Genetics, Inc |
| *npr1Δ* | BY4742 *npr1Δ::KanMX* | Research Genetics, Inc |
| *env7Δ* | BY4742 *env7Δ::KanMX* | Research Genetics, Inc |
| *yck1Δ* | BY4742 *yck1Δ::KanMX* | Research Genetics, Inc |

| | | |
|---|---|---|
| *ypk3Δ* | BY4742 *ypk3Δ::KanMX* | Research Genetics, Inc |
| *ssk22Δ* | BY4742 *ssk22Δ::KanMX* | Research Genetics, Inc |
| *ypl150wΔ* | BY4742 *ypl150wΔ::KanMX* | Research Genetics, Inc |
| *yck2Δ* | BY4742 *yck2Δ::KanMX* | Research Genetics, Inc |
| *swe1Δ* | BY4742 *swe1Δ::KanMX* | Research Genetics, Inc |
| *sks1Δ* | BY4742 *sks1Δ::KanMX* | Research Genetics, Inc |
| *frk1Δ* | BY4742 *frk1Δ::KanMX* | Research Genetics, Inc |
| *yck3Δ* | BY4742 *yck3Δ::KanMX* | Research Genetics, Inc |
| *sps1Δ* | BY4742 *sps1Δ::KanMX* | Research Genetics, Inc |
| *sky1Δ* | BY4742 *sky1Δ::KanMX* | Research Genetics, Inc |
| *ypk2Δ* | BY4742 *ypk2Δ::KanMX* | Research Genetics, Inc |
| *rtk1Δ* | BY4742 *rtk1Δ::KanMX* | Research Genetics, Inc |
| *slt2Δ* | BY4742 *slt2Δ::KanMX* | Research Genetics, Inc |
| *skm1Δ* | BY4742 *skm1Δ::KanMX* | Research Genetics, Inc |
| *yak1Δ* | BY4742 *yak1Δ::KanMX* | Research Genetics, Inc |
| *elm1Δ* | BY4742 *elm1Δ::KanMX* | Research Genetics, Inc |
| *sat4Δ* | BY4742 *sat4Δ::KanMX* | Research Genetics, Inc |
| *smk1Δ* | BY4742 *smk1Δ::KanMX* | Research Genetics, Inc |
| *tos3Δ* | BY4742 *tos3Δ::KanMX* | Research Genetics, Inc |
| *tpk2Δ* | BY4742 *tpk2Δ::KanMX* | Research Genetics, Inc |
| *tpk3Δ* | BY4742 *tpk3Δ::KanMX* | Research Genetics, Inc |
| *vhs1Δ* | BY4742 *vhs1Δ::KanMX* | Research Genetics, Inc |
| *pkh3Δ* | BY4742 *pkh3Δ::KanMX* | Research Genetics, Inc |
| *psk2Δ* | BY4742 *psk2Δ::KanMX* | Research Genetics, Inc |
| *tel1Δ* | BY4742 *tel1Δ::KanMX* | Research Genetics, Inc |
| *tor1Δ* | BY4742 *tor1Δ::KanMX* | Research Genetics, Inc |
| *tda1Δ* | BY4742 *tda1Δ::KanMX* | Research Genetics, Inc |
| *ygk3Δ* | BY4742 *ygk3Δ::KanMX* | Research Genetics, Inc |
| *gin4Δ* | BY4742 *gin4Δ::KanMX* | Research Genetics, Inc |
| *kin3Δ* | BY4742 *kin3Δ::KanMX* | Research Genetics, Inc |
| *pbs2Δ* | BY4742 *pbs2Δ::KanMX* | Research Genetics, Inc |
| *pho85Δ* | BY4742 *pho85Δ::KanMX* | Research Genetics, Inc |
| *pkh1Δ* | BY4742 *pkh1Δ::KanMX* | Research Genetics, Inc |
| *prr1Δ* | BY4742 *prr1Δ::KanMX* | Research Genetics, Inc |
| *prr2Δ* | BY4742 *prr2Δ::KanMX* | Research Genetics, Inc |
| *psk1Δ* | BY4742 *psk1Δ::KanMX* | Research Genetics, Inc |
| *ssn3Δ* | BY4742 *ssn3Δ::KanMX* | Research Genetics, Inc |
| *ste20Δ* | BY4742 *ste20Δ::KanMX* | Research Genetics, Inc |
| *tpk1Δ* | BY4742 *tpk1Δ::KanMX* | Research Genetics, Inc |
| *nnk1Δ* | BY4742 *nnk1Δ::KanMX* | Research Genetics, Inc |
| *rck2Δ* | BY4742 *rck2Δ::KanMX* | Research Genetics, Inc |

| | | |
|---|---|---|
| *kin2Δ* | BY4742 *kin2Δ::KanMX* | Research Genetics, Inc |
| *ksp1Δ* | BY4742 *ksp1Δ::KanMX* | Research Genetics, Inc |
| *mlp1Δ* | BY4742 *mlp1Δ::KanMX* | Research Genetics, Inc |
| yJP544 | BY4741 *hog1Δ::KanMX* | This lab |
| *ypk1Δ* | BY4741 *ypk1Δ::KanMX* | Research Genetics, Inc |
| YFR206 | BY4742 *met15Δ0 fpk1Δ::KanMX fpk2Δ::KanMX* | (Roelants et al., 2010) |
| *fus3Δ* | BY4742 *fus3Δ::KanMX* | Research Genetics, Inc |
| *ste11Δ* | BY4742 *ste11Δ::KanMX* | Research Genetics, Inc |
| *ste7Δ* | BY4742 *ste7Δ::KanMX* | Research Genetics, Inc |
| *cla4Δ* | BY4742 *cla4Δ::KanMX* | Research Genetics, Inc |
| *kk18Δ* | BY4742 *kkq8Δ::KanMX* | Research Genetics, Inc |
| *kin4Δ* | BY4742 *kin4Δ::KanMX* | Research Genetics, Inc |
| *fpk2Δ* | BY4742 *kin82Δ::KanMX* | Research Genetics, Inc |
| *pkp2Δ* | BY4742 *pkp2Δ::KanMX* | Research Genetics, Inc |
| *gcn2Δ* | BY4742 *gcn2Δ::KanMX* | Research Genetics, Inc |
| *ssk2Δ* | BY4742 *ssk2Δ::KanMX* | Research Genetics, Inc |
| *hal5Δ* | BY4742 *hal5Δ::KanMX* | Research Genetics, Inc |
| *ctk1Δ* | BY4742 *ctk1Δ::KanMX* | Research Genetics, Inc |
| *rim15Δ* | BY4742 *rim15Δ::KanMX* | Research Genetics, Inc |
| *vps15Δ* | BY4742 *vps15Δ::KanMX* | Research Genetics, Inc |
| *bud32Δ* | BY4742 *bud32Δ::KanMX* | Research Genetics, Inc |
| *pkh2Δ* | BY4742 *pkh2Δ::KanMX* | Research Genetics, Inc |
| *snf1Δ* | BY4742 *snf1Δ::KanMX* | Research Genetics, Inc |
| *fpk1Δ* | BY4742 *fpk1Δ::KanMX* | Research Genetics, Inc |
| $kin28^{ts}$ | BY4741 $kin28^{ts}$*::KanMX* | (Costanzo et al., 2010) |
| $dbf4^{ts}$ | BY4741 *dbf4-3::KanMX* | (Costanzo et al., 2010) |
| $ipl1^{ts}$ | BY4741 *ipl1-1::KanMX* | (Costanzo et al., 2010) |
| $cdc28^{ts}$ | BY4741 *cdc28-1::KanMX* | (Costanzo et al., 2010) |
| $rio2^{ts}$ | BY4741 *rio2-1::KanMX* | (Costanzo et al., 2010) |
| $pkc1^{ts}$ | BY4741 *pkc1-1::KanMX* | (Costanzo et al., 2010) |
| $cak1^{ts}$ | BY4741 *cak1-23::KanMX* | (Costanzo et al., 2010) |
| $tor2^{ts}$ (JTY5468) | BY4741 *tor2-29::KanMX* | (Costanzo et al., 2010) |
| $sln1^{ts}$ (JTY5473) | BY4741 *sln1-ts4::KanMX* | (Costanzo et al., 2010) |
| $cdc5^{ts}$ | BY4741 *cdc5-1::KanMX* | (Costanzo et al., 2010) |
| $cdc7^{ts}$ | BY4741 *cdc7-1::KanMX* | (Costanzo et al., 2010) |
| $cdc15^{ts}$ | BY4741 *cdc15-2::KanMX* | (Costanzo et al., 2010) |
| $sgv1^{ts}$ | BY4741 *sgv1-35::KanMX* | (Costanzo et al., 2010) |
| *TOR1-1 avo3*$^{\Delta CT}$ | *MATa TOR1-1 avo3Δ1274-1430 trp1 his3 ura3 leu2 rme1* (TB50 strain background) | (Gaubitz et al., 2015) |
| yAM135-A | BY4741 Ypk1(L424A)::*URA3 ypk2Δ::*KanMX4 | (Muir et al., 2014) |
| yKL4 | BY4741 Tor2::$Hyg^R$ | (Muir et al., 2014) |

| | | |
|---|---|---|
| yNM695 | BY4741 Tor2::Hyg$^{R}$ Avo3-3C-3xFLAG::KanMX | This lab |
| yDB344 | BY4741 3xFlag-Orm1 *ypk1Δ*::K.l. URA3 | (Roelants et al., 2011) |
| YFR302B | BY4741 *sln1-ts4::KanMX hog1Δ::HygR* | This study |
| yKL15 | BY4741 Sln1-6HA::HygR TIR1::HIS3 | This study |
| yKL18 | BY4741 Sln1-AID*-6HA::HygR TIR1::HIS3 | This study |
| yKL20 | BY4741 *lys2Δ0* Sln1-AID*-6HA::HygR *hog1Δ*::KanMX TIR1::HIS3 | This study |
| yKL26A | BY4741 Sln1-AID*-6HA::HygR *skn7Δ::KanMX* TIR1::HIS3 | This study |
| yKL27A | BY4741 Sln1-AID*-6HA::HygR *ssk2Δ::KanMX ssk22Δ::URA3* TIR1::HIS3 | This study |
| yKL16 | BY4741 Sln1-AID*-6HA *slt2Δ::URA3* TIR1::HIS3 | This study |
| yKL22 | BY4741 MET+ Sln1-AID*-6HA *hog1Δ::KanMX slt2Δ::URA3* TIR1::HIS3 | This study |
| YFR523 | BY4741 Sln1-AID*-6HA::HygR TIR1::HIS3 Avo2(T144A, T219A, S233A, S240A, S249A, T310A, S315A, T330, S333)::URA3 | This study |
| SEY6210.1 (Tether WT) | MATa *leu2-3,112 ura3-52 his3-Δ200 trp1-Δ901 lys2-801 suc2-Δ9* | (Robinson et al., 1988) |
| ANDY198 (*tetherΔ*) | SEY6210.1 *ist2Δ::HISMX6 scs2Δ::TRP1 scs22Δ::HISMX6 tcb1Δ::KANMX6 tcb2Δ::KANMX6 tcb3Δ::HISMX6* | (Manford et al., 2012) |

**Table 2.2** Plasmids used in this study

| Plasmid | Description | Source or Reference |
|---|---|---|
| pRS313 | *CEN, HIS3,* vector | (Sikorski and Hieter, 1989) |
| pRS315 | *CEN*, *LEU2*, vector | (Sikorski and Hieter, 1989) |
| p416 | *CEN, URA3,* vector | (Sikorski and Hieter, 1989) |
| pFR246 | pRS315 Ypk1(T51A, T71A, T504A, S644A, T662A)-myc | This study |
| pFR249 | pRS315 Ypk1(T51A,T57A, T71A, T504A, S644A, T662A)-myc | This study |
| pFR252 | pRS315 Ypk1(T51A,T57A, T71A, T504A, S644A, S653A, T662A)-myc | (Muir et al., 2015) |
| pFR255 | pRS315 Ypk1(T51A,T57A, S63A, S64A, T71A, T504A, S644A, S653A, T662A)-myc | This study |
| pFR264 | pRS315 Ypk1(T51A,T57A, S63A, S64A, T71A, T504A, S644A, S653A, T662A, S671A, S672A)-myc | (Roelants et al., 2011) |
| pJEN9 | pRS315 Ypk1(T51A,T57A, S63A, S64A, T71A, T504A, S644A, S653A, T662A, S671A, S672A, S678)-myc | This study |
| pKL28 | pRS315 Ypk1(T51A,T57A, S63A, S64A, T71A, T504A, S644A, S653A, T662A, 671S, S672A)-myc | This study |
| pKL29 | pRS315 Ypk1(T51A,T57A, S63A, S64A, T71A, T504A, S644A, S653A, T662A, S671A, 672S)-myc | This study |
| BG1805 | *2 μm*, *URA3*, $P_{GAL1}$, C-terminal tandem affinity (TAP) tag vector | Open Biosystems, Inc. |
| pAX50 | BG1805 Ypk1(L424A) | (Muir et al., 2014) |
| pAM20 | pRS315 Ypk1-myc | (Roelants et al., 2011) |
| pFR221 | pRS315 Ypk1(T662A)-myc | (Roelants et al., 2011) |
| pFR284 | pRS315 Ypk1(T662E)-myc | This study |
| pJEN3 | pRS315 Ypk1(S653A, S671A, S672A, S678A)-myc | This study |
| pJEN6 | pRS315 Ypk1(S653E, S671D, S672E, S678E)-myc | This study |
| pFR220 | pRS315 Ypk1(S644A)-myc | This study |
| pFR253 | pRS315 Ypk1(S653A)-myc | This study |
| pFR268 | pRS315 Ypk1(S671A, S672A)-myc | This study |
| pJEN8 | pRS315 Ypk1(S678A)-myc | This study |
| pFR234 | pRS315 Ypk1(D242A)-myc | This study |
| pKL7 | pRS315 Ypk1(D242A, T662A)-myc | This study |
| pJEN4 | pRS315 Ypk1(D242A, S653A, S671A, S672A, S678A)-myc | This study |
| pPL215 | p416 $MET25_{prom}$ Ypk1-3HA | (Niles et al., 2012) |
| pJEN5 | p416 $MET25_{prom}$ Ypk1(S653A, S671A, S672A, S678A)-3HA | This study |
| pKL32 | p416 $MET25_{prom}$ Ypk1(T662A)-3HA | This study |

| | | |
|---|---|---|
| pFR111 | YEp352GAL-Ypk1(T504A)-myc | (Roelants et al., 2010) |
| pAM76 | YEp352GAL-Ypk1-myc | (Roelants et al., 2002) |
| pFR112 | Yep352GAL-Ypk1-myc | This study |
| pKL27 | p416 pMET25 Ypk1$^{D242A}$-3HA | (Roelants et al., 2017) |
| pFR267 | pRS315 Ypk1(S51A, T57A, S63A, S64A, S71A, T504A, S644A, S653A, S671A, 672A)-myc | (Roelants et al., 2011) |
| pKL1 | pRS315 Avo2-3xFLAG | This study |
| pKL2 | pRS315 Avo2(T144A, T219A, S233A, S240A, S249A, T310A, S315A, T330, S333)-3xFLAG | This study |
| pAX126 | pRS315 $P_{LAC1}$ 3xFLAG-Lac1 | (Guerreiro et al., 2016) |
| pAX129 | pRS315 $P_{LAC1}$ 3xFLAG-Lac1 (S23A, S24A) | (Guerreiro et al., 2016) |

**Chapter 3. New insights about TORC2 phosphorylation of Ypk1: Yeast TORC2 activates protein kinase Ypk1 by phosphorylating four additional sites distinct from the turn and hydrophobic motifs**

## INTRODUCTION

The eukaryotic plasma membrane (PM) is a highly organized, yet dynamic, structure composed of specific proteins and several classes of lipids (Simons and Sampaio, 2011). The composition and distribution of the lipids in the PM affects many different processes mediated by this cell envelope, including endocytosis (Platta and Stenmark, 2011), solute transport (Divito and Amara, 2009) and signal transduction (Groves and Kuriyan, 2010). Eukaryotic cells have evolved, therefore, mechanisms to sense and respond to environmental stresses that affect PM status, such as fluctuations in temperature or osmolarity, and other perturbations, such as sphingolipid limitation, and thereby to adjust cell physiology appropriately to maintain homeostasis.

Using budding yeast (*Saccharomyces cerevisiae*) as the experimental organism, it has been shown by us (Roelants et al., 2011; Muir et al., 2014; Muir et al., 2015; Roelants et al., 2017) and others (Berchtold and Walther, 2009; Berchtold et al., 2012; Niles et al., 2012; Sun et al., 2012; Fröhlich et al., 2016) that the large multi-subunit protein kinase Target of Rapamycin (TOR) Complex 2 (TORC2) plays an essential role in sensing and ensuring maintenance of PM homeostasis. TORC2 is one of two evolutionarily conserved TOR-containing protein complexes (Kunz et al., 1993; Helliwell et al., 1994; Loewith et al., 2002; Wedaman et al., 2003). TORC1 is sensitive to inhibition by rapamycin, whereas TORC2 is normally insensitive to this agent (Jacinto et al., 2004). In both yeast and mammalian cells, TORC2 action influences not only reactions that affect PM lipid and protein composition, but also assembly and function of the actin cytoskeleton (Bartlett and Kim, 2014; Gaubitz et al., 2016). The catalytic subunit of the TORC1 and TORC2 complexes is the very large TOR polypeptide; metazoans possess a single TOR-encoding gene (human mTOR, 2,549 residues), whereas budding yeast (Heitman et al., 1991), fission yeast (Ikai et al., 2011) and other fungi (Eltschinger and Loewith, 2016) encode two TOR proteins, Tor1 and Tor2 (2,470 and 2,474 residues, respectively, in *S. cerevisiae*). TORC1 is functional when its catalytic subunit is either Tor1 and Tor2, whereas only Tor2 can serve as the catalytic subunit in TORC2 (Loewith et al., 2002; Wedaman et al., 2003). Both Tor1 and Tor2 bind and are greatly stabilized by the small *beta*-propeller protein Lst8 (Yang et al., 2013; Aylett et al., 2016; Baretić et al., 2016), which thus is present in both TORC1 and TORC2. However aside from Lst8, all of the other known subunits in TORC2, namely Avo1, Avo2, Avo3/Tsc11, Bit2, Bit61, Slm1 and Slm2, are separate and distinct from those in TORC1 (Loewith et al., 2002; Eltschinger and Loewith, 2016). Recent structural, genetic and biochemical analysis revealed that TORC2 is only insensitive to rapamycin because the C-terminus of Avo3 (mammalian homolog is Rictor) blocks the ability of rapamycin-bound FKBP12 (Fpr1 in *S. cerevisiae*) to bind to the FRB domain of Tor2; deleting a portion of the Avo3 C-terminus renders TORC2 sensitive to rapamycin inhibition (Gaubitz et al., 2015). In a yeast cell where such an *avo3* truncation is combined with a dominant point mutation (*TOR1-1*) in the FRB domain of Tor1 that blocks its association with rapamycin-Fpr1 (Heitman et al., 1991), TORC2 can be uniquely inhibited by addition of rapamycin (Gaubitz et al., 2015).

TORC2 is localized at the PM (Berchtold and Walther, 2009; Niles et al., 2012) and responds to activating perturbations and stresses by directly phosphorylating and thereby stimulating the activity of the downstream AGC-family protein kinase Ypk1 and its paralog Ypk2/Ykr2 (Chen et

al., 1993; Roelants et al., 2002), which are orthologs of mammalian SGK1 (Casamayor et al., 1999). An allele of Ypk2 (Ypk2$^{D239A}$) (Kamada et al., 2005), or a corresponding Ypk1 allele (Ypk1$^{D242A}$) (Roelants et al., 2011), which does not require TORC2-mediated phosphorylation for full activity, rescues the lethality of a *tor2* temperature-sensitive mutation at restrictive temperature, indicating that the functions of TORC2 required for viability are all exerted through the action of Ypk1 and/or Ypk2. Because a *YPK1*$^{+}$ *ypk2Δ* strain exhibits no deleterious phenotype (Chen et al., 1993; Roelants et al., 2002), Ypk1 alone is able to execute all of the essential functions carried out by these enzymes. Indeed, subsequent analysis of the substrates of Ypk1 has shown that this protein kinase maintains PM homeostasis in multiple ways. Ypk1 reduces aminoglycerophospholipid flipping from the outer to the inner leaflet of the PM by phosphorylating and inhibiting two protein kinases Fpk1 and Fpk2 that stimulates the P-type ATPases ("flippases") that catalyze this inward translocation (Roelants et al., 2010). Ypk1 also stimulates production of complex sphingolipid by phosphorylating Orm1 and Orm2 and thereby relieving the inhibition that these two tetraspanins exert on L-serine:palmitoyl-CoA acyltransferase, which catalyzes the first committed step in sphingolipid biosynthesis (Roelants et al., 2011), as well as by phosphorylating and stimulating the activity of Lac1 and Lag1, the catalytic subunits of the ceramide synthase complex (Muir et al., 2014). Alleviation of the inhibitory phosphorylation that Ypk1 exerts on the glycerol-3P dehydrogenase isoform Gpd1 (Lee et al., 2012) and of the channel-opening phosphorylation of the aquaglyceroporin Fps1 (Muir et al., 2015) both play important roles in promoting cell survival in response to hyperosmotic shock. Ypk1-mediated phosphorylation also blocks the ability of certain endocytic adaptors (alpha-arrestins) to promote internalization of integral PM protein (Alvaro et al., 2016).

As observed for other AGC family protein kinases (Pearce et al., 2010), Ypk1 is regulated by phosphorylation on residues situated within three conserved sequences. First, phosphorylation of Ypk1 on Thr504 in a conserved T$^{504}$FCGTPEY motif within its activation loop (T-loop) is required for Ypk1 activity, a modification installed by the upstream eisosome-associated protein kinases Pkh1 and Pkh2 (Roelants et al., 2002; Roelants et al., 2004). However, for cell survival in response to certain stresses (*e.g.* sphingolipid depletion, heat shock, or hypotonic conditions), Ypk1 activity must be upregulated by further phosphorylation at Thr662 in a shorter conserved sequence F/W-T$^{662}$-F/Y near its C-terminus (Roelants et al., 2004; Kamada et al., 2005; Roelants et al., 2011; Berchtold et al., 2012; Niles et al., 2012; Sun et al., 2012), dubbed the hydrophobic motif. As first revealed by analysis of Ypk2, phosphorylation at the hydrophobic motif is mediated by TORC2, which also phosphorylates another C-terminal site (Ser644 in Ypk1) within another conserved sequence (P-V/I-DS$^{644}$VV-D/N-E/D), dubbed the turn motif (Kamada et al., 2005). Thus, TORC2 plays a key role in stimulating Ypk1 activity, thereby allowing cells to cope with these stresses.

Given its importance in activating Ypk1 function, I sought to characterize TORC2-mediated phosphorylation of Ypk1 in greater detail. In doing so, I discovered that TORC2 phosphorylates Ypk1 at several previously uncharacterized C-terminal sites distinct from the "classical" turn and hydrophobic motifs. As I document here, phosphorylation at these additional sites is essential for full Ypk1 function. My findings suggest that differential phosphorylation by TORC2 may provide a means for modulating the activity of Ypk1 in a graded manner, thereby dynamically adjusting the level of Ypk1 activity to meet the needs of the cell.

## RESULTS

**Ypk1 is phosphorylated at four previously uncharacterized sites**. Prior work from this laboratory, as well as from others, have shown previously that at least five different protein kinases phosphorylate Ypk1 (Figure 3.1A). Pkh1 and Pkh2 phosphorylate Ypk1 at Thr 504 in the activation loop (Casamayor et al., 1999; Roelants et al., 2002); TORC2 phosphorylates Ypk1 at the turn (Ser644) and hydrophobic (Thr662) motifs (Kamada et al., 2005; Roelants et al., 2011; Niles et al., 2012); and Fpk1 and Fpk2 phosphorylate Ypk1 at Ser51 and Ser71 in the N-terminus (Roelants et al., 2010). To gain additional insight into Ypk1 regulation, I asked if Ypk1 is phosphorylated at any additional sites other than the five characterized previously. Toward this end, I expressed a Ypk1 mutant, Ypk1$^{5A}$-myc, that lacks the five previously characterized phosphorylation sites (due to their mutation to Ala) and resolved lysates from these cells by phosphate-affinity SDS-PAGE (Phos-tag™ gels) (Kinoshita et al., 2015). This technique slows the mobility of phosphorylated species; the more highly phosphorylated a protein, the slower its migration (Figure 3.2). When resolved by Phos-tag SDS-PAGE, Ypk1$^{5A}$-myc showed multiple slower mobility bands which were largely eliminated when the extract was treated with phosphatase, indicating that Ypk1 is phosphorylated at additional sites other than the five previously described (Figure 3.1B). To identify the previously uncharacterized phosphorylation sites revealed by my Phos-tag gel analysis, Ypk1 immuno-purified from yeast was analyzed by mass spectrometry (MS). Reassuringly, the MS analysis identified phosphorylation at four of the five previously described sites in Ypk1 but, in agreement with my Phos-tag gel analysis, indicated other candidate phosphorylated residues (Figure 3.1C). For this reason, I then began systematically installing into Ypk1$^{5A}$-myc Ala substitution mutations of these presumptive sites and analyzed the resulting change in migration on Phos-tag gels. Although detected as phosphorylated in the MS analysis, T57A and S64A (as well as S63A) mutants showed no difference in migration from that of Ypk1$^{5A}$-myc when examined by Phos-tag gel SDS-PAGE. However, mutants at three C-terminal residues, S653A, S671A and S672A, all showed a readily detectable change in migration compared to Ypk1$^{5A}$-myc (Figure 3.1D). Although Ser671 was not identified by MS as phosphorylated, band shift analysis showed that both Ser671 and Ser672 are phosphorylated *in vivo* (Figure 3.1E). Because all three of the phosphorylation sites I was able to confirm were located at the C-terminus of Ypk1, I then asked whether Ser678 was the phosphorylation site responsible for the single band shifted species exhibited by Ypk1$^{11A}$-myc on Phos-tag™ gels. Gratifyingly, mutating Ser678 to Ala to generate Ypk1$^{12A}$-myc eliminated the slower mobility band (Figure 3.1D).

To investigate the extent to which these residues (Ser653, Ser671, Ser672 and Ser678) in Ypk1 are conserved in Ypk1 orthologs in other species, I aligned the amino acid sequence of the C-terminal end of Ypk1 against the corresponding region in Ypk1 orthologs from 15 other yeast species as well as with its *S. cerevisiae* paralog (Ypk2) and its human ortholog (SGK1) (Casamayor et al., 1999) (Figure 3.3). Notably, the phosphorylated residues in Ypk1, as well as sequence context surrounding these residues, are well conserved in many other fungal homologs of Ypk1. Even though more distantly related relatives, such as *S. pombe* Gad8 and *H. sapiens* SGK1, share less homology with *S. cerevisiae* Ypk1, their C-termini still contain putative phosphorylation sites at approximately the same positions, suggesting that phosphorylation at multiple C-terminal sites may be an evolutionarily conserved feature of the regulation of this class of protein kinase.

**FIGURE 3.1**

A

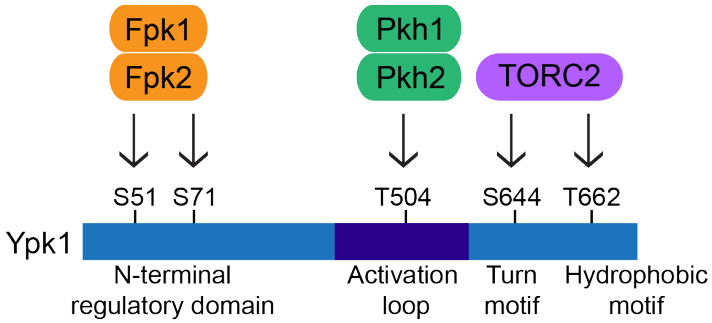


B

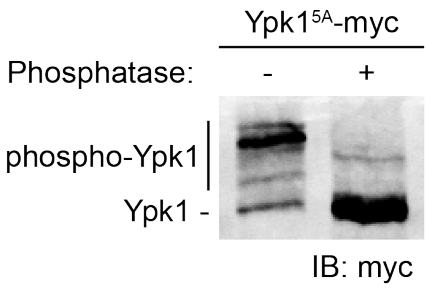


C

```
  1 MYSWKSKFKF GKSKEEKEAK HSGFFHSSKK EEQQNNQATA GEHDASITRS SLDRKGTINP
 61 SNSSVVPVRV SYDASSSTST VRDSNGGNSE NTNSSQNLDE TANIGSTGTP NDATSSSGMM
121 TIKVYNGDDF ILPFPITSSE QILNKLLASG VPPPHKEISK EVDALIAQLS RVQIKNQGPA
181 DEDLISSESA AKFIPSTIML PGSSTLNPLL YFTIEFDNTV ATIEAEYGTI AKPGFNKIST
241 FDVTRKLPYL KIDVFARIPS ILLPSKTWQQ EMGLQDEKLQ TIFDKINSNQ DIHLDSFHLP
301 INLSFDSAAS IRLYNHHWIT LDNGLGKINI SIDYKPSRNK PLSIDDFDLL KVIGKGSFGK
361 VMQVRKKDTQ KVYALKAIRK SYIVSKSEVT HTLAERTVLA RVDCPFIVPL KFSFQSPEKL
421 YFVLAFINGG ELFYHLQKEG RFDLSRARFY TAELLCALDN LHKLDVVYRD LKPENILLDY
481 QGHIALCDFG LCKLNMKDDD KTDTFCGTPE YLAPELLLGL GYTKAVDWWT LGVLLYEMLT
541 GLPPYYDEDV PKMYKKILQE PLVFPDGFDR DAKDLLIGLL SRDPTRRLGY NGADEIRNHP
601 FFSQLSWKRL LMKGYIPPYK PAVSNSMDTS NFDEEFTREK PIDSVVDEYL SESVQKQFGG
661 WTYVGNEQLG SSMVQGRSIR
```

Regions covered by mass spectrometry

Identified as phosphorylated by mass spectrometry

Sites mutated in Ypk1$^{12A}$

D

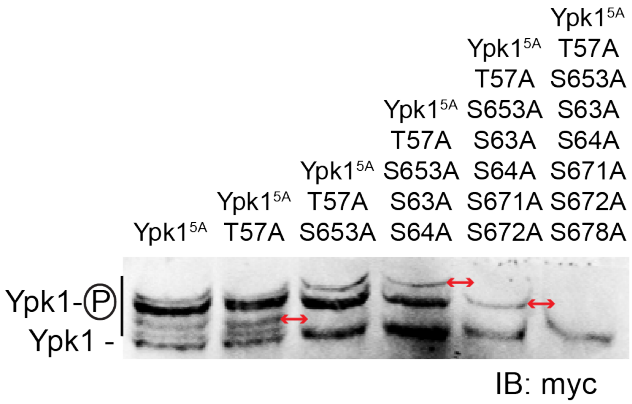


E

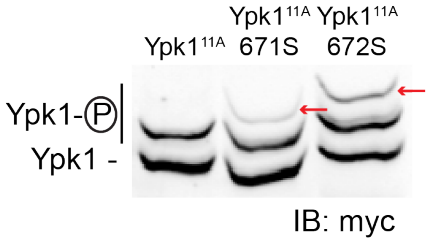

**Figure 3.1**. **Ypk1 is phosphorylated at four previously uncharacterized sites**. (A) Ypk1 is phosphorylated at Ser51 and Ser71 by Fpk1 (and its paralog Fpk2), at Thr504 in its activation loop by Pkh1 (and its paralog Pkh2), and at its turn (Ser664) and hydrophobic (Thr662) motifs by TORC2. (B) BY4741 expressing Ypk1$^{5A}$-myc (pFR246) were grown to exponential phase, harvested, lysed, the resulting whole-cell extracts incubated in the absence or presence of phosphatase (CIP), and samples resolved by Phos-tag™ SDS-PAGE and analyzed by immunoblotting with anti-myc mAb 9E10. (C) Phosphopeptides derived from Ypk1 immunoprecipitated from yeast were analyzed by mass spectrometry. Sequences recovered (underlined in blue); phosphorylation sites identified (boxed); sites mutated in Ypk1$^{12A}$ (red); phosphorylation sites confirmed by bandshift (red asterisk). (D) BY4741 expressing Ypk1$^{5A}$-myc (pFR246), Ypk1$^{6A}$-myc (pFR249), Ypk1$^{7A}$-myc (pFR252), Ypk1$^{9A}$-myc (pFR255), Ypk1$^{11A}$-myc (pFR264) or Ypk1$^{12A}$-myc (pJEN9) were analyzed as in (B), but without phosphatase treatment. (E) BY4741 cells expressing Ypk1$^{11A}$-myc (pFR264), Ypk1$^{11A\ 671S}$-myc (pKL28) or Ypk1$^{11A\ 672S}$-myc (pKL29) were analyzed as in (D).

**FIGURE 3.2**

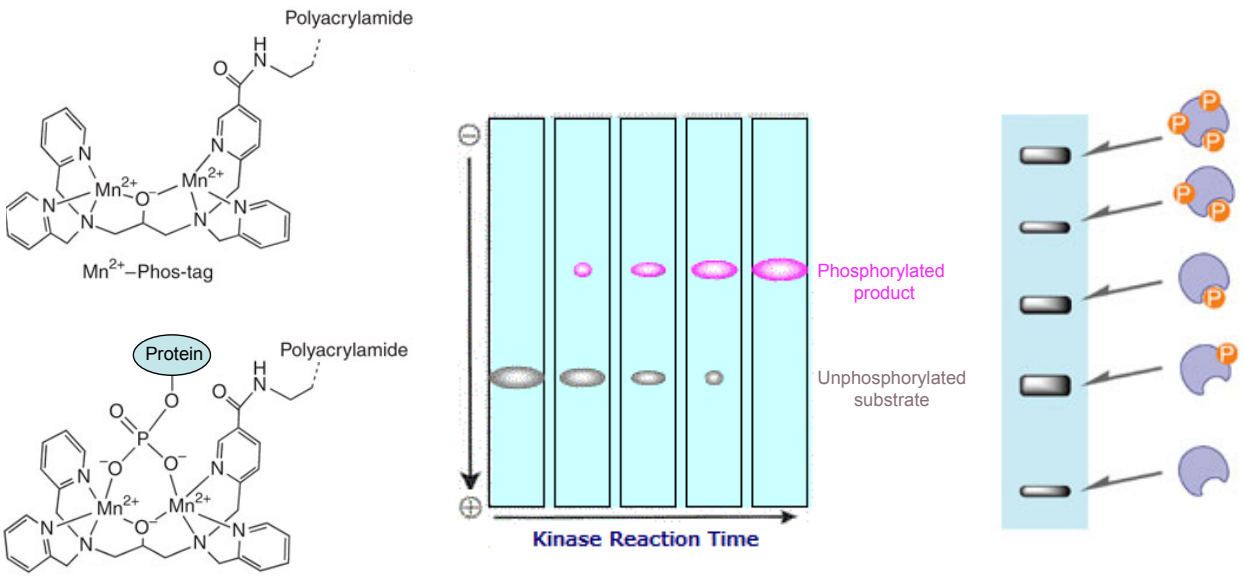


**Figure 3.2**. **Phosphate-affinity (Phos-tag™) SDS-PAGE**. Phosphorylated species are retarded differentially during their migration via non-covalent interaction of phosphorylated residues with the divalent cation bound to the covalently immobilized Phos-tag™ chelator attached to the polyacrylamide gel matrix. For any given protein, the choice of divalent cation— $Mg^{2+}$, $Mn^{2+}$, $Zn^{2+}$, $Co^{2+}$ or $Ni^{2+}$ —can sometimes improve the separation of species achieved. Panels adapted from images available in Kinoshita et al., 2009 and at URL http://www.wako-chem.co.jp/english/labchem/product/life/Phos-tag/Acrylamide.htm.

**FIGURE 3.3**

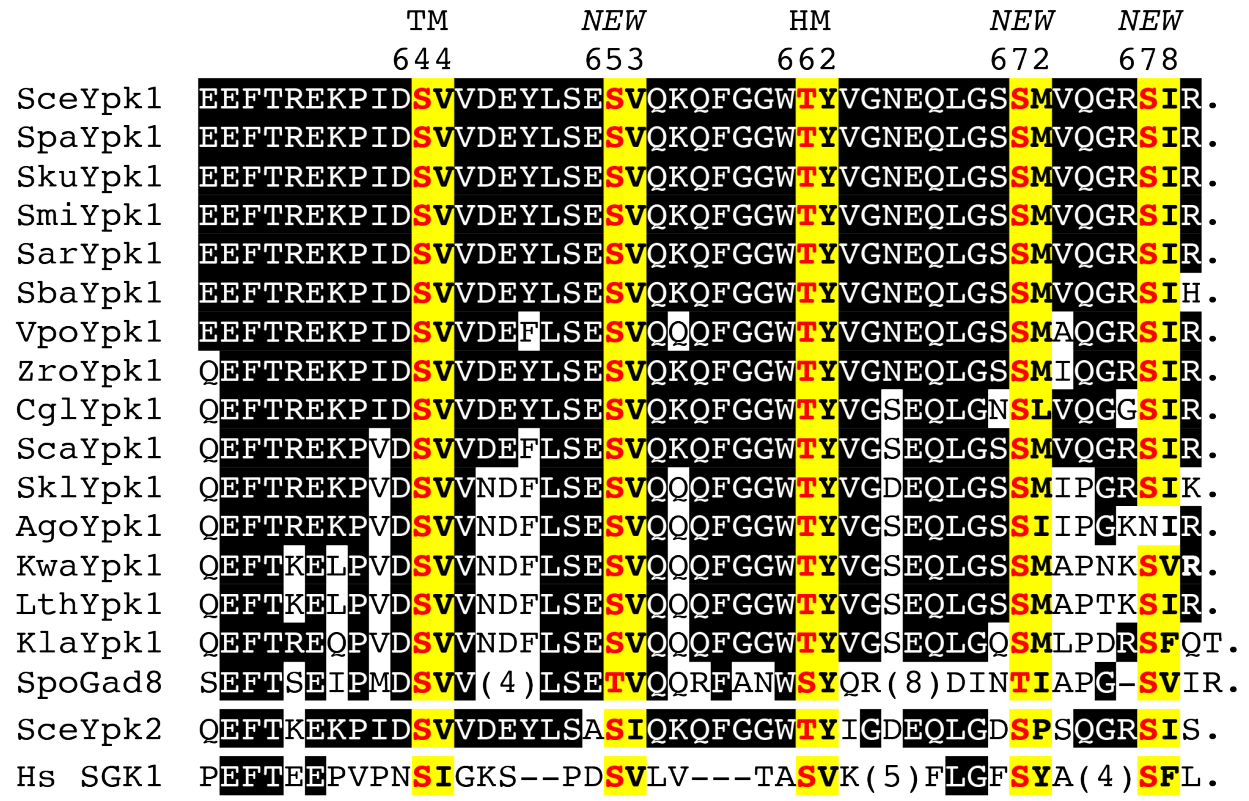
TM
NEW
HM
NEW
NEW
644
653
662
672
678
SceYpk1 EEFTREKPIDSVVDEYLSESVQKQFGGWTYVGNEQLGSSMVQGRSIR.
SpaYpk1 EEFTREKPIDSVVDEYLSESVQKQFGGWTYVGNEQLGSSMVQGRSIR.
SkuYpk1 EEFTREKPIDSVVDEYLSESVQKQFGGWTYVGNEQLGSSMVQGRSIR.
SmiYpk1 EEFTREKPIDSVVDEYLSESVQKQFGGWTYVGNEQLGSSMVQGRSIR.
SarYpk1 EEFTREKPIDSVVDEYLSESVQKQFGGWTYVGNEQLGSSMVQGRSIR.
SbaYpk1 EEFTREKPIDSVVDEYLSESVQKQFGGWTYVGNEQLGSSMVQGRSIH.
VpoYpk1 EEFTREKPIDSVVDEFLSESVQQQFGGWTYVGNEQLGSSMAQGRSIR.
ZroYpk1 QEFTREKPIDSVVDEYLSESVQKQFGGWTYVGNEQLGSSMIQGRSIR.
CglYpk1 QEFTREKPIDSVVDEYLSESVQKQFGGWTYVGSEQLGNSLVQGGSIR.
ScaYpk1 QEFTREKPVDSVVDEFLSESVQKQFGGWTYVGSEQLGSSMVQGRSIR.
SklYpk1 QEFTREKPVDSVVNDFLSESVQQQFGGWTYVGDEQLGSSMIPGRSIK.
AgoYpk1 QEFTREKPVDSVVNDFLSESVQQQFGGWTYVGSEQLGSSIIPGKNIR.
KwaYpk1 QEFTKELPVDSVVNDFLSESVQQQFGGWTYVGSEQLGSSMAPNKSVR.
LthYpk1 QEFTKELPVDSVVNDFLSESVQQQFGGWTYVGSEQLGSSMAPTKSIR.
KlaYpk1 QEFTREQPVDSVVNDFLSESVQQQFGGWTYVGSEQLGQSMLPDRSFQT.
SpoGad8 SEFTSEIPMDSVV(4)LSETVQQRFANWSYQR(8)DINTIAPG-SVIR.
SceYpk2 QEFTKEKPIDSVVDEYLSASIQKQFGGWTYIGDEQLGDSPSQGRSIS.
Hs SGK1 PEFTEEPVPNSIGKS--PDSVLV---TASVK(5)FLGFSYA(4)SFL.

**Figure 3.3**. **Comparison of the sequences of the C-terminal ends of the Ypk1 orthologs from sixteen yeast species and human SGK1**. The amino acid sequence of the C-terminal end of *Saccharomyces cerevisiae* (Sce) Ypk1 (*top line*) was aligned with the corresponding segment of the Ypk1 orthologs from fifteen other yeast species, as indicated, including the *sensu stricto* group *Saccharomyces paradoxus* (Spa), *Saccharomyces kudriavzevii* (Sku), *Saccharomyces mikatae* (Smi), *Saccharomyces arboricola* (Sar) and *Saccharomyces bayanus* (Sba), the more divergent species *Vanderwaltozyma polyspora* (Vpo), *Zygosaccharomyces rouxii* (Zro), *Candida glabrata* (Cgl), *Saccharomyces castellii* (Sca), *Saccharomyces kluyveri* (Skl), *Ashbya gossypii* (Ago), *Kluveromyces waltii* (Kwa), *Lachancea thermotolerans* (Lth), *Kluveromyces lactis* (Kla) and *Schizosaccharomyces pombe* (Spo), as well as its *S. cerevisiae* paralog Ypk2 and the human Ypk1 counterpart, SGK1 (*bottom line*). As a means to emphasize its degree of relatedness to *S. cerevisiae* Ypk1, only identities between each other protein and *S. cerevisiae* Ypk1 are indicated (*white letters on black boxes*). One-residue gaps (*hyphens*) and insertions of the indicated length (*in parentheses*) were introduced to maximize the alignment of the most distant orthologs. Period (.) indicates the end of the open-reading-frame. Matches to the consensus TORC2 phospho-acceptor site motif (-S/T-Hpo-, where Hpo denotes any hydrophobic residue) (*yellow boxes with phosphorylation site in bold red and hydrophobic residue in bold black*). The two "classical" sites for TORC2-mediated phosphorylation— the so-called Turn Motif (*TM*) and Hydrophobic Motif (*HM*) (Pearce *et al.* 2010) —as well as the additional sites (*NEW*) discovered in this study are indicated above, along with the corresponding residue positions in *S. cerevisiae* Ypk1. Sequence sources were: Sce (strain S288C) from the Saccharomyces Genome Database (http://www.yeastgenome.org/locus/ S000001609/protein); Spa, Sku, Smi, Sba, Sca and Skl from Cliften *et al.,* 2003 and Kellis *et al.*, 2003; Sar (GenBank EJS42953.1), Vpo (GenBank EDO19622.1), Zro (EMBL Bank CAR29179.1) and Lth (EMBL Bank CAR22493.1); Cgl, Ago, Kwa, Kla, Spo and Sce Ypk2 from the Fungal Orthogroups database at the Broad Institute (https://portals.broadinstitute.org/cgi-bin/regev/orthogroups/
show_orthogroup.cgi?orf=YKL126W); and, *Homo sapiens* (Hs) SGK1, isoform 2 (GenBank ACD35864.1).

**TORC2 phosphorylates Ypk1 at four C-terminal sites distinct from the turn and hydrophobic motifs**. To determine which protein kinase(s) is responsible for phosphorylating Ypk1 at Ser653, Ser671, Ser672 and Ser678, a screen was conducted in which Ypk1 phosphorylation at the new sites was monitored by band shift analysis in strains either deleted for non-essential serine/threonine protein kinases or containing temperature-sensitive alleles of essential serine/threonine protein kinases. The only serine/threonine protein kinase that showed a marked reduction in Ypk1 phosphorylation at the C-terminal sites upon deletion or inactivation was Tor2. In a temperature-sensitive *tor2*$^{ts}$ strain, Ypk1$^{5A}$-myc was already substantially less phosphorylated at 26°C compared to a wild-type strain; and, after shifting cells to the restrictive temperature for 2 h, Ypk1$^{5A}$-myc phosphorylation was completely abolished (Figure 3.4A). Thus, Tor2 activity is required for phosphorylation of Ypk1 at the new sites. Because Tor2 can function in both TORC1 and TORC2 (Loewith et al., 2002), I examined Ypk1$^{5A}$-myc phosphorylation in a *TOR1-1 avo3*$^{\Delta CT}$ strain (Gaubitz et al., 2015), in which TORC1 is resistant to and TORC2 is susceptible to inhibition by rapamycin. After treatment with rapamycin, the vast majority of Ypk1$^{5A}$-myc was unphosphorylated (Figure 3.4B), confirming by an independent means that TORC2 activity is required for phosphorylation of Ypk1 at the four new C-terminal sites. TORC2-mediated phosphorylation of Ypk1 at the hydrophobic motif is known to stimulate Ypk1 activity (Roelants et al., 2011). Although Ypk1$^{5A}$-myc itself is inactive (because it cannot be phosphorylated at its activation loop), I ruled out the possibility that its phosphorylation at the new sites was due to autophosphorylation *in trans* by endogenous Ypk1 or Ypk2. Ypk1$^{5A}$-myc showed no change in migration pattern when expressed in *ypk1*$^{as}$ *ypk2Δ* cells, regardless of whether or not they were treated with the Ypk1$^{as}$ inhibitor (3-MB-PP1) (Figure 3.4C). Additionally, TORC2 immunoprecipitated from yeast (Figure 3.4D) was able to phosphorylate purified Ypk1 *in vitro*, demonstrating that Ypk1 is a bona fide substrate of TORC2 (Figure 3.4E).

**FIGURE 3.4**

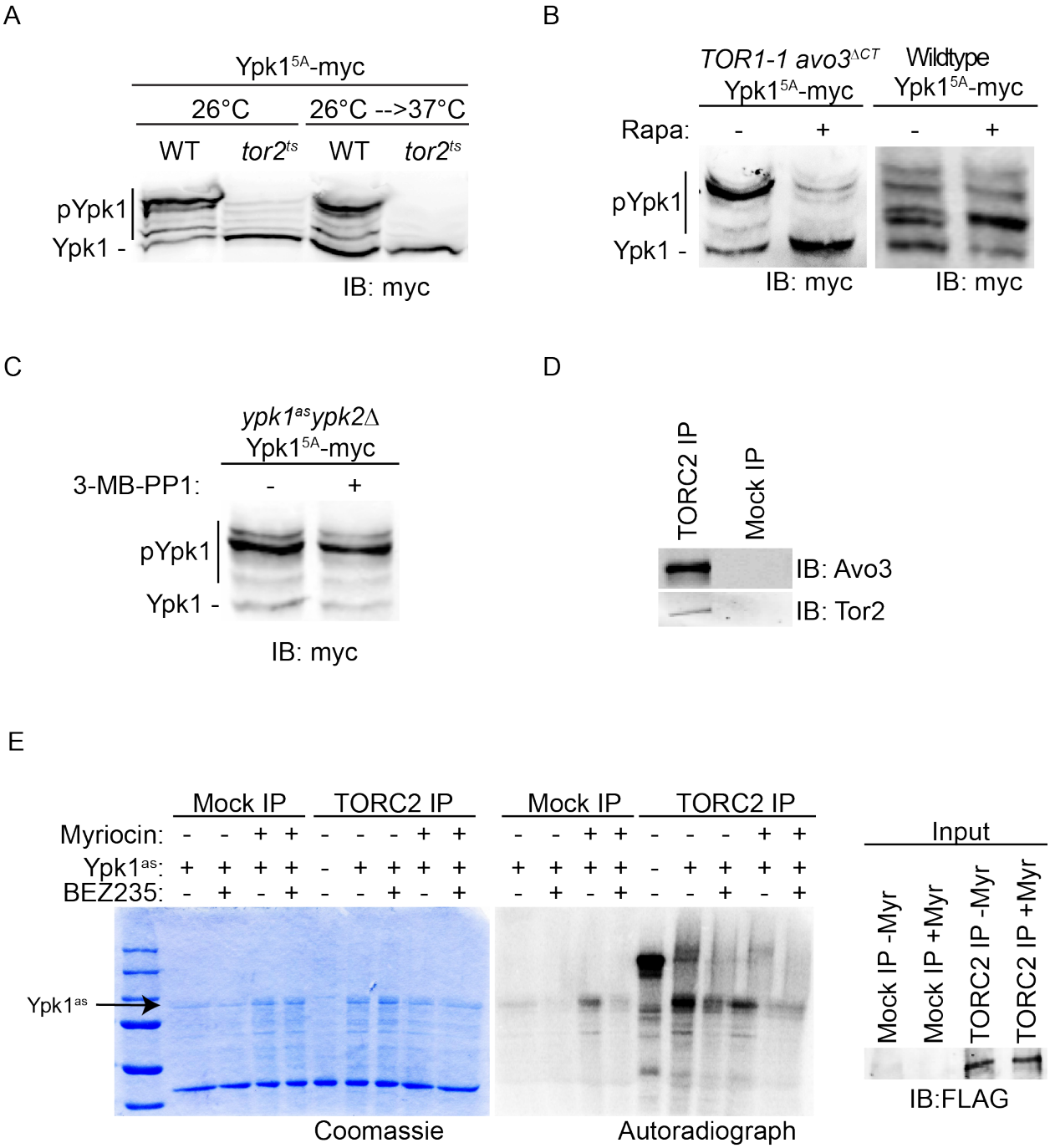
A
Ypk1^5A-myc
26°C
26°C -->37°C
WT
tor2ts
WT
tor2ts
pYpk1
Ypk1 -
IB: myc
B
TOR1-1 avo3ΔCT
Ypk1^5A-myc
Wildtype
Ypk1^5A-myc
Rapa:
-
+
-
+
pYpk1
Ypk1 -
IB: myc
IB: myc
C
ypk1asypk2Δ
Ypk1^5A-myc
3-MB-PP1:
-
+
pYpk1
Ypk1 -
IB: myc
D
TORC2 IP
Mock IP
IB: Avo3
IB: Tor2
E
Mock IP
TORC2 IP
Mock IP
TORC2 IP
Myriocin:
Ypk1as:
BEZ235:
Input
Mock IP -Myr
Mock IP +Myr
TORC2 IP -Myr
TORC2 IP +Myr
Ypk1as
IB:FLAG
Coomassie
Autoradiograph

**Figure 3.4. TORC2 phosphorylates Ypk1 at four C-terminal sites distinct from the turn and hydrophobic motifs**. (A) Wild-type (BY4741) or otherwise isogenic *tor2*$^{ts}$ (*tor2-29*) cells expressing Ypk1$^{5A}$-myc (pFR246) were grown at 26°C to exponential phase and then either kept at 26°C or shifted to 37°C for 2 h, harvested, lysed, and samples of the resulting extracts resolved by Phos-tag$^{TM}$ SDS-PAGE and analyzed by immunoblotting with anti-myc mAb 9E10. (B) *TOR1-1 avo3*$^{\Delta CT}$ or wild-type (BY4741) cells expressing Ypk1$^{5A}$-myc (pFR246) were grown to exponential phase and then treated with vehicle or 200 nM rapamycin for 20 min. Cells were then collected and analyzed as in (A). (C) Strain yAM135-A (*ypk1*$^{as}$ *ypk2Δ*) expressing Ypk1$^{5A}$-myc (pFR246) was grown to mid-exponential phase and then treated with either vehicle control (DMSO) or 10 μM 3-MB-PP1 for 1 h, harvested and then analyzed as in (A). (D) Wild-type "Mock IP" (yKL4) and Avo3-3C-3xFLAG "TORC2 IP" (yNM695) strains were grown in YPD to mid-exponential phase and then harvested. The cells were lysed and TORC2 was immunoprecipitated with anti-FLAG antibody coupled-agarose resin. Immunoprecipitated proteins were resolved by SDS-PAGE and analyzed by immunoblotting with anti-Avo3 and anti-Tor2 antibodies. (E) Wild-type "Mock IP" (yKL4) and Avo3-3C-3xFLAG "TORC2 IP" (yNM695) were grown to mid-exponential phase and treated with either vehicle (methanol) or 1.25 μM myriocin for 2 h prior to harvesting. Cells were lysed and TORC2 was immunoprecipitated with anti-FLAG antibody coupled-agarose resin and eluted from the resin by enzymatic cleavage with PreScission Protease. The IP eluates were incubated with purified analog-sensitive Ypk1$^{as}$ (pAX50) and [γ-$^{32}$P]ATP in the absence and presence of the TORC2 inhibitor BEZ235. Reaction products were resolved by SDS-PAGE and analyzed by Coomassie staining and, after drying the gel, by autoradiography.

**TORC2-dependent phosphorylation of Ypk1 at its C-terminus is necessary for full Ypk1 function**. The antibiotic myriocin (Myr), also known as ISP-1 (Miyake et al, 1995; Ikushiro et al., 2004; Yeung, 2011), inhibits eukaryotic cell growth because it is a transition state mimic that potently blocks L-serine:palmitoyl-CoA C-palmitoyltransferase (decarboxylating) [EC 2.3.1.50], the first enzyme unique to the sphingolipid biosynthetic pathway (Dunn et al., 2004; Dickson et al., 2006; Megyeri et al., 2016; Olson et al., 2016). Moreover, prior work has demonstrated that Ypk1-deficient cells are hyper-sensitive to the growth-inhibitory action of Myr (Momoi et al., 2004; Roelants et al., 2004). Subsequent studies revealed that TORC2-stimulated Ypk1-mediated phosphorylation of several substrates that control sphingolipid production is required for cell survival in response to sphingolipid limitation (Roelants et al., 2011; Berchtold et al., 2012; Muir et al., 2014). Hence, the degree of resistance or sensitivity to Myr provides a convenient phenotypic read-out for the efficacy of Ypk1 function *in vivo*.

Therefore, to assess whether TORC2-dependent phosphorylation of Ypk1 at its C-terminal sites modulates Ypk1 function, I tested the Myr sensitivity of various unphosphorylatable and phospho-mimetic alleles of Ypk1 in *ypk1Δ* cells. As expected, a Ypk1$^{T662A}$-myc mutant, which cannot be phosphorylated by TORC2 at the hydrophobic motif, displayed much greater sensitivity to Myr than cells expressing Ypk1$^{WT}$-myc (Figure 3.5A). Similarly, a mutant lacking the four newly identified C-terminal phosphorylation sites (Ypk1$^{AAAA}$-myc) exhibited increased Myr sensitivity, but at a somewhat higher concentration of this compound. In marked contrast, a mutant in which the same four residues were mutated to glutamate or aspartate (Ypk1$^{EDEE}$-myc), supported robust growth in the presence of Myr, indicating that mimicking phosphorylation at these four sites allows for full Ypk1 function. Individual unphosphorylatable site mutants displayed no noticeable Myr sensitivity at the concentrations tested (Figure 3.5B), suggesting that the effects of phosphorylation at these positions may be additive in stimulating Ypk1 action. I found that a Ypk1 turn motif mutant (Ypk1$^{S644A}$-myc) could not grow even at the lowest Myr concentrations tested, revealing that turn motif phosphorylation is critical for Ypk1 function,

It has been shown previously that the N-terminal mutation D242A bypasses the need for TORC2-mediated phosphorylation of Ypk1 (Roelants et al., 2011), suggesting that the N-terminal domain exerts some negative regulatory constraint on the C-terminal catalytic domain and, further, that the role of TORC2-mediated phosphorylation, like the D242A mutation, is to alleviate that inhibitory constraint. Consistent with that model, installing the D242A mutation in either Ypk1$^{T662A}$-myc or Ypk1$^{AAAA}$-myc fully restored their ability to support growth in the presence of Myr (Figure 3.5C).

Our laboratory has shown previously that Myr treatment stimulates Ypk1 phosphorylation of Orm1 and that mutating a critical TORC2 target site in Ypk1, such as Thr662, substantially reduces the ability of Ypk1 to phosphorylate Orm1 after Myr treatment (Roelants et al., 2011). Therefore, to assess the effect of C-terminal phosphorylation at the newly defined TORC2 sites on the ability of Ypk1 to phosphorylate a known substrate *in vivo*, we monitored Ypk1-dependent phosphorylation of Orm1 after Myr treatment. Cells expressing Ypk1$^{AAAA}$-myc showed a marked reduction in Orm1 phosphorylation in response to Myr treatment compared to cells expressing Ypk1$^{WT}$-myc, whereas cells expressing either Ypk1$^{D242A\ +\ AAAA}$ or Ypk1$^{EDEE}$-myc exhibited a level of Orm1 phosphorylation equivalent to that of wild-type Ypk1-myc or Ypk1$^{D242A}$-myc cells (Figure 3.5D). Collectively, these observations indicate that lack of TORC2 phosphorylation of Ypk1 at the four newly discovered sites significantly compromises Ypk1 function.

**FIGURE 3.5**

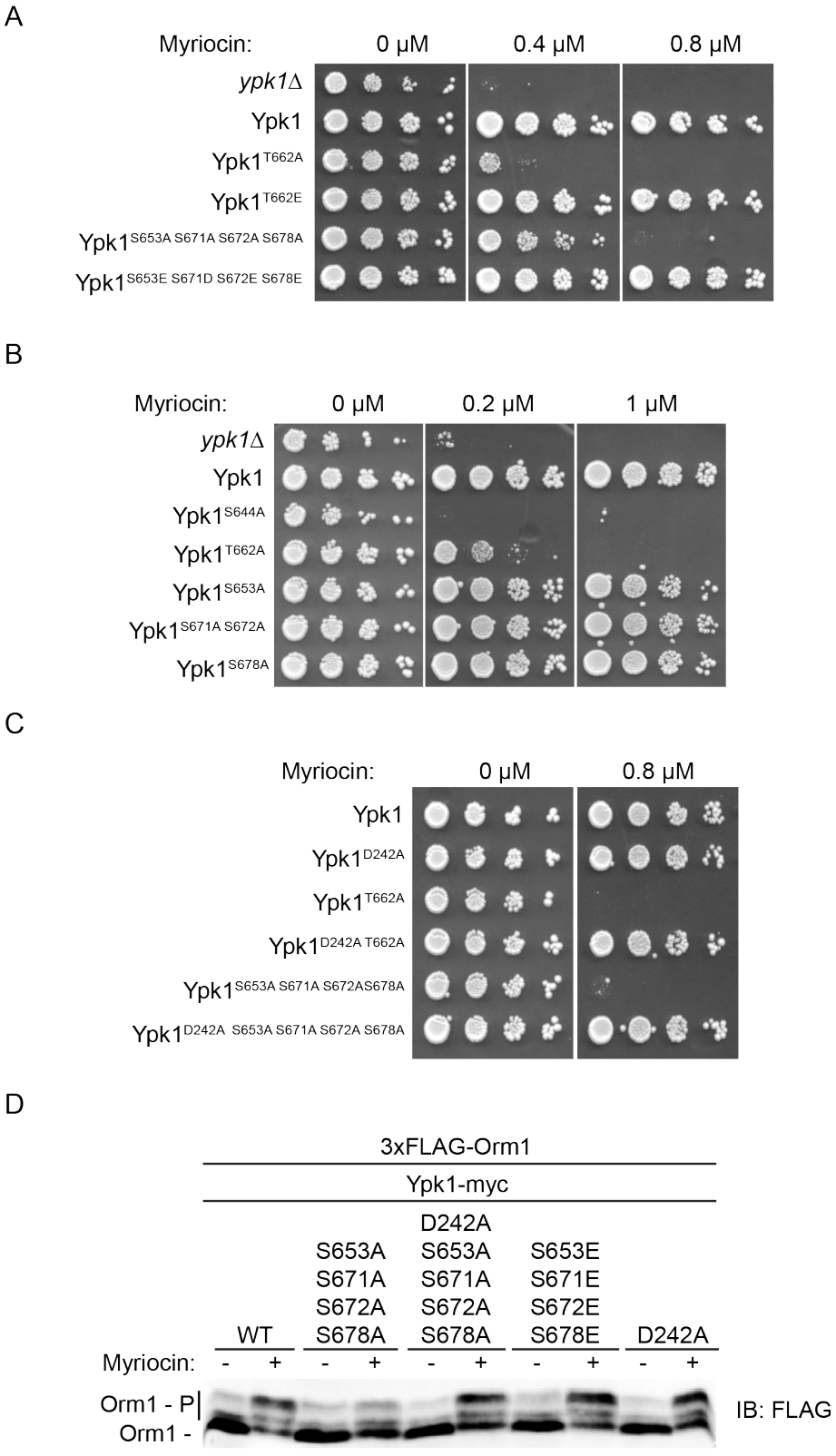
A
Myriocin:
0 μM
0.4 μM
0.8 μM
ypk1Δ
Ypk1
Ypk1T662A
Ypk1T662E
Ypk1S653A S671A S672A S678A
Ypk1S653E S671D S672E S678E
B
Myriocin:
0 μM
0.2 μM
1 μM
ypk1Δ
Ypk1
Ypk1S644A
Ypk1T662A
Ypk1S653A
Ypk1S671A S672A
Ypk1S678A
C
Myriocin:
0 μM
0.8 μM
Ypk1
Ypk1D242A
Ypk1T662A
Ypk1D242A T662A
Ypk1S653A S671A S672AS678A
Ypk1D242A S653A S671A S672A S678A
D
3xFLAG-Orm1
Ypk1-myc
WT
S653A S671A S672A S678A
D242A S653A S671A S672A S678A
S653E S671E S672E S678E
D242A
Myriocin:
- + - + - + - + - +
Orm1 - P
Orm1 -
IB: FLAG

**Figure 3.5**. **TORC2-dependent phosphorylation of Ypk1 at the C-terminus is required for full Ypk1 function**. (A) Cultures of *ypk1Δ* cells containing either empty vector (pRS315) or the same plasmid expressing Ypk1$^{WT}$-myc (pAM20), Ypk1$^{T662A}$-myc (pFR221), Ypk1$^{T662E}$-myc (pFR284), Ypk1$^{S653A\ S671A\ S672A\ S678A}$-myc (pJEN3) or Ypk1$^{S653E\ S671D\ S672E\ S678E}$-myc (pJEN6) were adjusted such that $A_{600\ nm}$ = 1.0 and then spotted in 10-fold serial dilutions onto SCD-Leu plates containing the indicated concentrations of Myr and incubated at 30°C for 3 days. (B) Serial dilutions of *ypk1Δ* cells containing either empty vector (pRS315) or the same plasmid expressing Ypk1$^{WT}$-myc (pAM20), Ypk1$^{S644A}$-myc (pFR220), Ypk1$^{T662A}$-myc (pFR221), Ypk1$^{S653A}$-myc (pFR253), Ypk1$^{S671A\ S672A}$-myc (pFR268) or Ypk1$^{S678A}$-myc (pJEN8) were analyzed as in (A). (C) Cultures of *ypk1Δ* cells containing either empty vector (pRS315) or the same plasmid expressing Ypk1$^{WT}$-myc (pAM20), Ypk1$^{D242A}$–myc (pFR234), Ypk1$^{T662A}$-myc (pFR221), Ypk1$^{D242A,\ T662A}$-myc (pKL7), Ypk1$^{S653A\ S671A\ S672A\ S678A}$-myc (pJEN3) or Ypk1$^{D242A\ 653A\ S671A\ S672A\ S678A}$-myc (pJEN4) were analyzed as in (A). (D) Strain yDB344 (3xFLAG-*ORM1 ypk1Δ*) expressing either Ypk1$^{WT}$-myc (pAM20), Ypk1$^{S653A,\ S671A,\ S672A,\ S678A}$-myc (pJEN3), Ypk1$^{D242A\ S653A\ S671A\ S672A\ S678A}$-myc (pJEN4), Ypk1$^{S653E\ S671D\ S672E\ S672E}$-myc (pJEN6) or Ypk1$^{D242A}$-myc (pFR234) were grown to exponential phase in selective medium, treated with either vehicle (methanol) or 1.25 μM myriocin for 2 h. After harvesting, whole-cell extracts were prepared, resolved by SDS-PAGE as described in Chapter 2 and analyzed by immunoblotting with anti-FLAG M2 antibody.

**Ypk1 C-terminal phosphorylation is necessary for efficient hydrophobic motif phosphorylation**. In addition to effects on activity, phosphorylation of a protein can alter its function in other ways, such as by changing its stability or localization. Thus, I asked next whether phosphorylation of Ypk1 at the four new C-terminal sites affected its stability. To do so, I examined the steady-state levels of various Ypk1 unphosphorylatable and phospho-mimetic mutants by immunoblotting (Figure 3.6A). When extracts from untreated cells were examined by standard SDS-PAGE, Ypk1-myc migrated as a doublet; the slower mobility species represents Ypk1 isoforms phosphorylated by Fpk1 (and Fpk2) (Roelants et al., 2010). Fpk1 and Fpk2 are themselves phosphorylated and inhibited by Ypk1 (Roelants et al., 2010). Thus, when cells are treated with Myr, and Ypk1 activity is stimulated, Ypk1-dependent phosphorylation of Fpk1/Fpk2 increases, resulting in reduced Fpk-mediated phosphorylation of Ypk1. Hence, in cells pre-treated with Myr, Ypk1-myc ran predominantly as the faster mobility species, whereas Ypk1$^{T662A}$-myc which prevents robust TORC2 activation of Ypk1 did not undergo this shift, but the phospho-mimetic allele Ypk1$^{T662E}$-myc did (Figure 3.6A). Moreover, as reported by others (Tanoue et al., 2005), mutation of the hydrophobic motif phosphorylation site (Thr662) did not compromise the stability of Ypk1. Strikingly, however, I found that the level of Ypk1$^{AAAA}$-myc was significantly lower than that of Ypk1$^{WT}$-myc, Ypk1$^{T662A}$-myc, or Ypk1$^{T662E}$-myc and its pattern did not change upon Myr treatment, suggesting that TORC2-dependent phosphorylation at the four new C-terminal sites is important for Ypk1 stability. Consistent with this hypothesis, under the same conditions, the level of the phospho-mimetic mutant Ypk1$^{EDEE}$-myc was even higher than that of Ypk1$^{WT}$-myc. These results indicate that the effect on Ypk1 stability is specific to the four new C-terminal sites. Although these results suggest that phosphorylation at the four new C-terminal sites is important for both Ypk1 function and stability, it is possible that these properties of Ypk1$^{AAAA}$-myc arise simply from a low level of expression because my preliminary kinetic analysis indicates that Ypk1$^{AAAA}$-myc and Ypk1$^{WT}$-myc are turned over at similar rates (data not shown). Nonetheless, additional observations demonstrate that the deficiencies observed in the function of Ypk1$^{AAAA}$-myc cannot be accounted for merely by its low level of expression. For example, installation of the D242A mutation which fully restores function to Ypk1$^{AAAA}$-myc, as judged by Myr sensitivity and Orm1 phosphorylation, does not do so by increasing the level of the protein at all (Figure 3.6B). In fact, the D242A mutation seemed to destabilize Ypk1$^{WT}$-myc and especially Ypk1$^{T662}$-myc (Figure 3.6B). Hence, the phenotypes associated with the Ypk1$^{AAAA}$-myc mutant must be due, at least in large part, to impairment of its activity.

My observation that the Ypk1$^{D242A\ AAAA}$-myc protein is present at much lower levels compared to Ypk1$^{WT}$-myc, but exhibits no deleterious phenotypes, suggested that phosphorylation at the four new C-terminal sites may be important for priming Ypk1 for full activation via phosphorylation at other important sites. Indeed, as has been shown previously, for Ypk1 to be fully active, it must be phosphorylated at Thr504 in its activation loop by Pkh1 (and Pkh2) (Casamayor et al., 1999; Roelants et al., 2002; Roelants at el., 2004) and, as I have recapitulated here, it must also be phosphorylated at Ser644 in its turn motif and at Thr662 in its hydrophobic motif by TORC2, a modification stimulated when cells are treated with Myr (Roelants et al., 2002; Roelants et al., 2011; Berchtold et al., 2012). To examine which of these sets of phosphorylations might be compromised when Ypk1 cannot be phosphorylated at the four new sites, I took advantage of phospho-site-directed antibodies that allow me to detect specifically the Pkh1 site (P-Thr504) and an important TORC2 site (P-Thr662). Our laboratory has

demonstrated before that a commercial phospho-site antibodies directed against the highly homologous PDK1 sites in human SGK1 robustly and specifically detects P-Thr504 in Ypk1 (Roelants et al., 2010). Prof. Ted Powers (UC Davis) has developed and generously provided to me phospho-site antibodies that specifically detect P-Thr662 in Ypk1 (Niles et al., 2012). Using these reagents, I found that, compared to $Ypk1^{WT}$-3HA, phosphorylation of Thr662 is abolished in $Ypk1^{AAAA}$-3HA, down to the background level observed for a $Ypk1^{T662A}$-3HA mutant that totally lacks the site (Figure 3.6C), whereas the level of phosphorylation of Thr504 in $Ypk1^{S644A\ T662A}$-3HA, which lacks two critical TORC2 sites was quite comparable to that in $Ypk1^{WT}$-3HA and, thus, unaffected (Figure 3.6D). These results show, first, that modifications at Thr504 and Thr662 occur independently of each other. Second, and by contrast, my findings indicate that multiple phosphorylations at the C-terminus (namely at Ser653, Ser671, Ser672 and Ser678) are a prelude to and prerequisite for efficient TORC2 modification of Thr662 (and, presumably, Ser644).

**FIGURE 3.6**

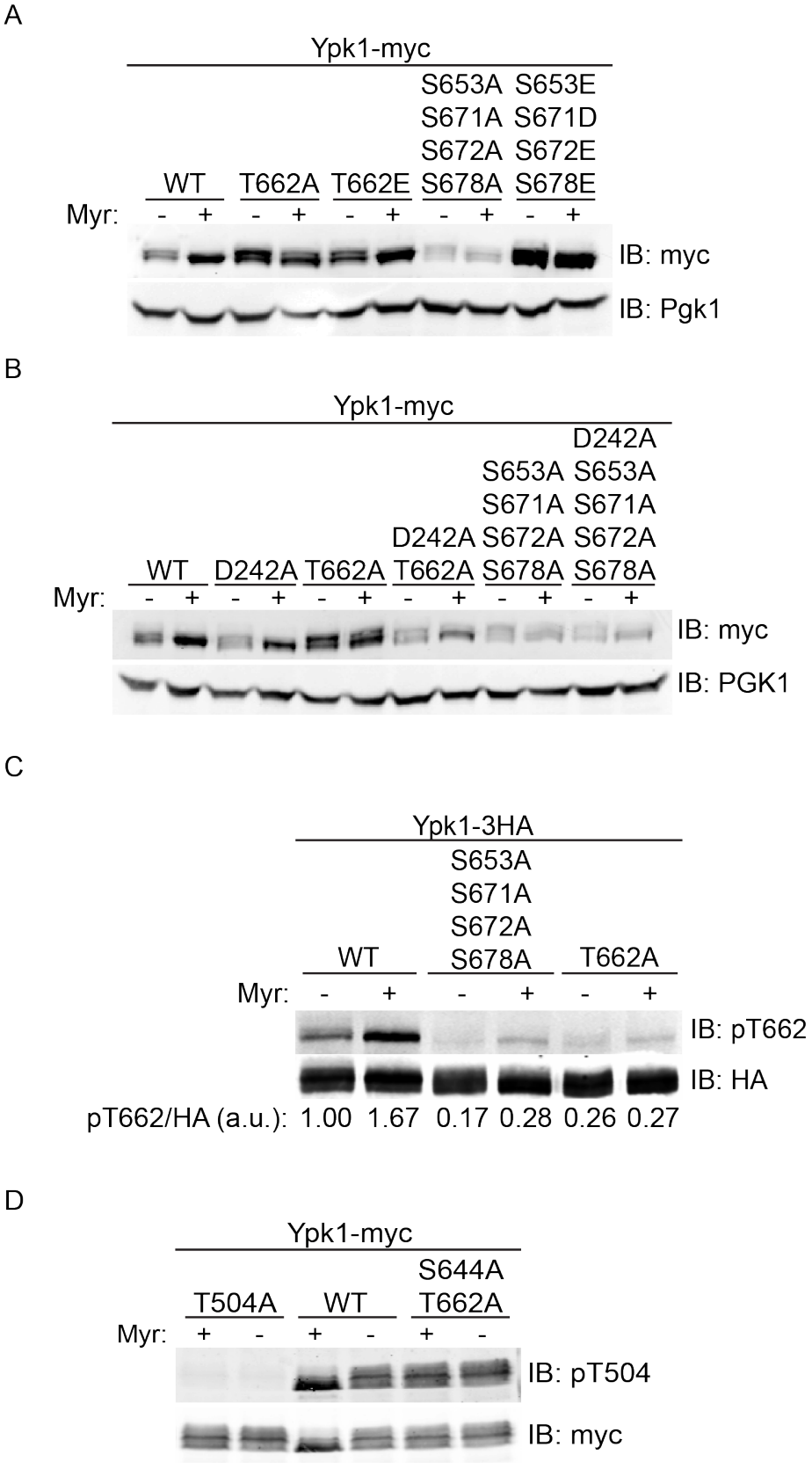
A
Ypk1-myc
S653A S653E
S671A S671D
S672A S672E
WT T662A T662E S678A S678E
Myr: - + - + - + - + - +
IB: myc
IB: Pgk1
B
Ypk1-myc
D242A
S653A S653A
S671A S671A
D242A S672A S672A
WT D242A T662A T662A S678A S678A
Myr: - + - + - + - + - + - +
IB: myc
IB: PGK1
C
Ypk1-3HA
S653A
S671A
S672A
WT S678A T662A
Myr: - + - + - +
IB: pT662
IB: HA
pT662/HA (a.u.): 1.00 1.67 0.17 0.28 0.26 0.27
D
Ypk1-myc
S644A
T504A WT T662A
Myr: + - + - + -
IB: pT504
IB: myc

**Figure 3.6**. **Phosphorylation of Ypk1 at the C-terminus is necessary for efficient Ypk1 activation**. (A) Cultures of *ypk1Δ* cells containing empty vector (pRS315) or the same plasmid expressing Ypk1$^{WT}$-myc (pAM20), Ypk1$^{T662A}$-myc (pFR221), Ypk1$^{T662E}$-myc (pFR284), Ypk1$^{S653A\ S671A\ S672A\ S678A}$-myc (pJEN3) or Ypk1$^{S653E\ S671D\ S672E\ S678E}$-myc (pJEN6) were grown to exponential phase and then treated with vehicle (methanol) or 1.25 μM myriocin for 2 h. After harvesting, whole-cell lysates were prepared, resolved by SDS-PAGE and analyzed by immunoblotting with anti-myc mAb 9E10. (B) Cultures of *ypk1Δ* cells containing empty vector (pRS315) or the same plasmid expressing Ypk1$^{WT}$-myc (pAM20), Ypk1$^{D242A}$–myc (pFR234), Ypk1$^{T662A}$-myc (pFR221), Ypk1$^{D242A\ T662A}$-myc (pKL7), Ypk1$^{S653A\ S671A\ S672A\ S678A}$-myc (pJEN3) or Ypk1$^{D242A\ S653A\ S671A\ S672A\ S678A}$-myc (pJEN4) were treated and analyzed as in (A). (C) Cultures of *ypk1Δ* cells containing plasmids expressing Ypk1-3HA (pPL215), Ypk1$^{S653A\ S671A\ S672A\ S678A}$-3HA (pJEN5), or Ypk1$^{T662A}$-3HA (pKL32) were grown to exponential phase in SCD-Ura then treated with either vehicle (methanol) or 1.25 μM myriocin for 2 h. After harvesting, whole-cell extracts were prepared, resolved by SDS-PAGE and analyzed by immunoblotting with anti-HA and anti-phosphoT662 Ypk1 antibodies. (D) Strain BY4741 (*YPK1*$^{+}$) containing plasmids expressing from the *GAL* promoter Ypk1$^{T504A}$-myc (pFR111), Ypk1$^{WT}$-myc (pAM76) or Ypk1$^{S644A\ T662A}$-myc (pFR112), as described in Chapter 2, were treated with vehicle (methanol) or 1.25 μM myriocin for 2 h. After harvesting, whole-cell extracts were prepared, resolved by SDS-PAGE and analyzed by immunoblotting with anti-myc mAb 9E10 and anti-phospho-Thr256 SGK1 antibodies.

## DISCUSSION

Reversible phosphorylation is an important method for regulating protein function. Like all eukaryotic protein kinases, AGC-family protein kinases share a common catalytic domain structure consisting of a small N-terminal lobe (N-lobe) and larger C-terminal lobe (C-lobe) with the active site sandwiched between the N-lobe and C-lobe (Pearce et al., 2010). In this protein kinase sub-family, phosphorylation at several conserved sites is necessary for full catalytic function. The first conserved site is in the activation loop, which is situated adjacent to the ATP-binding site in the kinase domain. The activation loop, when phosphorylated, makes vital contacts with the catalytic loop and the αC helix, and the cumulative conformational changes so induced are essential for opening up the active site cleft, for positioning the catalytic Asp in the proper location, and for enhancing contacts with ATP in its binding pocket, all of which are necessary for catalytic activity (Yang et al., 2002a; Komander et al., 2005). The second conserved phosphorylation site is in the hydrophobic motif which extends from the C-lobe and wraps around the N-lobe and fits into a hydrophobic groove partially composed of the αC helix. Hydrophobic motif phosphorylation stabilizes the αC helix in the active conformation (Yang et al., 2002a; Yang et al., 2002b). Some AGC-family protein kinases also have a third conserved site, known as the turn motif, which is located in the C-terminal tail upstream of the hydrophobic motif. When phosphorylated, the turn motif interacts with a positively charged patch in the N-lobe and helps the C-terminal tail wrap around the N-lobe (Grodsky et al., 2006; Hauge et al., 2007). Thus, phosphorylations at the activation loop, hydrophobic motif and turn motif all contribute to and are necessary for full activation of AGC-family protein kinases.

As a member of the AGC-family of protein kinases, Ypk1 is known to be regulated by phosphorylation at both its activation loop (Thr504) and the hydrophobic motif (Thr662). Pkh1/Pkh2 mediate activation loop phosphorylation which is required for basal Ypk1 activity. Ypk1 Thr504 phosphorylation increases in certain conditions, such as during heat stress (Omnus et al., 2016). Hydrophobic motif phosphorylation is mediated by TORC2 and is known to be stimulated by certain stresses, such as sphingolipid depletion (Berchtold et al., 2012; Roelants et al., 2011), hypotonic conditions (Berchtold et al., 2012), heat shock (Omnus et al., 2016) and acetic acid stress (Guerreiro et al., 2016). To my knowledge, Ypk1 mRNA level before and after these treatments has not been measured and it would be of significant interest and important to determine whether *YPK1* expression is under any stress-dependent transcriptional control. It is clear, however, that YPK2 is induced by heat shock (Gasch et al., 2000).

As I have confirmed here, the turn motif in Ypk1 (Roelants et al., 2004) is also essential for Ypk1 function. Moreover, I discovered that TORC2 also mediates phosphorylation at four other C-terminal sites in Ypk1, namely Ser653, Ser671, Ser672 and Ser678. Phosphorylation at these four sites is necessary for full Ypk1 function. Taken together, the most parsimonious interpretation of my data is that TORC2 phosphorylates its preferred sites at the C-terminus of Ypk1 sequentially, starting from the very carboxy terminus. Presumably, installation of each successive modification helps destabilize and peel back the C-terminal segment of the protein making the next site more accessible, eventually allowing TORC2 access to the hydrophobic motif and the turn motif. In this way, phosphorylation of the four new sites primes Ypk1 for phosphorylation at its hydrophobic motif, consistent with my findings that preventing phosphorylation of Ypk1 at the four C-terminal sites prevents hydrophobic motif phosphorylation. Our MS analysis indicated an increase in phosphorylation of Ypk1 at Ser653 following Myr treatment (data not shown); and, in agreement with our observation, a recent

phosphoproteomics study reported phosphorylation of Ypk1 at S653 and at Ser672 increases following Myr treatment (Lebesgue et al., 2017). Thus, it does appear that TORC2 responds to sphingolipid depletion by enhancing phosphorylation of Ypk1 at the four C-terminal sites which, in turn, allows for efficient hydrophobic motif phosphorylation.

Ser644 in the turn motif is also thought to be under the control of TORC2. Indeed, our MS study showed an increase in Ser644 phosphorylation after Myr treatment (data not shown). Additionally, I found that turn motif phosphorylation is critical for Ypk1 function; a Ypk1$^{S644A}$-myc mutant was inviable even at the lowest concentrations of Myr tested and was even more sensitive to Myr than a Ypk1$^{T662A}$-myc mutant. Turn motif phosphorylation has been reported to be important for proper carboxyl-terminal folding and protein stability for the mammalian AGC-family protein kinases Akt and PKC (Facchinetti et al., 2008; Ikenoue et al., 2008). Thus, turn motif phosphorylation is likely very important for Ypk1 stability. Unfortunately, I did not have a phospho-site specific antibody available that could reliable report this modification in Ypk1. Interestingly, in this regard, mutation of the four new C-terminal phosphorylation sites in Ypk1 to Ala resulted in a diminished steady-state level of Ypk1, suggesting that TORC2-mediated phosphorylation at the four C-terminal sites may be needed to allow for modification of Ser644 and its role in stabilizing Ypk1. Additional experiments are needed to determine how TORC2-mediated phosphorylation influences the stability of Ypk1. Nonetheless, full TORC2-dependent phosphorylation of Ypk1 is necessary for optimal Ypk1 function.

To date, there is no available crystal or NMR structure for Ypk1. There is a reported crystal structure for SGK1, the closest human ortholog of Ypk1; however, in this structure, the N-terminal 154 residues were deleted and six substitution mutations (S169A S173A R287A S492A S496A S517D) were introduced to "stabilize" the protein to obtain the resolution achieved (1.9 Å) (Zhao et al., 2007). Ypk1 contains a well-conserved C-terminal kinase domain as well as an upstream N-terminal domain. The exact function of the Ypk1 N-terminal domain is unknown, but likely serves a regulatory role as overexpressing an N-terminally truncated Ypk1ΔN mutant is toxic to cells, whereas overexpressing a kinase-dead Ypk1ΔN mutant is not (Roelants et al., 2002). Interestingly, the need for TORC2-dependent phosphorylation of Ypk1 can be eliminated by mutating Asp242 in the N-terminal domain to Ala (Roelants et al., 2011). Thus, the D242A bypass mutation rescues the need for phosphorylation of Ypk1 at the turn motif, hydrophobic motif and four C-terminal sites. How the single D242A point mutation bypasses the need for TORC2 phosphorylation to activate Ypk1 is not known. However, Ypk1$^{D242A}$ is not more phosphorylated by TORC2 (Figure 3.7). In fact, Ypk1$^{D242A}$ seems to be less phosphorylated by TORC2 than Ypk1$^{WT}$, presumably due to the higher basal activity of Ypk1$^{D242A}$ which feedbacks to negatively regulate TORC2. One possible explanation is that Asp242 in the N-terminal regulatory domain of Ypk1 interacts, perhaps by the formation of a salt bridge with a basic residue(s) in the kinase domain in such a way that the active site is occluded or kinase function is impeded due to some other conformational constraint. Mutating the negatively charged Asp242 to an uncharged residue may alleviate the constraint, thereby permitted greater conformational freedom, thus allowing the kinase to more frequently adopt its active state. Conversely, the role of TORC2-mediated phosphorylation may be to add negative charge to the Ypk1 C-terminus, which would break the same hypothetical salt bridge due to charge repulsion, consistent with the fact that unlike the Ala substitution mutations, conversion of the same four residues to Glu (and Asp), which should also cause charge repulsion with Asp242, did not deleteriously affect Ypk1 function. Additional experiments are needed to test this speculative explanation for the

**FIGURE 3.7**

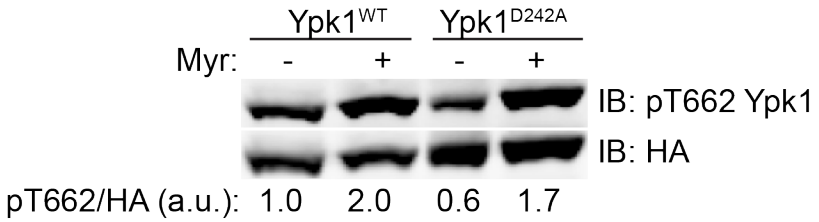


**Figure 3.7. Ypk1$^{D242A}$ is not hyper-phosphorylated by TORC2.** Cells (*ypk1Δ*) expressing Ypk1$^{WT}$-3HA (pBL215) or Ypk1$^{D242A}$-3HA (pKL27) were grown to exponential phase in SCD-Ura and then treated with either vehicle (methanol) or 1.25 μM myriocin for two h prior to harvesting. Whole-cell extracts were prepared, resolved by SDS-PAGE and analyzed by immunoblotting.

phenotype of the D242A mutation.

The identification of four, new conserved TORC2-dependent phosphorylation sites in Ypk1 has allowed for the prediction of a preferred phosphoacceptor site motif for yeast TORC2. Based on the sites now found in Ypk1 that have been demonstrated to be TORC2-dependent, it seems that the common feature is only a bulky hydrophobic residue +1 to the Ser/Thr phosphorylation site. It is worth noting in this same regard that several other phosphorylation sites identified in our MS experiments, namely Thr57, Ser64 and Ser343 also have a bulky hydrophobic residue at +1 and Thr57 phosphorylation was elevated after Myr treatment. Although phosphorylation at these sites could not be followed by mobility shift on Phos-tag gels, I have not ruled out the possibility that these phosphorylation sites may also be under TORC2 control and/or direct targets of TORC2.

Several global phosphoproteomic studies (Holt et al., 2009; Swaney et al., 2013) have identified phosphorylation at the residues in Ypk2 that correspond to Ser653 and Ser672 in Ypk1, suggesting that Ypk2 might also be regulated by TORC2 in a similar manner to Ypk1. However, in Ypk2, the residue corresponding to Ypk1 Ser671 is a negatively charged Asp, which cannot be subject to reversible phosphorylation. Additionally, Ser671 is not conserved in more distant Ypk1 orthologs, whereas Ser672 (and sites corresponding to Ser653 and Ser678 in Ypk1) is. Thus, although both Ser671 and Ser672 are phosphorylated in Ypk1 in a TORC2-dependent manner, Ser672 is likely the primary and important site. Interestingly, the residue in Ypk2 that corresponds to Ser672 in Ypk1 is followed by proline suggesting that TORC2 might also recognize phosphorylation sites with Pro at the +1 position. The AGC-family protein kinase and TORC1 substrate Sch9 has been reported to also be phosphorylated at multiple C-terminal sites in addition to the turn and hydrophobic motifs by TORC1 (Urban et al., 2007). As with the newly characterized C-terminal phosphorylation sites in Ypk1, the TORC1 phosphorylation sites in Sch9 indicate a preference for bulky, hydrophobic and aromatic amino acids in the -4 and +1 positions (Urban et al., 2007), which may explain why either Tor1 or Tor2 can both function in TORC1. Mammalian TOR (mTOR) has also been reported to prefer proline, hydrophobic and aromatic residues in the +1 position (Hsu et al., 2011). Thus, the phosphoacceptor site specificity of TOR seems to have been well conserved.

I have shown that TORC2-mediated phosphorylation of Ypk1 at the four C-terminal sites distinct from the turn and hydrophobic motifs is necessary for full Ypk1 activation. Our laboratory has reported that phosphorylation of Ypk1 at the C-terminal sites is dramatically reduced when TORC2 activity is down-regulated by hyperosmotic shock (Muir et al., 2015). In a similar manner, TORC1-mediated phosphorylation of Sch9 at C-terminal sites other than the turn and hydrophobic motifs also changes in response to stresses that are known to modulate TORC1 activity, such as carbon and nitrogen starvation (Urban et al., 2007). In mammalian cells, the AGC-family protein kinase Akt is phosphorylated in an mTORC2-dependent manner at C-terminal sites in addition to the turn and hydrophobic motifs (Liu et al., 2014). Consistent with what I have observed for Ypk1, phosphorylation of Akt at the C-terminus is necessary for efficient hydrophobic motif phosphorylation (Liu et al., 2014). In conclusion, extensive C-terminal phosphorylation is a conserved mechanism by which TOR complexes activate AGC-family protein kinases.

**ACKNOWLEDGEMENTS**

The mass spectrometry analysis of Ypk1-derived phosphopeptides was conducted in collaboration with David Breslow (University of California, San Francisco; now Assistant Professor, Yale University) and Bernd Bodenmiller (Stanford University; now Assistant Professor, University of Zürich, Switzerland). We thank Professor Ted Powers (University of California, Davis) for the generous gift of anti-phospho-T662 Ypk1 antibodies and certain plasmids.

## Chapter 4. New insights about TORC2 regulation by hyperosmotic stress: Sln1-Hog1 osmotic stress sensing pathway regulates TORC2-Ypk1 signaling

### INTRODUCTION

Cells continuously sense and respond to changes in their external environment in order to maintain homeostasis. The ability to adapt to changes in external osmolarity is important for maintaining proper intracellular water activity for biochemical reactions to occur. The budding yeast *Saccharomyces cerevisiae* preferentially maintains an intracellular osmolarity that is higher than its extracellular environment (Hohmann, 2015). Therefore, water tends to flow into the cell (Harold, 2002). A strong, but elastic, cell wall limits cell swelling and also protects the cell from mechanical stress (Levin, 2011; Orlean, 2012). The osmotic force driving water into the cell is balanced by the intracellular turgor pressure exerted against the PM and cell wall (Harold, 2002; Kock et al., 2015). Turgor pressure provides necessary force for cell expansion and, during periods of cell growth, the cell wall is remodeled to both accommodate and direct cell expansion (Klis et al., 2006; Free, 2013).

In *S. cerevisiae,* two mitogen-activated protein kinase (MAPK) pathways sense and respond to changes in extracellular osmotic conditions and other stresses that compromise intracellular turgor pressure, the PM and the cell wall. Each MAPK pathway contains a core protein kinase cascade consisting of a MAPK kinase kinase (MAPKKK), a MAPK kinase (MAPKK) and a MAPK that is activated in response to specific environmental cues (Chen and Thorner, 2007). Under hypertonic conditions, the high osmolarity glycerol (HOG) pathway and its eponymous MAPK Hog1 are required for cell survival (Saito and Posas, 2012; Brewster and Gustin, 2014). Under hypotonic conditions, the cell wall integrity (CWI) pathway and its MAPK Slt2 (also known as Mpk1) are required for cell viability (Jendretzki et al., 2011; Levin, 2011). However, the CWI pathway is also activated by cell wall damaging agents (Rodríguez-Peña et al., 2013), heat shock (Kamada et al., 1995) and other stresses that threaten the structure and function of the yeast cell envelope (Fuchs and Mylonakis, 2009). Moreover, the CWI pathway is activated at specific points in the cell cycle to facilitate the polarized growth needed for bud formation (Levin, 2011). The CWI pathway consists of cell surface receptors that, when activated, mediate the PM recruitment and activation of the GEF Rom2 (Ozaki et al., 1996). Activated Rom2 stimulates GTP-loading of the small GTPase Rho1. GTP-bound Rho1 then binds to and activates Pkc1 (Kamada et al., 1996), which subsequently serves as a MAPKKK kinase and activates the CWI MAPK cascade (Figure 4.1). The CWI MAPK Slt2 promotes cell wall maintenance by transcriptionally up-regulating genes involved in cell wall synthesis and remodeling (Jung et al., 2002; Levin, 2011).

Hyperosmotic stress can activate the MAPKK of the HOG pathway, Pbs2, by either of two distinct osmostress sensing systems (Maeda et al., 1995; Westfall et al., 2004): the Sln1 branch or the Sho1 branch (Figure 4.2). The Sln1 branch comprises a two-component phosphorelay, the Sln1-Ypd1-Ssk1 complex (Saito and Posas, 2012). Sln1 is an integral PM protein and senses cell turgor pressure via its extracellular domain (Ostrander and Gorman, 1999; Tamás et al., 2000; Schaber et al., 2010). Under normal osmotic conditions, Sln1 is active and autophosphorylates at a histidine residue (His576) in its histidine kinase domain (Maeda et al., 1994; Fassler and West, 2010). This phosphoryl group is transferred to an aspartate residue (Asp1144) in the Sln1 receiver domain, and then to a histidine residue (His64) in the phospho-transfer protein Ypd1. Phospho-Ypd1, in turn, transfers its phosphate to an aspartate residue (Asp554) in the receiver

domain of the regulatory protein Ssk1 (Posas et al., 1996). In its phosphorylated state, Ssk1 is unable to stimulate the paralogous MAPKKKs Ssk2 and Ssk22. Hence, under low to normal osmotic conditions, where Sln1 is active, phosphorylated Ssk1 prevents Pbs2 activation. Upon hyperosmotic shock, Sln1 becomes inactivated and consequently Ssk1 accumulates in its unphosphorylated form, which then binds to and activates Ssk2 and Ssk22, which then phosphorylate and activate Pbs2 (Posas and Saito, 1998). The mechanism by which the Sho1 branch of the HOG pathway (Saito and Posas, 2012) is activated is less clear, but involves the interactions of two, highly O-glycosylated, mucin-like integral PM proteins (Msb2 and Hkr1), the tetraspanin Sho1, and another integral membrane protein Opy2, which collectively constitute an osmosensor complex (Figure 4.2). Upon exposure of cells to strongly hyperosmotic conditions, the osmosensing complex of the Sho1 branch stimulates GTP loading of the small GTPase Cdc42, likely via localized recruitment of its GEF (Cdc24) to Msb2 (Bender and Pringle, 1992; Cullen et al., 2004). GTP-bound Cdc42, in turn, stimulates the PM-associated p21-activated protein kinases Cla4 and Ste20 (Lamson et al., 2002; Tatebayashi et al., 2006). The substrate of Ste20 is the MAPKKK Ste11 (Drogen et al., 2000; Raitt et al., 2000b). Ste11 is positioned at the PM for several reasons; first, its tightly bound non-catalytic subunit Ste50 (Posas et al., 1998; Wu et al., 1999) has a Cdc42-binding domain (Tatebayashi et al., 2006; Truckses et al., 2006) and also interacts with Opy2 (Ekiel et al., 2009; Yamamoto et al., 2010). Second, while Pbs2 is the MAPKK of the Hog1 pathway, it also serves as a scaffold that binds Ste11 (Posas and Saito, 1997) and is also anchored by a Pro-rich region to an SH3 domain at the C-terminus of Sho1 (Maeda et al., 1995). Therefore, once phosphorylated and activated, Ste11 is then able, in turn, to efficiently phosphorylate and activate Pbs2 (Maeda et al., 1995; Tatebayashi et al., 2006). Pbs2 then dually phosphorylates and activates Hog1 in the same manner that Sln1 branch activation does. Thus, the Sho1 and the Sln1 branches converge on activation of Pbs2 and, subsequently, Hog1.

Active Hog1 phosphorylates a number of targets, both in the cytosol and in the nucleus, to promote cell survival during hyperosmotic conditions (Saito and Posas, 2012). Hog1 stimulates the production and retention of the osmolyte glycerol, which is critical for minimizing water loss and restoring turgor pressure (Yancey et al., 1982; Albertyn et al., 1994). Hog1 also reportedly phosphorylates targets that retard cell-cycle progression (Clotet et al., 2006; Yaakov et al., 2009) and also modulates gene expression (de Nadal and Posas, 2015). Although active Hog1 translocates into the nucleus, our laboratory has shown that nuclear localization is dispensable for cell survival as tethering Hog1 to the PM by a membrane-targeting CaaX domain (or by fusion to the GPCR Ste2) has no deleterious effect on cell growth in the presence of 1 M sorbitol (Westfall et al., 2008). Consistent with that observation, quantitative studies of the HOG response have shown that 80% of the increase in glycerol flux can be explained by changes in cell metabolism whereas induction of gene expression only contributes 20% (Bouwman et al., 2011). When osmotic balance is restored, Hog1 is dephosphorylated, primarily by nuclear tyrosine phosphatases Ptp2 and Ptp3 (Jacoby et al., 1997) and PM-localized Ser/Thr phosphatases Ptc1 and Ptc2 (Warmka J et al, 2001; Young et al., 2002), back to near basal levels and Sln1 histidine kinase activity returns.

Other studies from our laboratory have shown that down-regulation of TORC2-Ypk1 signaling also plays a critical role in the cellular response to hyperosmotic stress (Lee et al., 2012; Muir et al., 2015). TORC2 localizes to the PM and ensures that PM homeostasis is maintained in response to certain stresses by directly phosphorylating and thereby stimulating Ypk1 and its

paralog Ypk2, which are AGC-family protein kinases. As described in the preceding section (Chapter 3) of this thesis, TORC2 phosphorylates Ypk1 at its conserved turn (Ser644) and hydrophobic (Thr662) motifs as well as at four additional C-terminal sites, which are all necessary for full Ypk1 activity. Ypk1, in turn, directly phosphorylates and regulates the function of its substrates. Two documented Ypk1 targets are directly involved in the synthesis and accumulation of glycerol: (i) cytosolic glycerol-3-phosphate dehydrogenase (Gpd1) (Lee et al., 2012), which catalyzes the conversion of dihydroxyacetone-phosphate to glycerol-3-phosphate (which then can be rapidly dephosphorylated to produce glycerol); and, (ii) PM-localized aquaglyceroporin Fps1 (Muir et al., 2015). In normal osmotic conditions, active Ypk1 inhibits Gpd1 and keeps the Fps1 glycerol channel open. However, upon hyperosmotic shock, TORC2-Ypk1 signaling is rapidly down-regulated, resulting in relief of Gpd1 inhibition and closure of the Fps1 channel, thereby promoting both glycerol production and retention.

The upstream signals that modulate TORC2 in response to hyperosmotic stress are not well understood. Although prior work from this laboratory has shown that *short-term* down-regulation of TORC2-Ypk1 signaling immediately after exposure to hyperosmotic stress does not require Hog1 (Muir et al., 2015), I have discovered that activation of Hog1 via the Sln1 branch of the HOG MAPK pathway exerts negative regulation on TORC2-Ypk1 signaling that is more sustained. I show further, in agreement with evidence that the HOG and CWI pathways can act coordinately in the regulation of other stress responses (Rodríguez-Peña et al., 2010), that the down-regulation of TORC2 depends on both the Hog1 and Slt2 MAPKs. My results provide unique insights about how known stress-sensing pathways cooperate to modulate TORC2 function. These findings are novel because control of TORC2 function by MAPK action has not previously been reported.

**FIGURE 4.1**

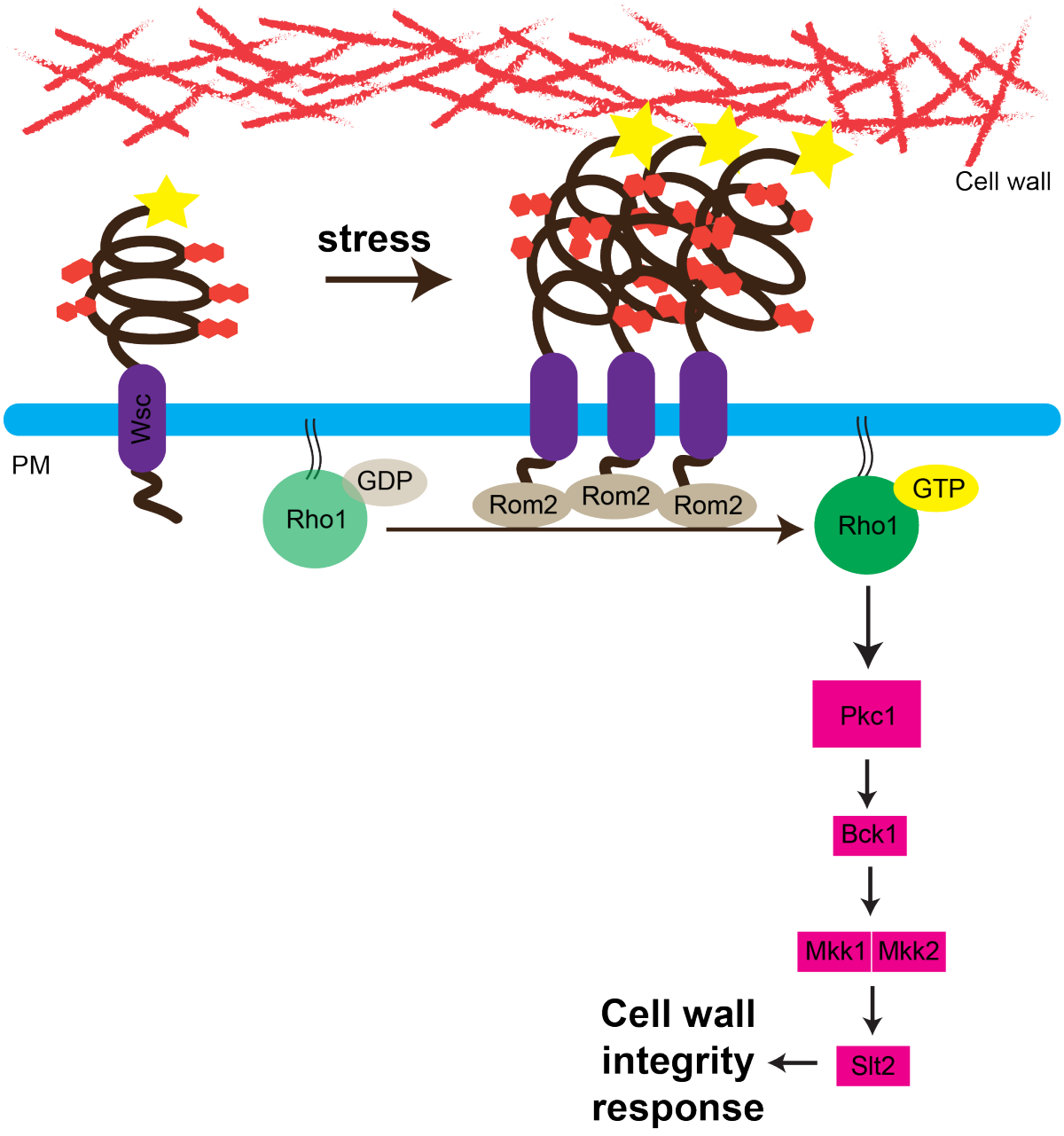


**Figure 4.1**. **Schematic depiction of the cell wall integrity pathway**. Cell wall stress is sensed by a battery of cell surface receptors (Slg1/Wsc1; the related protein Wsc2 and its paralog Wcs3; Mid2 and its paralog Mtl1), which all signal to the small GTPase Rho1 via the Rho1 GEF Rom2. GTP-bound Rho1 activates Pkc1, which then initiates signaling through the cell wall integrity (CWI) MAPK cascade.

**FIGURE 4.2**

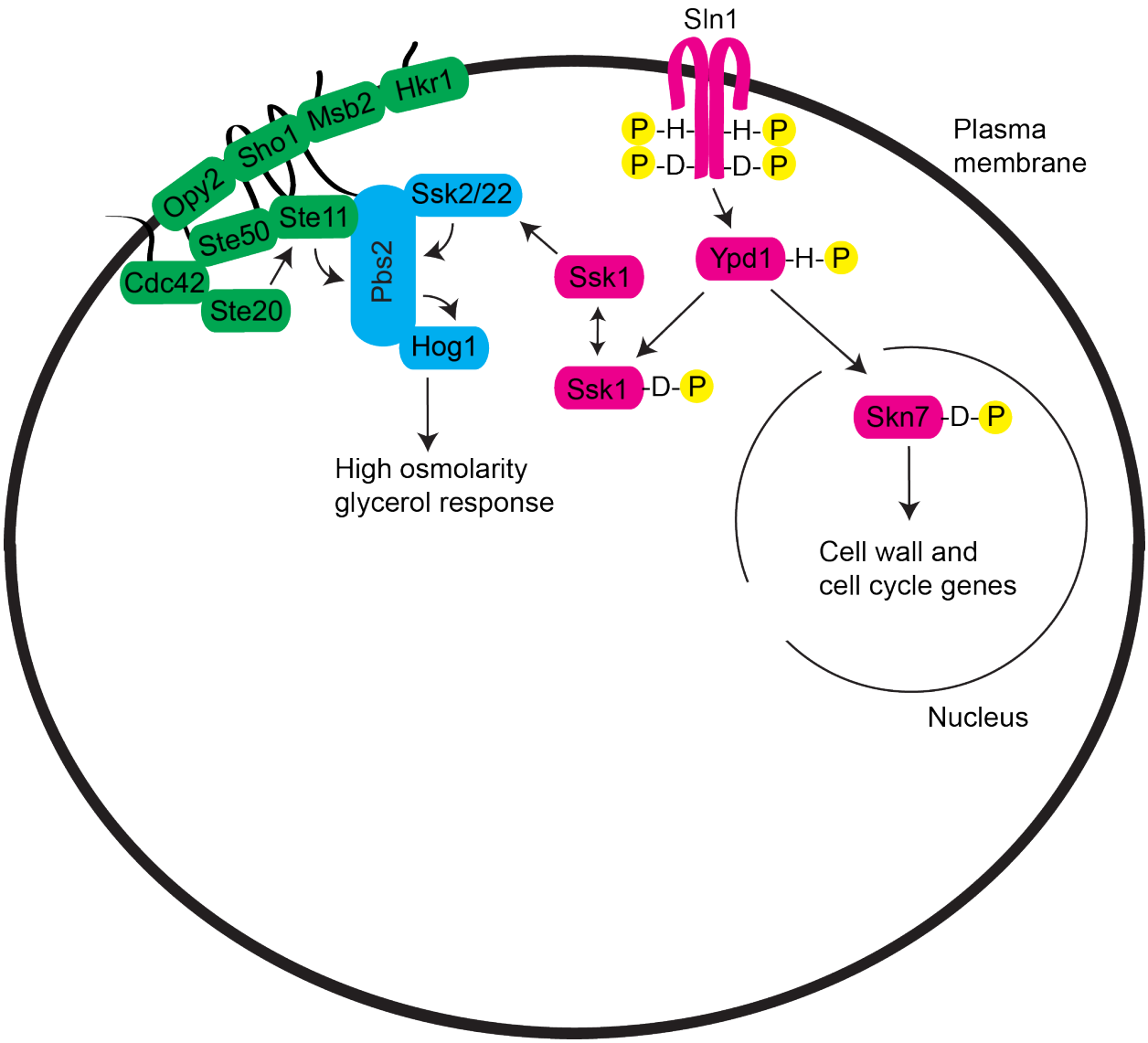


**Figure 4.2. Schematic depiction of the high osmolarity glycerol pathway.** The high osmolarity glycerol (HOG) MAPK cascade (shown in blue) can be activated by two, independent upstream branches: the Sln1 branch (shown in pink) and the Sho1 branch (shown in green). Both branches converge on activation of the HOG MAPKK Pbs2.

## RESULTS

**The Sln1 branch of the HOG pathway negatively regulates TORC2-Ypk1 signaling.** Our laboratory has previously shown that TORC2 is an upstream activator of Ypk1. As described in Chapter 3, TORC2 stimulates Ypk1 activity by phosphorylating Ypk1 at its turn (Ser644) and hydrophobic (Thr662) motifs and at four additional C-terminal sites (Ser653, Ser671, Ser672 and Ser678). The screen used to identify the kinase responsible for those modifications, pinpointed Tor2, the catalytic subunit of TORC2, but also uncovered one other candidate, namely the His-Asp phosphorelay enzyme Sln1. Shifting a temperature-sensitive Sln1 allele to the restrictive temperature for 2 h to inactivate its function (Figure 4.3A), caused a loss of TORC2-mediated phosphorylation of Ypk1 nearly as complete as that caused by inactivation of a temperature-sensitive allele of Tor2 (see Figure 3.4). This loss of TORC2 phosphorylation of Ypk1 occurred at both the newly characterized C-terminal phosphorylation sites as well as at the hydrophobic motif (Thr662) (Figure 4.3B), indicating a general down-regulation of TORC2 activity upon Sln1 inactivation. Given that Sln1 is not an enzyme able to phosphorylate Ser or Thr residues, our observation indicated that the loss of Sln1 function was acting indirectly to impede TORC2-mediated phosphorylation of Ypk1, most likely via the action of Hog1, which becomes activated when Sln1 is not functional. Indeed, in agreement with that conclusion, under the same conditions, when Sln1 was inactivated by temperature-shift in cells lacking Hog1, phosphorylation of Ypk1 at its TORC2 sites was unaffected (Figure 4.3A and 4.3B).

Sln1 acts via a phosphorelay system (Sln1 → Ypd1 → Ssk1) that prevents activation of Hog1 because phosphorylated Ssk1 is unable to bind and activate the paralogous HOG pathway MAPKKKs Ssk2 and Ssk22 (Figure 4.2). If Hog1 action is responsible for the observed loss of TORC-dependent Ypk1 phosphorylation, then the onset of that effect should only occur after Sln1 has been inactivated for a sufficient period to prevent Ssk1 phosphorylation, thereby promoting significant Hog1 activation. Indeed, kinetic analysis of Hog1 activation and loss of Ypk1 phosphorylation upon Sln1 inactivation showed exactly this reciprocal relationship (Figure 4.3C), providing further support for a role for Hog1 in negatively regulating TORC2.

To address this issue by an independent approach and to avoid any potential confounding effects that might arise from temperature shifts, I constructed a strain that expresses Tir1 and an allele of Sln1 tagged with a modified auxin-inducible degron (AID*) (Morawska and Ulrich, 2013). Tir1 is an F-box protein from plants that is able to couple to the yeast Skp1-Cdc53/cullin-Rbx1/RING protein:ubiquitin ligase (SCF E3) (Nishimura et al., 2009) and recognizes the AID* sequence only when the plant hormone auxin (or a more cell-permeable auxin analog) is provided. In this way, AID-tagged proteins are degraded in SCF-mediated auxin-regulated manner (McIsaac et al., 2011). Thus, my Sln1-AID* allele provided a temperature-independent method to specifically inactivate Sln1 and induce Hog1 signaling. Constitutive Hog1 activation is toxic to cells and, consequently, a *sln1Δ* mutation is lethal, but rescued by a *hog1Δ* mutation (Maeda et al., 1994). Likewise, efficient auxin-induced degradation of Sln1 should phenocopy a *sln1* null mutation and lead to a level of persistent Hog1 activation that should prevent growth. Consistent with this expectation, I found that cells expressing Sln1-AID*-6HA were unable to grow on synthetic medium containing 1 mM 1-NAA, whereas otherwise isogenic cells lacking Hog1 (Sln1-AID*-6HA *hog1Δ*) grew as well as control cells expressing Sln1 lacking the AID degron (Sln1-6HA) (Figure 4.4A).

Using this engineered inducible Sln1 degradation system, I examined the kinetics of Sln1 degradation, subsequent Hog1 activation, and loss of Ypk1 phosphorylation following the

addition of 1-NAA. The majority of Sln1 was degraded within the first 20 min and, strikingly, by the time the remaining residual Sln1 was no longer detectable (60-90 min), robust Hog1 activation occurred (Figure 4.4B). Moreover, just as I observed when the $sln1^{ts}$ allele was inactivated by shift to the restrictive temperature (Figure 4.3C), the onset of the reduction in TORC2 phosphorylation of Ypk1 coincided with the timing of Hog1 activation (Figure 4.4B). Both Hog1 activation and the loss of TORC2 phosphorylation of Ypk1 were sustained for several hours, as expected, because of the persistent very low level of Sln1 (Figure 4.4.B).

In addition to regulating HOG pathway activation, Sln1 also regulates the activity of a nuclear response regulator, the transcription factor Skn7 (Brown et al., 1993; Brown et al., 1994b; Raitt et al., 2000a), via the phosphorelay pathway (Sln1 → Ypd1 → Skn7). Skn7 was first isolated as a multicopy suppressor of a mutation that causes cell wall defects (Brown et al., 1993). Under hypotonic conditions Sln1 is active and phosphorylated Skn7 promotes the transcription of genes, such as *OCH1*, a mannosyltransferase involved in cell wall synthesis (Fassler et al., 1997; Ketela et al., 1998; Li et al., 2002). However, Skn7 activity is only partially regulated by Sln1. Skn7 has been to shown to bind to Rho1, the small GTPase which mediates activation of the CWI MAPK pathway, when Rho1 is GTP-bound (Alberts et al., 1998). Additionally, overexpression of the cell wall stress sensor Mid2, an upstream activator of Rho1, increases Skn7 transcriptional activity (Ketela et al., 1999). Thus, I wanted to know if the down-regulation of TORC2 that occurs upon Sln1 inactivation is dependent on Skn7. When Sln1 is inactivated in Sln1-AID*-6HA *skn7Δ* cells by the addition of 1-NAA, TORC2-dependent phosphorylation of Ypk1 decreases just as it does in Sln1-AID*-6HA cells treated with 1-NAA (Figure 4.4C). Thus, Skn7 is not required for the down-regulation of TORC2 upon Sln1 inactivation. In marked contrast, just like Sln1-AID*-6HA cells lacking Hog1, Sln1-AID*-6HA *skk2Δ ssk22Δ* cells, which lack the paralogous MAPKKKs of the HOG pathway, exhibited no loss in TORC2-dependent phosphorylation of Ypk1 upon 1-NAA induced Sln1 degradation (Figure 4.4C). Therefore, the down-modulation of TORC2 signaling upon Sln1 destruction requires activation of the Hog1 MAPK.

It has been shown that stresses that can activate the CWI pathway and the Slt2 MAPK, for example, heat shock, can also lead to activation of the Hog1 MAPK (Winkler et al., 2002). Moreover, it has even been reported that activated Hog1 can cause transcriptional induction of *SLT2* expression (Hahn and Thiele, 2002). For these reasons, I also examined the status of Slt2 upon Sln1 degradation and found that the Slt2 MAPK was concomitantly activated upon Sln1 degradation (Figure 4.4B).

**FIGURE 4.3**

A

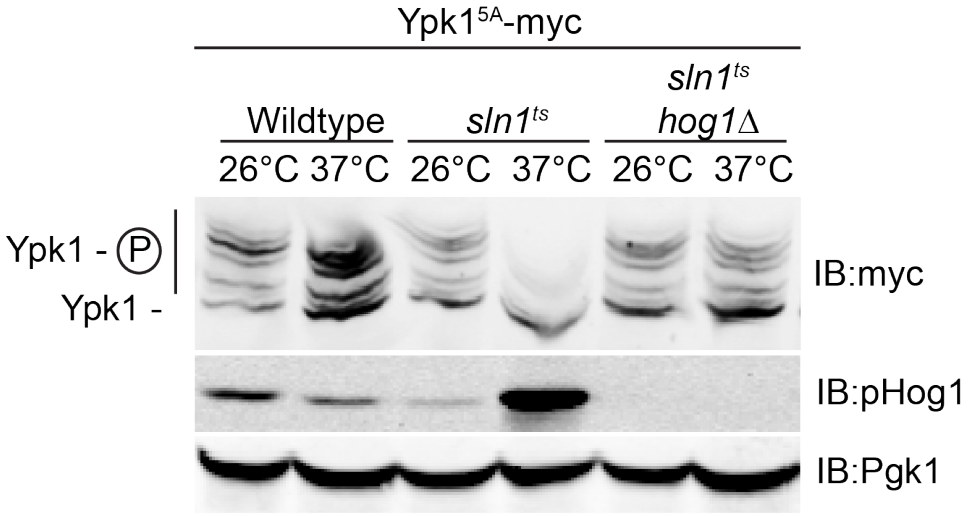


B

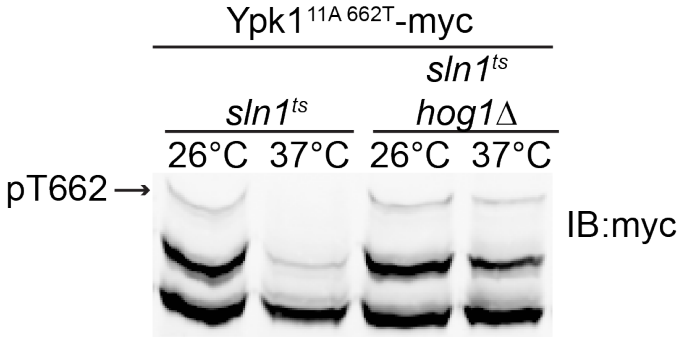


C

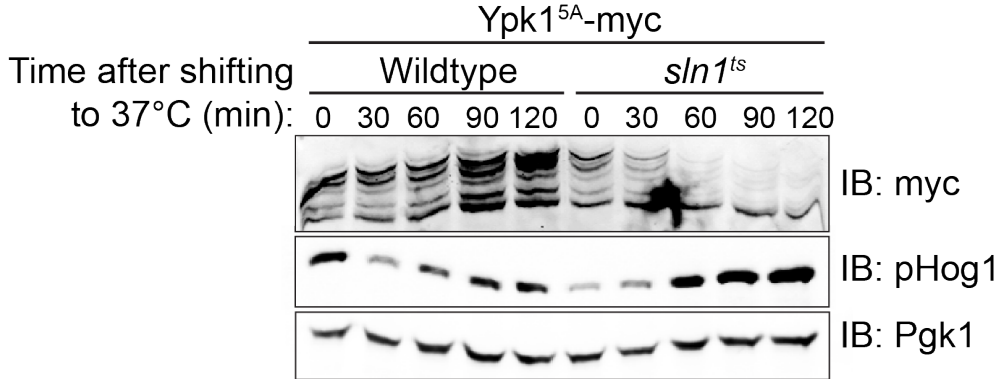

**Figure 4.3**. **Sln1 is a novel regulator of TORC2**. (A) Wild-type (BY4741), *sln1$^{ts}$* (JTY5473) or *sln1$^{ts}$ hog1Δ* (YFR302B) cells expressing Ypk1$^{5A}$-myc (pFR246) were grown at 26°C to exponential phase and then either kept at 26°C or shifted to 37°C for 2 h. Cells were harvested and whole-cell extracts were prepared. Ypk1 phosphorylation was analyzed by Phos-tag SDS-PAGE and detected by immunoblotting with anti-myc mAb 9E10. Hog1 phosphorylation was monitored by resolving the proteins in cell lysates by standard SDS-PAGE and immunoblotting with anti-phospho-p38 MAPK antibody (p38 is the mammalian ortholog of yeast Hog1; Han et al., 1994). Pgk1 was used as a loading control and detected with anti-Pgk1 antibody. (B) *sln1$^{ts}$* (JTY5473) or *sln1$^{ts}$ hog1Δ* (YFR302B) cells expressing Ypk1$^{11A\ 662T}$-myc (pFR267) were grown at 26°C to exponential phase and then either kept at 26°C or shifted to 37°C for 2 h. Cells were harvested whole-cell extracts were prepared, and Ypk1$^{11A\ 662T}$-myc was detected as in (A). (C) Wild-type (BY4741) or *sln1$^{ts}$* (JTY5473) cells expressing Ypk1$^{5A}$-myc (pFR246) were grown at 26°C and then shifted to 37°C and samples were taken at the indicated time points, and Ypk1$^{5A}$-myc, Hog1 phosphorylation, the Pgk1 loading control were all monitored as in (A).

**FIGURE 4.4**

A

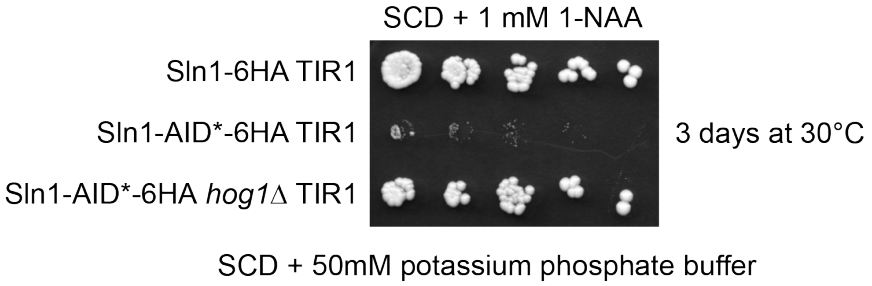


B

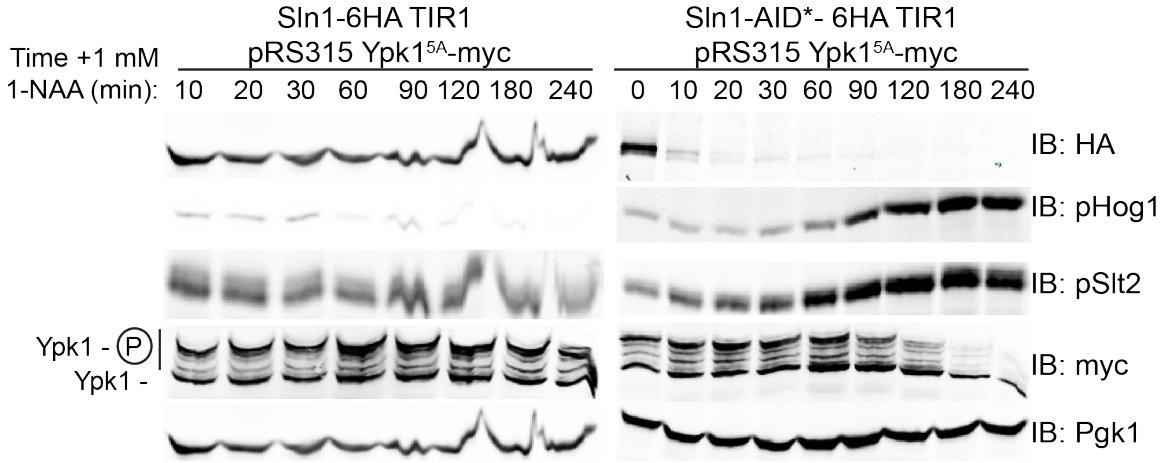


C

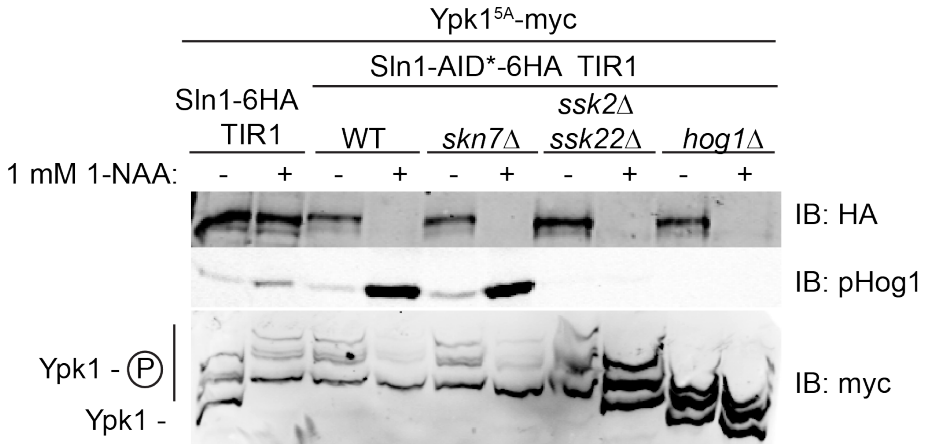

**Figure 4.4**. **The Sln1-Hog1 pathway negatively regulates TORC2-Ypk1 signaling**. (A) Overnight cultures of Sln1-6HA TIR1 (yKL15), Sln1-AID*-6HA TIR1 (yKL18) and Sln1-AID* TIR1 *hog1Δ* (yKL20) cells were adjusted to an $A_{600\ nm}$ = 1.0 and then spotted in 10-fold serial dilutions onto SCD plates containing 50 mM potassium phosphate buffer and 1 mM 1-NAA, which were incubated at 30°C for 3 days. (B) Sln1-6HA TIR1 (yKL15) or Sln1-AID*-6HA TIR1 (yKL18) strains expressing Ypk1$^{5A}$-myc (pFR246) were grown to exponential phase in selective minimal media containing 50 mM potassium phosphate buffer pH 6.2, treated with 1-NAA (1 mM final concentration) and samples withdrawn at the indicated times. Whole-cell extracts were prepared and resolved by Phos-tag SDS-PAGE to monitor Ypk1 phosphorylation and by standard SDS-PAGE to monitor the other proteins, which were detected by immunoblotting with the following antibodies: Ypk1$^{5A}$-myc, mouse anti-myc mAb 9E10; Hog1, rabbit anti-p38 MAPK phospho-Thr180/phospho-Tyr182 mAb; Slt2, rabbit anti-phospho-p44/42 MAPK (Erk1/2) (Thr202/Tyr204) mAb; Pgk1, rabbit polyclonal anti-Pgk1 antibodies. (C) Sln1-6HA TIR1 (yKL15), Sln1-AID*-6HA TIR1 (yKL18), Sln1-AID*-HA *skn7Δ* (yKL26A), Sln1-AID*-HA *ssk2Δ ssk22Δ* (yKL27A) and Sln1-AID*-HA *hog1Δ* (yKL20) cells expressing Ypk1$^{7A}$-myc (pFR252) were grown to exponential phase in selective minimal media containing 50 mM potassium phosphate buffer pH 6.2. Cells were then treated with either vehicle (DMSO) or 1 mM 1-NAA for 2 h prior to harvesting. Whole-cell extracts were prepared and resolved by Phos-tag SDS-PAGE to observe Ypk1 phosphorylation and by standard SDS-PAGE to measure the levels of Sln1-6HA and active Hog1. Proteins were detected as in (B), except for Sln1-6HA, which was detected with mouse anti-HA.11 mAb.

**Table 4.1**. Consensus MAPK phosphoacceptor sites in TORC2 subunits.

| **TORC2 subunit** | **Molecular weight** (kDa) | **MAPK phosphoacceptor sites**[1] |
|---|---|---|
| Avo3 | 164 | 11 *(5)* |
| Avo2 | 47 | 9 *(4)* |
| Avo1 | 131 | 8 *(3)* |
| Tor2 | 282 | 10 *(1)* |
| Lst8 | 34 | 2 *(0)* |
| Bit2 | 61 | 3 *(0)* |
| Bit61 | 61 | 4 *(0)* |
| Slm1 | 78 | 6 *(1)* |
| Slm2 | 75 | 7 *(2)* |

[1]Value indicates the total number of -SP- or -TP- sites in the indicated protein and the number in parentheses indicates the number of such sites that are detectably phosphorylated *in vivo* in various phosphoproteomic studies catalogued for each protein at the Saccharomyces Genome Database (http://www.yeastgenome.org).

**Down-regulation of TORC2 upon Sln1 inactivation is dependent on MAPKs Hog1 and Slt2**. To investigate the mechanism by which activated Hog1 and Slt2 down-modulate TORC2 phosphorylation of Ypk1, I decided to test the hypothesis that these MAPKs may negatively regulate the function of TORC2 by directly phosphorylating one or more of the subunits that constitute the TORC2 complex. In this regard, I found by inspection that many TORC2 components contain potential MAPK phosphoacceptor sites (Ser/Thr-Pro) some of which have already been shown to be phosphorylated *in vivo* in global MS studies (Holt et al., 2009; Swaney et al., 2013) (Table 4.1). I decided to focus, first, on the subunit Avo2 for several reasons. Although Avo2 (47 kDa) is one of the smaller TORC2 components, it has nine potential MAPK phosphoacceptor sites, four of which have already been shown to be phosphorylated *in vivo* (Holt et al., 2009; Swaney et al., 2013). Also, because *AVO2* is a non-essential gene, mutational analysis of Avo2 should, in theory, not cause any deleterious effects on cell viability under non-stress conditions.

Using the *sln1$^{ts}$* strain, I found that at the permissive temperature, Avo2 already exists in a series of different phospho-isoforms as resolved by Phos-tag SDS-PAGE (Figure 4.5A). Strikingly, however, after shifting the *sln1$^{ts}$* strain to the restrictive temperature for 2 h, the pattern displayed by Avo2 was markedly shifted to a spectrum of slower mobility, i.e. more highly phosphorylated, bands (Figure 4.5A). As a first approach to determine whether this apparent increase in Avo2 phosphorylation was due to an increase in phosphorylation by MAPKs, I examined in the same manner an Avo2$^{9A}$ mutant, in which all nine potential MAPK phosphoacceptor sites were mutated to Ala. I found that at the permissive temperature, Avo$^{9A}$ is still phosphorylated, but distinctly less so than Avo2$^{WT}$, indicating that MAPK(s), as well as other kinase(s), phosphorylate Avo2 under basal conditions. Consistent with the observed shift to slower mobility isoforms arising from MAPK-mediated phosphorylation of Avo2, the Avo2$^{9A}$ mutant did not exhibit this shift when the *sln1$^{ts}$* cells were incubated at the restrictive temperature. Thus, Avo2 does undergo phosphorylation at its MAPK sites upon Sln1 inactivation. Moreover, in further agreement with this conclusion, a change in the phosphorylation pattern of Avo2 upon shift of *sln1$^{ts}$* cells to non-permissive temperature also was eliminated in cells lacking Hog1 (Figure 4.5A). I noted, however, that even in *sln1$^{ts}$ hog1Δ* cells shifted to restrictive temperature, Avo2$^{WT}$ displays more phospho-isoforms than the Avo2$^{9A}$ mutant, indicating that a MAPK other than Hog1 also participates in phosphorylating Avo2 at the -SP- and -TP- sites

Given the concomitant activation of Slt2 that we observed upon Sln1 degradation (Figure 4.4B), it was the most likely candidate MAPK to phosphorylate Avo2, in addition to Hog1. Indeed, crosstalk is known to occur between the HOG and CWI pathways (Fuchs and Mylonakis, 2009). In particular, hyperosmotic stress has been shown to induce a delayed and transient activation of Slt2 (García-Rodríguez et al., 2005). Given such evidence for some degree of coordination between the HOG and CWI pathways, I carried out experiments to determine whether and to what extent Slt2 action contributes to the Avo2 phosphorylation observed after Sln1 inactivation. For this analysis, and to avoid the known ability of heat stress to activate Slt2 (Truman et al., 2007), I used my Sln1-AID* system and monitored Hog1 and Slt2 activation and the pattern of Avo2 phosphorylation after Sln1 inactivation. Just as I observed in the *sln1$^{ts}$* strain, by 2 h after auxin treatment, Avo2$^{WT}$ was distinctly more phosphorylated in the Sln1-AID* strain (Figure 4.5B). Also, as I observed before (Figure 4.4.B), both Hog1 and Slt2 were robustly activated following sustained Sln1 inactivation (Figure 4.5B). Analysis of the *hog1Δ* and *slt2Δ*

single mutants under the same conditions revealed that lack of Slt2 did not affect Hog1 activation; but, strikingly, lack of Hog1 prevented Slt2 activation (Figure 4.5B), suggesting that the primary effect of inactivation of Sln1 is activation of Hog1, which then leads to activation of Slt2 as a secondary consequence. In agreement with this conclusion, the pattern of $Avo2^{WT}$ phospho-isoforms observed in the *hog1Δ slt2Δ* double mutant most closely resembled that of the *hog1Δ* single mutant, as expected if the *hog1Δ* mutation is epistatic to the *slt2Δ* mutation. In any event, $Avo2^{WT}$ phosphorylation did not increase in the Sln1-AID* *hog1Δ slt2Δ* cells after auxin treatment and more closely resembled the pattern displayed by $Avo^{9A}$, indicating that Slt2 contributes to the Avo2 phosphorylation observed after sustained Sln1 inactivation. Nonetheless, the presence of some residual phospho-isoforms of $Avo2^{WT}$ in the *hog1Δ slt2Δ* cells indicates that additional kinase(s) are able to modify some of the five -SP- and/or four -TP- sites in Avo2, albeit at a very low level compared to those modified by Hog1 and Slt2.

To assess whether the Slt2-mediated phosphorylation of Avo2 is as important as the Hog1-mediated phosphorylation of Avo2 in down-regulation of TORC2-dependent phosphorylation of Ypk1, I expressed $Ypk1^{5A}$-myc in the same set of Sln1-AID*-6HA strains and monitored its phosphorylation status using Phos-tag SDS-PAGE after Sln1 inactivation. I found that absence of Slt2 was just as efficacious as the absence of Hog1 in preventing the loss of TORC2-mediated phosphorylation observed in otherwise wild-type cells upon degradation of Sln1 (Figure 4.5C). The pattern of Ypk1-myc preserved in the Sln1-AID*-6HA *hog1Δ slt2Δ* double mutant provides some suggestion that that maintenance of TORC2 function conferred by the absence of each MAPK might be slightly additive. In any event, despite the fact that activation of Slt2 may be a secondary consequence of the activation of Hog1, Slt2 action is nonetheless required for the down-regulation of TORC2 function that occurs when Sln1 is inactivated (Figure 4.5C). Thus, when loss of Sln1 function is sustained, hyperactivation of Hog1 leads to Slt2 activation, and Slt2 then mediates the phosphorylation and down-regulation of TORC2.

Genetic findings I made also demonstrate significant coordination between the HOG and CWI pathways, based on the growth phenotype of various Sln1-AID* strains on YPD plates containing 1 mM 1-NAA. At this concentration of auxin, the Sln1-AID*-6HA strain grew on YPD plates at 30°C, but more slowly than the control Sln1-6HA strain (Figure 4.6). As I found previously (Figure 4.4A), the growth retardation observed for Sln1-AID*-6HA cells in the presence of auxin is due, in large part, to hyperactivation of Hog1 because, when Hog1 is absent, these cells grew better and comparable to the control (Sln1-6HA) cells. However, the Sln1-AID*-6HA cells also grew better at 37°C than at 30°C. Heat stress is known to activate the CWI pathway and its MAPK Slt2 (Tuman et el., 2007). The fact that the Sln1-AID*-6HA cells grew better at 37°C than 30°C suggests that activation of Slt2 somehow compensates for the deleterious effects of too much Hog1 activity. Consistent with a role for Slt2 in maintaining viability under these conditions, I found that Sln1-AID*-6HA *slt2Δ* cells were extremely sick on YPD + 1-NAA plates at both 30°C and 37°C. However, given its role in cell wall synthesis and remodeling, it is likely that cell wall defects in the *slt2Δ* strain enhance its permeability to 1-NAA, causing more facile Sln1 degradation and ensuing Hog1 activation. In agreement with that proposal, a *hog1Δ* mutation rescued the severe growth debility of the *slt2Δ* cells, especially at 30˚C and even detectably at 37˚C.

**FIGURE 4.5**

A

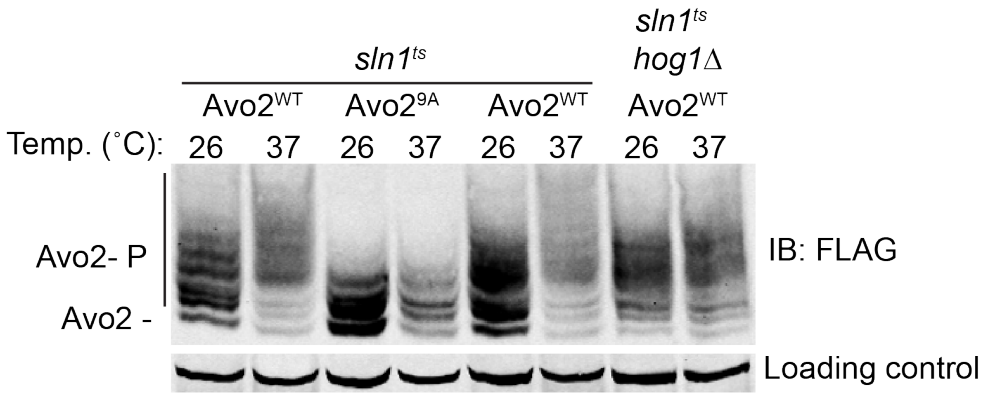


B

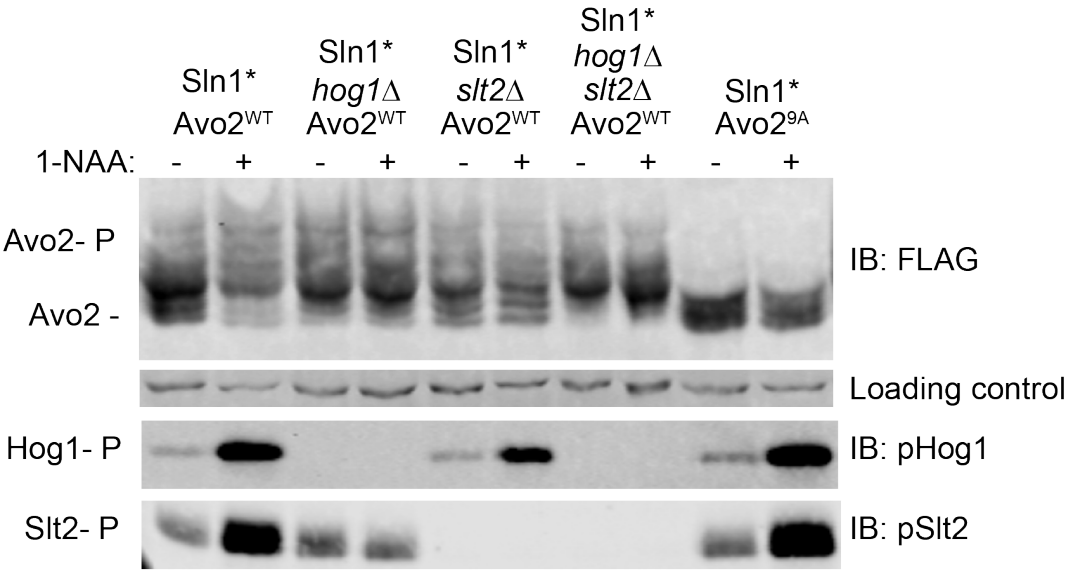


C

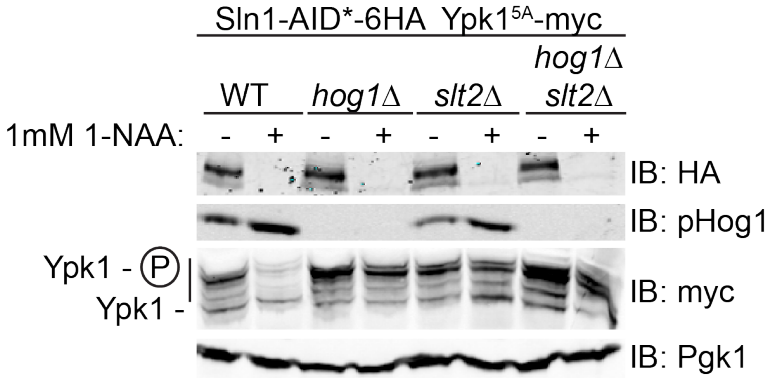

**Figure 4.5**. **MAPK-dependent phosphorylation of TORC2 subunit Avo2**. (A) *sln1$^{ts}$* (JTY5473) or *sln1$^{ts}$ hog1Δ* (YFR302B) cells expressing Avo2$^{WT}$-3xFLAG (pKL1) or Avo2$^{9A}$-3xFLAG (pKL2) were grown at 26°C to exponential phase and then either kept at 26°C or shifted to 37°C for 2 h prior to harvesting. Whole-cell extracts were prepared, resolved by Phos-tag SDS-PAGE and analyzed by immunoblotting with anti-FLAG antibody. The loading control is a non-specific band recognized by the anti-FLAG antibody. (B) Sln1-AID*- 6HA (yKL18), Sln1-AID*- 6HA *hog1Δ* (yKL20), Sln1-AID*- 6HA *slt2Δ* (yKL16) or Sln1-AID*- 6HA *hog1Δ slt2Δ* (yKL22) cells expressing Avo2$^{WT}$-3xFLAG (pKL1) or Avo2$^{9A}$-3xFLAG (pKL2), as indicated, were grown to exponential phase in selective minimal media containing 50 mM potassium phosphate buffer pH 6.2 and then treated with 1 mM 1-NAA or vehicle (DMSO) for 2 h. Avo2 phosphorylation was analyzed by Phos-tag SDS-PAGE and immunoblotting as in (A). Activated (dually phosphorylated) Hog1 and Slt2 were detected with anti-phospho-p38 MAPK and anti-phospho-p44/42 MAPK antibodies, respectively. (C) Sln1-AID*-6HA TIR1 (yKL18), Sln1-AID* TIR1 *hog1Δ* (yKL20), Sln1-AID* TIR1 *slt2Δ* (yKL16) and Sln1-AID* TIR1 *hog1Δ slt2Δ* (yKL22) cells expressing Ypk1$^{5A}$-myc (pFR246) were grown to exponential phase in selective minimal media containing 50 mM potassium phosphate buffer pH 6.2. Cells were then treated with either vehicle (DMSO) or 1 mM 1-NAA for 90 min prior to harvesting. Samples were prepared and extracts were resolved by Phos-tag SDS-PAGE and the proteins of interest detected by immunoblotting as described in the legend to Figure 4.4B.

**FIGURE 4.6**

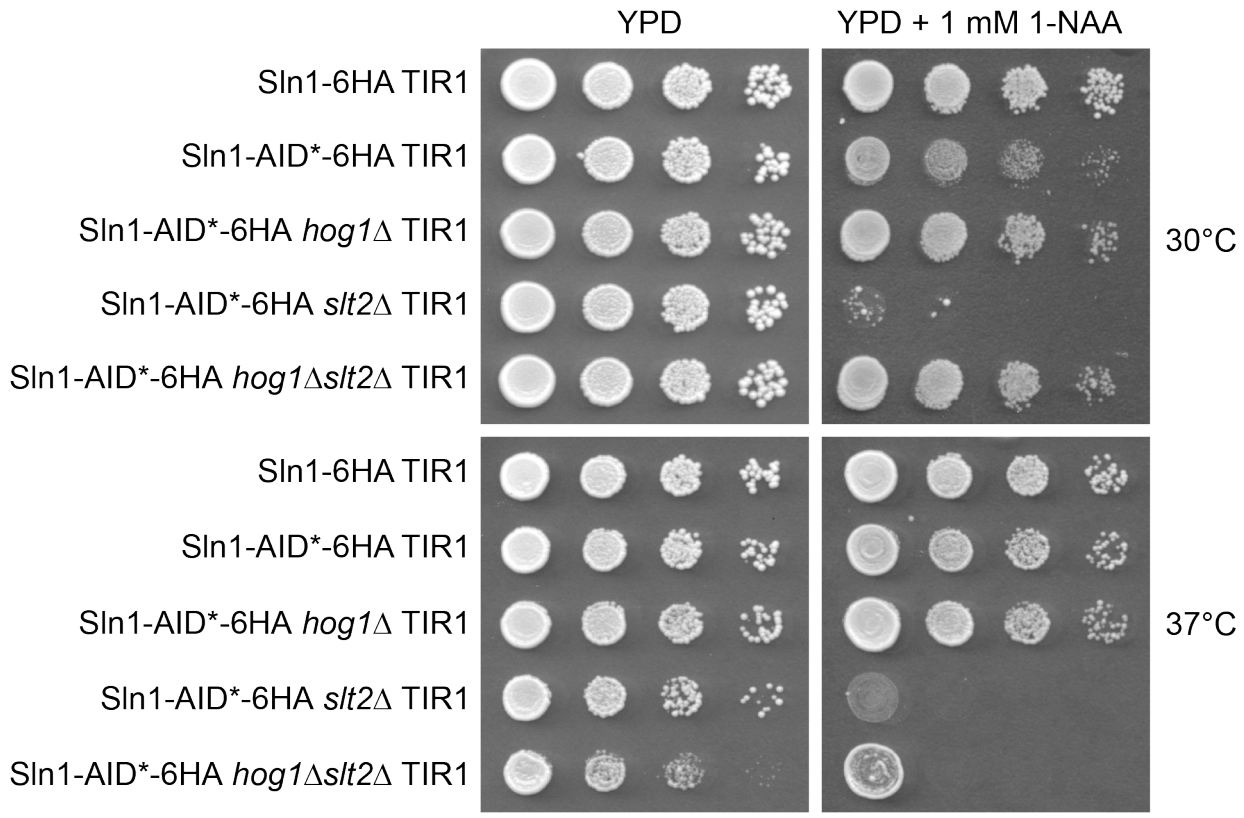


**Figure 4.6**. **Phenotypic evidence for coordination between Hog1 and Slt2**. Overnight cultures of Sln1-6HA TIR1 (yKL15), Sln1-AID*-6HA TIR1 (yKL18), Sln1-AID* TIR1 *hog1Δ* (yKL20), Sln1-AID* TIR1 *slt2Δ* (yKL16) *and* Sln1-AID* TIR1 *hog1Δ slt2Δ* (yKL22) cells were adjusted to an $A_{600\,nm}$ = 1.0 and then spotted in 10-fold serial dilutions onto YPD plates containing 50 mM potassium phosphate buffer pH 6.2 and either vehicle (DMSO) or 1 mM 1-NAA. Plates were incubated at either 30°C (*top panels*) or 37°C (*bottom panels*) for 2-3 days.

## DISCUSSION

I have shown here that the Sln1-Hog1 and TORC2-Ypk1 signaling pathways are coordinated during prolonged response to hyperosmotic stress. Specifically, when Sln1 is inactivated upon protracted exposure of cells to hypertonic conditions or by other means, Hog1 is activated and down-regulates TORC2 signaling. Prior work in our laboratory showed that short-term expose to hyperosmotic conditions causes rapid (minutes timescale) and dramatic down-regulation of TORC2-Ypk1 signaling that does not require Hog1 (Muir et al., 2015). However, my new findings document that, when Sln1 is inactive over a longer term (hours timescale), TORC2 down-regulation does require Hog1. Thus, TORC2-Ypk1 signaling is controlled by both Hog1-independent and Hog1-dependent mechanisms.

The PtdIns4,5$P_2$-binding proteins Slm1 and Slm2 are necessary for upregulation of TORC2 function in response to hypotonic conditions, as judged by the state of TORC2-dependent phosphorylation of Ypk1. Slm1/2 purportedly contribute to TORC2 signaling by helping to recruit Ypk1 to the PM (Niles et al., 2012) because Ypk1 has no identifiable membrane-targeting domains. At the PM, Ypk1 encounters, and is phosphorylated and thereby activated by TORC2. Under normal conditions, Slm1 is primarily localized to punctate PM domains termed eisosomes and only a small amount is available to bind to TORC2. Hypotonic conditions reportedly trigger the release of Slm1 from the eisosomes, increasing the amount of Slm1 that can associate with TORC2 and, subsequently, results in a modest enhancement of Ypk1 phosphorylation at its TORC2 sites (Berchtold et al., 2012). Sequestering Slm1 via inducible tethering of Slm1 to the eisosome component Sur7, so that it can no longer readily interact with TORC2, reduced the basal level of Ypk1 phosphorylation at a TORC2-dependent site (Thr662) (Berchtold et al., 2012). It is possible, therefore, but not yet demonstrated, that hyperosmotic shock may have the opposite effect from hypotonic conditions; specifically, hypertonic conditions may promote dissociation of Slm1/Slm2 from TORC2, thus perhaps preventing efficient TORC2-mediated phosphorylation of Ypk1 in a Hog1-independent manner. Sustained TORC2 activity is required to maintain Ypk1 modification at its TORC2 sites because inhibition of TORC2 in an Avo3$^{\Delta CT}$ strain, in which TORC2 can be inhibited by rapamycin, results in loss of Ypk1 hydrophobic motif (Thr662) phosphorylation within 5 min (Gaubitz et al., 2015), indicating that continuous TORC2-mediated phosphorylation of Ypk1 counter-acts the action of phosphatases. If, as I have proposed, hyperosmotic conditions disrupt Slm1/Slm2 interaction with TORC2, it might explain the equally rapid kinetics and Hog1-independence of the reduction of TORC2-mediated phosphorylation of Ypk1 observed when cells are treated with 1 M sorbitol (Lee et al., 2012; Muir et al., 2015). To address this issue experimentally, it might be informative to monitor Ypk1 phosphorylation in a strain in which Slm1/Slm2 is anchored to TORC2 and cannot dissociate upon hyperosmotic shock or inactivation by Sln1.

My construction of an auxin-inducible degron allele of Sln1 allowed for the activation of Hog1 in a precise and sustained manner and uncovered a previously uncharacterized role for MAPKs in enforcing down-regulation of TORC2 signaling during conditions that mimic prolonged exposure to hyperosmotic conditions. TORC2-Ypk1 signaling is modulated by external fluctuations that exert stress on the PM, such as changes in osmolarity and temperature, and adjusted to the appropriate level to maintain homeostasis (Roelants et al., 2011; Berchtold et al., 2012; Lee et al., 2012; Muir et al;, 2014; Muir et al., 2015). It is perhaps not too surprising, therefore, that MAPK pathways, which also are activated in response to a wide variety of environmental stresses, are involved in regulating TORC2. Both Hog1 action and TORC2-Ypk1

function play vital roles in cellular adaptation to hyperosmotic stress (Lee et al., 2012; Saito and Posas, 2012; Muir et al., 2015), primarily by regulating the production and accumulation of glycerol. In addition to its activation by hyperosmotic stress (Brewster and Gustin, 2014), Hog1 is also activated by heat stress (via the Sho1 branch) (Winkler et al., 2002), by citric acid stress (Lawrence et al., 2004), by cold shock (via the Sln1 branch) (Panadero et al., 2006), by hypoxia (Hickman et al., 2011), by sphingolipid depletion (Tanigawa et al., 2012) and by glucose starvation (Vallejo and Mayinger, 2015). Unlike hyperosmotic shock which robustly activates Hog1 and markedly down-regulates TORC2-Ypk1 signaling in a Hog1-dependent manner, some of the other stresses that activate Hog1, such as heat stress and sphingolipid depletion, are known to markedly stimulate TORC2-Ypk1 signaling (Roelants et al., 2011; Berchtold et al., 2012; Omnus et al., 2016). Thus, under those shared conditions where both Hog1 and TORC2-Ypk1 signaling are upregulated, there must be mechanisms, as yet undefined, to prevent Hog1 from negatively regulating TORC2 or to shield TORC2 from Hog1 action.

My finding that the CWI pathway MAPK Slt2 collaborates with Hog1 in down-regulating TORC2 signaling supports the premise that regulation of TORC2 is multifaceted. Deletion of either *HOG1* alone or *SLT2* alone (or both) prevented the down-regulation of TORC2 signaling observed upon Sln1 inactivation. Thus, neither Hog1 by itself nor Slt2 by itself is not sufficient to inhibit TORC2-dependent phosphorylation of Ypk1. Some of my data suggest that the role of Hog1 may be to initiate activation of Slt2 and that Slt2 may be critical for executing the events that actually down-regulate TORC2. To test whether activation of Slt2 alone, *i.e.* in the absence of concomitant Hog1 activation, is sufficient to down-regulate TORC2 signaling, it might be possible to active Slt2 independently of Hog1 by inducing expression of a known hyperactive Pkc1 allele ($Pkc1^{R398A, R405A, K406A}$ or Pkc1*) (Mascaraque et al., 2013) in *hog1Δ* cells or by treating *hog1Δ* cells with the cell-wall damaging agent Calcofluor White™ (García-Rodríguez et al., 2005), and then monitoring both Avo2 phosphorylation and TORC2-dependent phosphorylation of Ypk1.

Sustained inactivation of Sln1 promotes the Hog1- and Slt2-dependent phosphorylation of the TORC2 component Avo2. My results suggest that Hog1 is necessary for Slt2 activation following Sln1 inactivation and that it is Slt2 that then mediates phosphorylation of Avo2. Phosphorylation of recombinant Avo2 *in vitro* with purified activated Hog1 and with purified activated Slt2, alone, simultaneously, and sequentially (first with Hog1, then Slt2; and, vice-versa) should pinpoint which of the four -TP- and five -SP- sites in Avo2 are modified by which MAPK and whether initial phosphorylation by one serves to prime Avo2 for phosphorylation by the other.

It has been reported that hyperosmotic shock induces a delayed and transient activation of Slt2 that is dependent on the CWI pathway MAPKKK Bck1 and the HOG pathway MAPKK Pbs2 (García-Rodríguez et al., 2005). Hog1 activation promotes the production and accumulation of glycerol, primarily by upregulating *GDP1* expression (Albertyn et al., 1994) as well as by closing the glycerol efflux channel Fps1 (Lee et al., 2013). Remarkably, overproduction of Gpd1 is sufficient to induce Slt2 activation (García-Rodríguez et al., 2005). Additionally, hyperosmotic stress has been reported to induce a temporal upregulation of *SLT2* transcription that is dependent on Hog1 as well as the transcription factor Rlm1, a Slt2 target (Watanabe et al., 1997; Hahn and Thiele, 2002). Hog1 is not known to regulate Rlm1 directly. Therefore, Slt2 is likely activated in response to the increase in turgor pressure that results from the Hog1-mediated rise in intracellular glycerol levels. Hypotonic stress is a known activator of the CWI

pathway (Levin, 2011; Hohmann, 2015). Therefore, to elucidate whether Hog1 plays any role in Slt2 activation under hypertonic stress, kinetic studies to monitor the status of Hog1 and Slt2, as well as TORC2-Ypk1 signaling, might be helpful. Additionally, measuring Slt2 activation as well as TORC2-dependent phosphorylation of Ypk1 in a strain in which Hog1 is tethered to the PM via a CaaX motif and cannot translocate into the nucleus upon Sln1 inactivation (Westfall et al., 2008) would reveal whether nuclear Hog1 is required for induction of *SLT2* transcription.

How MAPK-mediated phosphorylation down-modulates TORC2 is not known. For my studies, I selected Avo2 as a convenient reporter for examining whether any components of TORC2 are subject to enhanced MAPK-dependent phosphorylation upon Sln1 inactivation. However, as pointed out in Table 4.1, every known constituent of TORC2 contains potential MAPK phosphoacceptor sites. Indeed, multiple TORC2 components have already been shown to be phosphorylated at MAPK phosphoacceptor sites *in vivo* (Holt et al., 2009; Swaney et al., 2013). So, in addition to Avo2, it is possible that other components of TORC2 undergo just as dramatic an increase in MAPK-mediated phosphorylation as I observed for Avo2 under conditions mimicking sustained exposure to hyperosmotic conditions. In fact, I have noted that TORC2-mediated phosphorylation of Ypk1 is down-regulated in a Sln1-AID* Avo2$^{9A}$ strain at the same rate and to the same extent as a Sln1-AID* Avo2$^{WT}$ strain (data not shown), suggesting that phosphorylation of other TORC2 components must also contribute to TORC2 down-regulation after Sln1 inactivation. In any event, the cumulative effect of such modifications could result in down-regulation of TORC2 function by altering its composition, stability, localization, membrane association, or specific catalytic activity (or any combination of such effects). One plausible mechanism could be that MAPK phosphorylation prevents Slm1/Slm2 association with TORC2 and, therefore, prevents efficient recruitment of Ypk1 to TORC2. Therefore, monitoring Ypk1 phosphorylation in a Sln1-AID* strain in which Slm1 is irreversibly tethered to TORC2 might be informative. It would also be informative to measure the kinase activity of TORC2 *in vitro* before and after incubation with constitutively-active Slt2.

Just as the short-term loss of TORC2-Ypk1 signaling and long-term elevation of Hog1 function have complementary roles in maintaining cell viability in response to hyperosmotic stress, previous studies have indicated functional interrelationships between TORC2 and the CWI pathway. The earliest characterized function of Tor2 activity is proper polarization of the actin cytoskeleton (Schmidt et al., 1996) which is known to be mediated by Rho1 and the CWI pathway. Overexpression of an activated allele of Pkc1 or CWI MAPK pathway components rescues the inviability and actin polarization defects associated with loss of TORC2 or Ypk1/2 function (Helliwell et al., 1998b; Roelants et al., 2002; Schmelzle et al., 2002). TORC2-Ypk1 activity is necessary for the proper localization of Rho1 as well as the Rho1 GEF Rom2 to bud tips (Niles and Powers, 2014; Hatakeyama et al., 2017). Treating Ypk1$^{as}$ *lcb4Δ* cells with the long-chain base PHS rescues the actin polarization defect observed in *torc2$^{ts}$* cells (Aronova et al., 2008) and restores proper localization of Rom2 to the bud tip (Niles and Powers, 2014). Additionally, ypk1$^{as}$ *fpk1Δ* cells display improved recruitment of Rom2 to the bud tip and bud neck compared to *ypk1$^{as}$* cells (Niles and Powers, 2014), indicating that both sphingolipids and flippase activity are important for the proper localization of Rom2 (Hatakeyama et al., 2017). Thus, TORC2-Ypk1 modulates CWI pathway activation via Rom2 and Rho1 PM localization by regulating the lipid composition and organization of the PM. Additionally, like Ypk1 and Ypk1, Pkc1 function requires its activation loop phosphorylation by Pkh1 and Pkh2 (Inagaki et al., 1999) and upregulation by TORC2 (Nomura and Inoue, 2015).

Heat stress and hypotonic shock have been reported to activate both TORC2 (Berchtold et al., 2012; Omnus et al., 2016) and the CWI pathway (Kamada et al., 1995; Zarzov et al., 1996). Therefore, it may seem contradictory that Slt2 is involved in the down-regulation of TORC2 function when Sln1 is inactivated. One possibility is that the joint action of Hog1 and Slt2 is required to inhibit TORC2. Another explanation, if one assumes that TORC2 action is antithetical to CWI pathway function, is that Slt2-mediated down-regulation of TORC2 signaling supports sustained and self-reinforcing CWI pathway activation. However, that view is not consistent with the substantial evidence that TORC2-Ypk1 signaling promotes activation of the CWI pathway. Cells lacking Ypk1 display significant defects in Slt2 phosphorylation and activation in response to heat stress (Schmelzle et al., 2002). Additionally, overexpression of Rom2 in *Ypk1*$^{as}$ cells results in increased Slt2 phosphorylation (Niles and Powers, 2014). One way to test whether Slt2 might participate in a negative feedback loop and down-regulate TORC2 signaling would be to activate the CWI MAPK pathway independently of TORC2, such as by overexpressing Pkc1*. If overexpression of hyperactive Pkc1* reduces TORC2-dependent phosphorylation of Ypk1, such a result would support the existence of a negative feedback loop between CWI signaling and TORC2.

I cannot yet exclude the possibility that among the effects ensuing from Sln1 inactivation is activation of a phosphatase that removes the TORC2-dependent phosphorylations on Ypk1. The identity of such a phosphatase(s) is unknown. However, hypertonic shock itself has been shown to increase cytosolic [$Ca^{2+}$] and thereby active the $Ca^{2+}$/calmodulin-dependent phosphatase calcineurin (PP2B) (Denis and Cyert, 2002). However, loss of TORC2-mediated Ypk1 phosphorylation after 1 M sorbitol treatment still occurred in a *cna1Δ cna2Δ* strain, indicating that calcineurin is not involved in the short-term down-regulation of TORC2 signaling upon hyperosmotic shock (Muir et al., 2015). It remains to be determined whether the down-regulation of TORC2 signaling observed upon Sln1 inactivation is calcineurin-dependent or not. The mammalian AGC-family protein kinase Akt is a target of mammalian TORC2 (mTORC2) and is dephosphorylated by the action of two PP2C type phosphatases PHLPP1 & PHLPP2 (Brognard et al., 2007). *S. cerevisiae* expresses seven PP2C type phosphatases: Ptc1 to Ptc7. Interestingly, the four cytosolic Ptc phosphatases (Ptc1 to Ptc4) have all been implicated in negatively regulating the HOG pathway (Maeda et al., 1993; Warmka et al., 2001; Young et al., 2002; Shitamukai et al., 2004). Therefore, it would be worth examining whether one or more of the yeast Ptc class of phosphatases might also act on Ypk1 to counteract its TORC2-mediated phosphorylation. Further experiments are underway to test this hypothesis.

In conclusion, the TORC2, HOG and CWI pathways comprise an elaborate signaling network whose mutual interactions adjust their levels of activity to optimally maintain the integrity of the PM and cell wall in response to environmental challenges. Specifically, the activation of Hog1 and Slt2, in response to protracted inactivation of Sln1, down-regulates TORC2 signaling by mediating the phosphorylation of at least one TORC2 subunit, Avo2. Although additional experiments are needed to elucidate the details of how this negative regulation is imposed, my results have revealed a novel mechanism by which TORC2 function is modulated by MAPK-dependent phosphorylation.

**Chapter 5: Perspectives**

TORC2 is essential for the maintenance of cellular homeostasis. In yeast, the TORC2 signaling network ensures the integrity of the cell's boundaries by modulating the lipid composition and organization of the PM and by responding to osmotic changes that stress the PM and cell wall. Significant progress has been made in elucidating the downstream effectors of TORC2 signaling. However, the upstream mechanisms that regulate TORC2-Ypk1 signaling are still being clarified. In Chapter 3, I provided additional insight into how TORC2 modulates the activity of its primary effector Ypk1. In Chapter 4, I established that the MAPKs Hog1 and Slt2 negatively regulate TORC2 signaling by promoting the phosphorylation of at least one component of TORC2 itself. My discovery is the first evidence that MAPKs can regulate TORC2. In this final chapter, I present data that provide additional insights about the regulation of TORC2 signaling and highlight promising areas for future study.

**ER-PM contact sites are required for signaling downstream of TORC2 but not for TORC2 activation**. Sphingolipids are important structural components of the PM, and also are the source of signaling molecules. The basic sphingolipid unit, called a ceramide, is composed of a long-chain base (LCB) to which is attached an amide-linked fatty acid. A ceramide can be further modified by linking additional substituents to a hydroxyl at the polar end of the LCB. In yeast, the major LCB is phytosphingosine and the major ceramide-derived complex sphingolipids are IPC, MIPC and $M(IP)_2C$. In all eukaryotes, sphingolipid synthesis begins in the endoplasmic reticulum (ER) with the formation of LCBs and ceramides, which are then transported to the Golgi for further modification to form complex sphingolipids. From the Golgi, sphingolipids are transported to their final destination in the outer leaflet of the PM (Hannun and Obeid, 2008; Megyeri et al, 2016).

Prior work in our laboratory has shown that TORC2-Ypk1 signaling plays a vital role in regulating ER sphingolipid metabolism to maintain the integrity of the PM. Ypk1-mediated phosphorylation at two control points enhances flux through the sphingolipid biosynthetic pathway: (i) the first and rate-limiting step in *de novo* sphingolipid synthesis, the condensation of serine and palmitoyl-CoA to form 3-ketodihydroxysphingosine catalyzed by L-serine: palmitoyl-CoA acyltransferase (SPT) (Alvarez-Vasquez et al., 2005); (ii) the N-acylation of LCBs with a fatty acid to form ceramide, catalyzed by the ceramide synthase complex. Ypk1 stimulates overall flux through the sphingolipid biosynthetic pathway by phosphorylating and relieving the negative regulation exerted by two proteins, Orm1 and Orm2, that would otherwise inhibit SPT (Roelants et al., 2011). Ypk1 also directs sphingolipid flux into the formation of ceramides and complex sphingolipids by phosphorylating and stimulating the activity of Lag1 and Lac1 (Muir et al., 2014), the catalytic subunits of the ceramide synthase complex (D'mello et al., 1994; Guillas et al., 2001). Thus, TORC2-Ypk1 signaling communicates the status of the PM (PM) to the ER, so that ER metabolism can be adjusted to meet the needs of the PM.

Cortical ER-PM junctions (Manford et al., 2012; Gatta and Levine, 2017) are also important sites of ER-PM crosstalk. ER-PM contact sites mediate the non-vesicular transport of glycerophosphoplipids and sterols between the ER and PM (Lev, 2010; Saheki and De Camilli, 2017) as well as regulate calcium dynamics as the ER is a major storage site for intracellular calcium (Stefan et al., 2013). Deletion of the proteins mediating the formation of these ER-PM junctions, which I will refer to as *tetherΔ* mutants, significantly diminishes the cortical ER network (Manford et al., 2012; Omnus et al., 2016). Additionally, *tetherΔ* cells are defective in

maintaining PM integrity during stress conditions as *tetherΔ* cells display higher levels of propidium iodide internalization after heat shock compared to wild-type cells (Omnus et al., 2016). The defects in PM maintenance of *tetherΔ* cells has been attributed to decreased ceramide synthase activity as *tetherΔ* cells contain lower levels of ceramide and higher levels of long-chain bases (LCBs) compared to wild-type cells (Omnus et al., 2016).

TORC2-Ypk1 signaling is intimately involved in regulating sphingolipid metabolism. Lag1 and Lac1, the catalytic subunits of the ceramide synthase complex, are direct substrates of Ypk1. Prior work in our laboratory has shown that Ypk1-mediated phosphorylation of Lag1 and Lac1 stimulates ceramide production (Muir et al., 2014). Given the importance of ER-PM contact sites in maintaining PM homeostasis, we wanted to know if ER-PM tethers are necessary for proper TORC2 signaling. In the absence of PM stress, Ypk1-dependent phosphorylation of Lac1 was significantly less efficient in *tetherΔ* cells compared to wild-type cells (Figure 5.1A). Moreover, Lac1 phosphorylation did not increase in *tetherΔ* cells when they were treated with the SPT inhibitor Myr to block *de novo* sphingolipid synthesis. This result suggests that ER-PM contact sites might be important for activating TORC2 in response to sphingolipid depletion or that the substrate Lac1, which is an ER-localized protein (Schorling et al., 2001), is less available to Ypk1 once Ypk1 has become activated by its TORC2-mediated phosphorylation. To distinguish between these possibilities, I performed additional experiments. In wild-type cells, TORC2 phosphorylation of Ypk1 increases upon blockade of sphingolipid synthesis, which can be achieved by treating cells with either the SPT inhibitor Myr or with Aba, which inhibits IPC synthase (Zhong et al., 1999). I found that treatment of *tetherΔ* cells with either Myr (Figure 5.1B) or Aba (Figure 5.1C) led to readily detectable enhancement of TORC2-dependent Ypk1 phosphorylation, indicating that *tetherΔ* cells are still able to detect and respond to sphingolipid limitation by upregulating TORC2 function. Thus, the more likely explanation for that lack of robust Ypk1-mediated Lac1 phosphorylation in the tetherΔ cells is that there is less ER and hence less Lac1 in the immediate vicinity of the PM where Ypk1 is activated by TORC2-dependent phosphorylation.

**BOX 1**

**Myriocin (also known as ISP-1)**

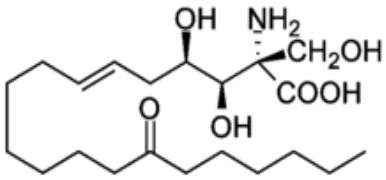


**Aureobasidin A**

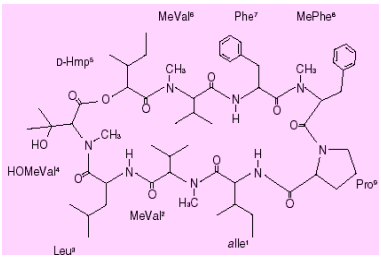


Interestingly, I noted that the effect of Myr on *tetherΔ* cells was somewhat less potent than on the control cells (Figure 5.1B), whereas that was not the case for Aba (Figure 5.1C). We were curious as to why Myr and Aba, which both block sphingolipid biosynthesis, but at different points, had differential effects on TORC2 activation in *tetherΔ* cells. Of course, whenever mutant cells are treated with an exogenously supplied compound, it is possible that any observed differences in potency could be due to differences in the permeability of wild-type versus mutant cells. Prior work has shown that cells with other kinds of mutations that reduce TORC2-Ypk1 signaling are more sensitive to *both* Myr and Aba due to their inability to fully activate Ypk1 and thereby compensate for the effects of these inhibitors by upregulating sphingolipid biosynthesis. I found that, compared to wild-type cells, the *tetherΔ* mutant was more resistant to Myr, but less resistant to Aba (Figure 5.1D). The structures of Myr and Aba are quite different (Box 1) ; and,

therefore, it is likely that they enter the cell through different mechanisms. Moreover, given the role of ER-PM junctions in lipid trafficking, the *tetherΔ* mutations likely have a more direct and profound effect on the PM lipid composition and, hence, the cell's permeability barrier than other mutations that compromise TORC2-Ypk1 signaling. This hypothesis is supported by the fact that the *tetherΔ* mutant was also more sensitive to the killing action of duramycin, an antibiotic that binds to phosphatidylethanolamine (PtdEth) in the outer leaflet of the PM and kills cells (Iwamoto et al., 2007; Roelants et al., 2015). PtdEth is translocated from the outer leaflet of the PM to the inner leaflet by the action of flippases (Pomorski et al., 2003). ER-PM junctions are the sites where PtdEth is converted to phosphatidylcholine (PtcCho) (Tavassoli et al., 2013). Thus, when such contact sites are absent, more of the PtdEth that reaches the PM will remain as PtdEth, thus causing *tetherΔ* cells to be more sensitive to duramycin. Thus, the changes in PM lipid composition that result from the lack of the ER-PM contact sites which are missing in the *tetherΔ* cells presumably impedes Myr entry and promotes Aba entry, likely explaining the Myr resistance and Aba sensitivity of these cells and, consequently, the extent to which these drugs inhibit sphingolipid biosynthesis. This differential permeability would thus also account for the fact that Aba was more potent than Myr in upregulating TORC2-dependent phosphorylation of Ypk1 (compare Figure 5.1B to Figure 5.1C). Given that Slm1 association with TORC2 is necessary for TORC2 phosphorylation of Ypk1, my results are consistent with the reported observation that, in both wild-type and *tetherΔ* cells, Slm1-GFP displays a similar cortical patch localization (Omnus et al., 2016).

Although ER-PM junctions are not required for TORC2 activation by sphingolipid limitation, they did appear to reduce the efficiency of even basal Ypk1-mediated Lac1 phosphorylation (Figure 5.1A). As mentioned above, because Lac1 is an ER-localized protein, this result could mean that, in *tetherΔ* cells, there is less of this target in the vicinity of activated Ypk1. On the other hand, our laboratory demonstrated that the phosphorylations installed in Lac1 (and Lag1) by Ypk1 are removed by the phosphatase calcineurin (Muir et al., 2014); and, in this regard, it has been reported that *tetherΔ* cells have 4-fold higher calcineurin activity compared to control cells (Omnus et al., 2016), as measured using a reporter gene that monitors the action of the calcineurin activated transcription factor Crz1 (Stathopoulos and Cyert, 1997). Thus, elevated calcineurin activity rather than lack of efficient Ypk1-Lac1 encounter might explain the marked reduction in both basal and Myr-induced Ypk1-mediated phosphorylation observed in the *tetherΔ* cells.

**FIGURE 5.1**

A

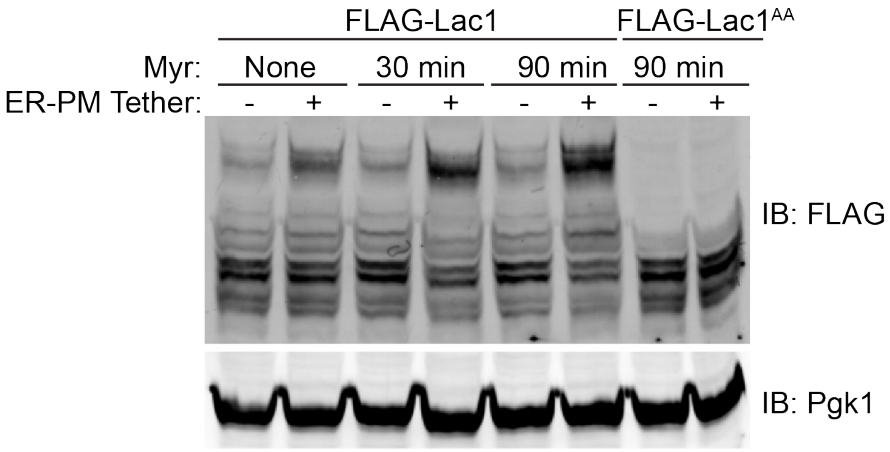


B

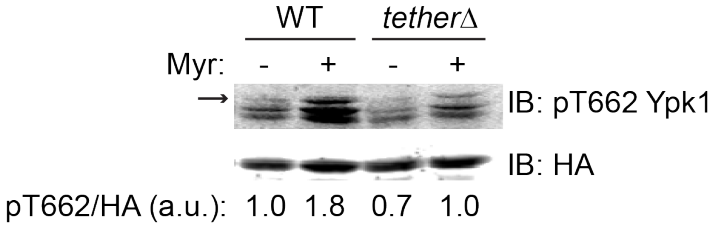


C

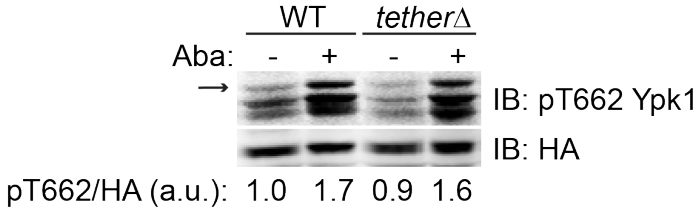


D

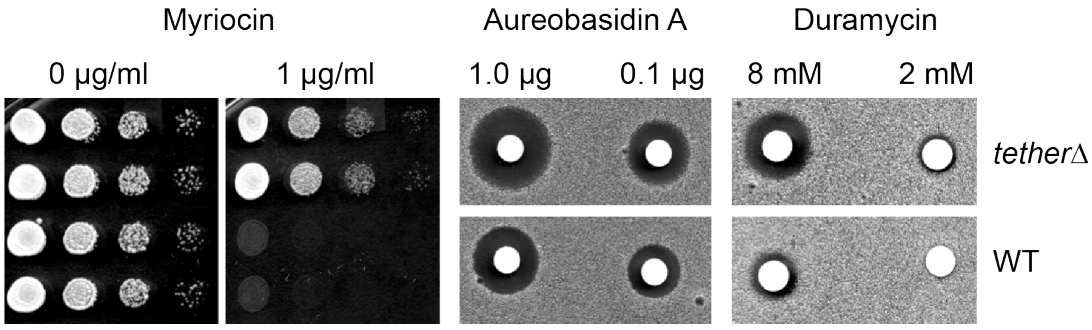

**Figure 5.1. Tricalbin-containing ER-PM tethers are not required for TORC2 activation in response to sphingolipid depletion**. (A) Wild-type or *tetherΔ* cells expressing FLAG-Lac1 or FLAG-Lac1(S23A S24A) lacking its Ypk1 phospho-acceptor sites were grown to mid-exponential phase and treated with vehicle (methanol) or 1.25 μM myriocin. Samples were taken at the indicated time points. Whole-cell lysates were prepared and resolved by Phos-tag SDS-PAGE. Proteins were detected by immunoblotting with anti-FLAG and anti-Pgk1 antibodies. (B) and (C) Wild-type or *tetherΔ* cells expressing Ypk1-3HA (pLB215) were grown to exponential phase in SCD-Ura and then treated with either vehicle (methanol) or 1.25 μM myriocin (B) or vehicle (ethanol) or 1.8 μM aureobasidin A (Aba) (C) for two h prior to harvesting. Whole-cell extracts were prepared, resolved by SDS-PAGE and analyzed by immunoblotting as in (A). (D) To test Myr sensitivity: overnight cultures of wild-type or *tetherΔ* cells were adjusted such that $A_{600\,nm}$ = 1.0 and spotted in 10-fold serial dilutions on plates lacking or containing Myr and incubated at 30°C for 2 days. To test aureobasidin A or duramycin sensitivity: wild-type or *tetherΔ* cells were each plated as a lawn on YPD plates, and 10 μL of a stock solution of aureobasidin A or duramycin at the indicated concentrations were spotted onto sterile filter paper disks and immediately placed onto the lawn, and the plates were incubated at 30 °C for 2 days.

**The Unfolded Protein Response does not activate TORC2**. In addition to its role in sphingolipid and sterol biosynthesis**,** the ER is also the major site for synthesis of both membrane and secreted proteins. Accumulation of misfolded proteins in the ER induces the unfolded protein response (UPR) (Malhotra and Kaufman, 2007; Walter and Ron, 2011). Moreover, alterations of lipid metabolism in the ER also can activate the UPR (Volmer and Ron, 2015). In this latter regard, it has been reported that *tetherΔ* cells have constitutive UPR activation and are hypersensitive to tunicamycin, a known UPR activator (Manford et al., 2012). Upon UPR induction, hundreds of genes are up-regulated to alleviate ER stress including genes involved in lipid metabolism (Travers et al., 2000; Gardner et al., 2013). Increased lipid synthesis concomitant with UPR activation is thought to be important for ER growth and expansion to accommodate the increased demand for protein synthesis (Ron and Hampton, 2004; Sriburi et al., 2004; Schuck et al., 2009). For example, the level of *LCB1* mRNA, which encodes one of the catalytic subunits of SPT, is higher upon UPR induction (Travers et al., 2000). Also, in cells in which the UPR has been induced, the levels of ceramides and complex sphingolipids are elevated (Epstein et al., 2012).

Given these observations, and the fact that TORC2-Ypk1 signaling is known to stimulate sphingolipid biosynthesis, I wanted to determine whether TORC2 activity is stimulated under conditions that induced the UPR. Therefore, I monitored TORC2 phosphorylation of Ypk1 after treating cells with tunicamycin, a known activator of the UPR (Kohno et al., 1993). I found that TORC2-dependent phosphorylation of Ypk1 did not increase after tunicamycin treatment of the cells (Figure 5.2A), indicating that TORC2 is not activated as part of the UPR. In fact, I found that TORC2-dependent phosphorylation of Ypk1 was lower in the tunicamycin-treated cells than in the matched control cells. This result could be explained if factors evoked by the UPR upregulate sphingolipid biosynthesis independently of TORC2 because it is clear from prior work in our laboratory (Roelants et al., 2011) that sphingolipids act in a negative feedback loop (Figure 5.2B) to hold TORC2 activity in check. Other observations also support this conclusion. For example, compared to wild-type cells, in various mutants in which sphingolipid biosynthesis is compromised (e.g., *lcb3Δ, csg2Δ* and *sur1Δ*) TORC2 activity is higher, as judged by increased phosphorylation of Ypk1 at Thr662 (Berchtold et al., 2012). However, in *ipt1Δ* cells, which lack the enzyme that converts MIPC to $M(IP)_2$, there was no increase in Thr662 phosphorylation (Berchtold et al., 2012), suggesting that production of IPC and/or MIPC is sufficient to mediate the feedback inhibition of TORC2 activity. There is some evidence that the activity of Ypk1 itself is required for this regulatory effect; for example, treatment of *ypk1$^{as}$ ypk2Δ* cells with the inhibitory analog 1-NM-PP1 increased TORC2-dependent phosphorylation of Ypk1 at Thr662 (Berchtold et al., 2012). However, it is also possible that this regulatory loop is actually exerted by Fpk1 (and its paralog Fpk2) because Ypk1 negatively regulates Fpk1 function and sphingolipids are required for Fpk1 activity. So, when Ypk1 is inhibited or sphingolipids are high, or both, Fpk1 is maximally active (Roelants et al., 2010).

It has been reported that *de novo* sphingolipid synthesis is required for the transport of newly synthesized GPI-anchored proteins from the ER to the Golgi. This requirement arises from the fact that maturation of the lipid moiety of GPI-anchored proteins requires the attachment of sphingolipid pathway-derived IPC (Umemura et al. 2007). Thus, treatment with Myr to block sphingolipid biosynthesis causes a rapid reduction in the ER-to-Golgi transport of GPI-anchored proteins (Horvath et al., 1994). Interestingly, the outer layer of the cell wall is highly enriched for GPI-anchored proteins (De Groot et al., 2003). The *S. cerevisiae* genome encodes for

approximately 70 GPI-anchored proteins (Caro et al., 1997) and about half of them reside in the cell wall (Smits et al., 1999). Induction of ER stress by tunicamycin, d-deoxyglucose or DTT triggers the activation of the CWI pathway illustrating the important functional relationship between ER protein metabolism and cell wall maintenance (Levin, 2011). Thus, by regulating sphingolipid biosynthesis, TORC2 also promotes cell wall integrity by ensuring the proper transport of GPI-anchored proteins through the secretory pathway to their final destination in the cell wall.

**FIGURE 5.2**

A

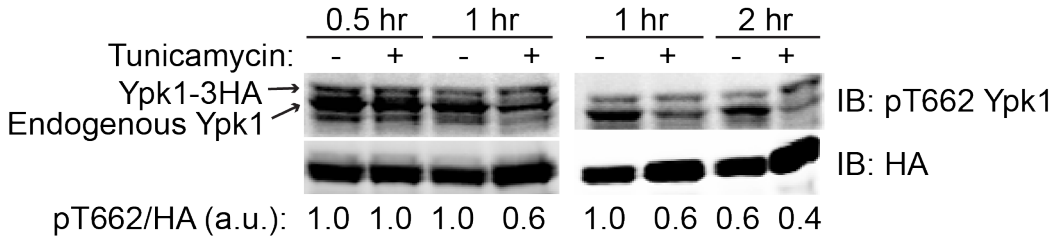


B

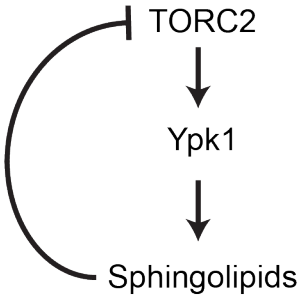


**Figure 5.2. The Unfolded Protein Response (UPR) does not activate TORC2.** (A) Wild-type (BY4741) cells expressing Ypk1-3HA (pLB215) were grown in SCD-Ura to mid-exponential phase and then treated with either vehicle (DMSO) or 1 μg/mL tunicamycin for the indicated time points prior to harvesting. Whole cell extracts were prepared, resolved by SDS-PAGE and analyzed by immunoblotting with anti-phosphoT662 Ypk1 and anti-HA antibodies. (B) Sphingolipids impose negative feedback on TORC2-Ypk1 signaling.

**Low extracellular glucose diminishes TORC2 activity**. The TOR complexes are generally thought of as master regulators of cell growth (Gonzales and Hall, 2017; Saxton and Sabatini, 2017). Growth requires sufficient levels of energy as well as cellular building blocks, such as amino acids, sugars and nucleotides. TORC1 has a well-established role in balancing anabolic and catabolic processes to regulate cell growth (Loewith and Hall, 2011; Dibble and Manning, 2013). In yeast, acute starvation for carbon, nitrogen, phosphate or amino acids all rapidly decreases TORC1 phosphorylation of its downstream substrate, the AGC-family protein kinase Sch9 (Urban et al., 2007; Binda et al., 2009). Less is known about how nutrient levels affect yeast TORC2 activity (Gaubitz et al., 2016). Mammalian TORC2 (mTORC2) promotes glucose uptake and metabolism in response to insulin signaling, although the mechanisms that connect insulin action and mTORC2 function are not well understood (Whiteman et al., 2002; Sarbassov et al., 2005; Manning and Cantley, 2007). It is possible that a downstream effector of mTORC2, like the protein kinases AKT and/or SGK, promote glucose uptake by phosphorylating and impeding the action of the mammalian a-arrestin TXNIP, which is known to down-regulate the mammalian glucose transporter GLUT1 (Wu et al., 2013), akin to what has been observed for Ypk1-mediated phosphorylation, which blocks the function of the yeast a-arrestin Rod1 (Alvaro et al., 2016).

Recently, it has been shown that *S. pombe* TORC2 (*Sp*TORC2) is activated by glucose in a manner that depends on the small Rab family GTPase Ryh1 (Tatebe et al., 2010; Hatano et al., 2015). Inducing glucose starvation by transferring cells grown in 2% dextrose to 0.02% dextrose rapidly, but transiently, diminished *Sp*TORC2-mediated phosphorylation of Gad8 (the *S. pombe* Ypk1 homolog) at its hydrophobic motif (Hatano et al., 2015). Addition of glucose to the medium restored *Sp*TORC2-dependent phosphorylation of Gad8. Expression of a dominant GTP-locked Ryh1 mutant, Ryh1(Q70L), was sufficient to maintain Gad8 in its SpTORC2-phosphorylated state, even after glucose depletion, indicating that *Sp*TORC2 somehow senses glucose levels in a manner that depends on the Ryh1 GTPase (Hatano et al., 2015).

Although it had not been shown previously that the exogenous glucose supply affects *Sc*TORC2 function, hints in the published literature suggested that this might be the case. In collaborative studies, our laboratory showed that TORC2-activated Ypk1 phosphorylates and inhibits the glycerol-3-phosphate dehydrogenase Gpd1, whereas its paralog Gpd2, which also functions in NADH-dependent reduction of dihydroxyacetone phosphate to glycerol-3-phosphate, is phosphorylated and inhibited by Snf1, the yeast ortholog of mammalian AMPK (Lee et al., 2012). Although Gpd1 and Gpd2 catalyze the same reaction, they have different functions in the cell and are regulated reciprocally in response to different environmental conditions. The main role of Gpd1 is to synthesize glycerol in response to hyperosmotic stress. Gpd1 activity and *GPD1* transcription are both upregulated upon hyperosmotic stress. Gpd2, on the other hand, functions primarily in cellular energy generation via its role in a mitochondrial redox shuttle that is important during aerobic growth. Given this function, negative regulation of Gpd2 by Snf1 makes physiological sense; Snf1 is activated mainly by AMP and ADP, which accumulate when ATP levels in the cell fall precipitously, such as when the glucose supply is low (Hardie, 2007; Hedbacker and Carlson, 2008; Oakhill et al., 2012; Carling, 2017). Conversely, Ypk1-mediated phosphorylation of Gpd1 is significantly decreased by 90 min after cells are shifted from high (2%) glucose medium to low (0.05%) glucose medium for 90 minutes (Lee et al., 2012), suggesting that Ypk1-dependent modification is less efficient when glucose availability is low. One explanation for that response would be if TORC2 is less active in phosphorylating Ypk1 under low-conditions. Therefore, as a readout of TORC2 function, I examined Ypk1

hydrophobic motif phosphorylation after shifting cells from high glucose medium to low glucose medium (Figure 5.3). I found that after 90 min in low glucose medium, Ypk1 was significantly less phosphorylated by TORC2 indicating that glucose depletion down-regulates TORC2 function. The TORC2 subunits Avo1 and Avo3 both have putative Ras-interacting domains. In *S. cerevisiae,* the small GTPase Ras regulates cell growth by activating adenylate cyclase which stimulates the production of 3',5'-cyclic AMP (cAMP), leading to activation of the cAMP-activated protein kinase PKA (in yeast, the catalytic subunits are Tpk1, Tpk2 and Tpk3 and the regulatory subunit is Bcy1). As a small GTPase, Ras is active when bound to GTP and inactive when bound to GDP (Boguski and McCormick, 1993). The nucleotide state of Ras is determined by the activities of its guanine exchange factor (GEF) Cdc25 (Lai et al., 1993) and GTPase-activating proteins (GAPs) Ira1 and Ira2 (Parrini et al., 1996). The addition of glucose to glucose-starved cells causes a rapid increase in the amount of GTP-bound Ras (Rudoni et al., 2001) and a subsequent increase in cAMP (Colombo et al., 2004). Although the regulation of TORC2 by glucose in *S. pombe* is reportedly independent of Ras-cAMP signaling (Hatano et al., 2015), it is possible that Ras or some other small Ras super-family GTPase might be involved in regulating TORC2 in *S. cerevisiae*. One way this hypothesis could be tested would be to monitor TORC2-mediated phosphorylation of Ypk1 after shifting cells from high glucose medium to low glucose medium in strains in which overexpression of constitutively GTP-locked or GDP-locked alleles of Ras or other candidate small GTPases has been induced.

TORC2 has been implicated in regulating the pentose phosphate pathway (PPP), which branches from glycolysis after the first committed step in glucose metabolism (Kliegman et al., 2013; Patra and Hay, 2014). The PPP produces several important metabolites that are needed for anabolic growth: the reducing equivalent NADPH, which is required for fatty acid synthesis, and pentose sugars for nucleic acid synthesis (Patra and Hay, 2014). Interestingly, NADPH also functions as a ROS scavenger (Patra and Hay, 2014). Inhibition of an analog-sensitive TORC2 allele causes a rapid reduction in multiple PPP metabolites, demonstrating that TORC2 activity stimulates PPP flux (Kliegman et al., 2013). My finding that TORC2 activity is reduced on low glucose can be readily rationalized; when carbon supply is limiting, down-modulation of TORC2 would cause a decrease in anabolic processes, like diminishing pentose sugar production with concomitant effects on cellular redox balance.

**FIGURE 5.3**

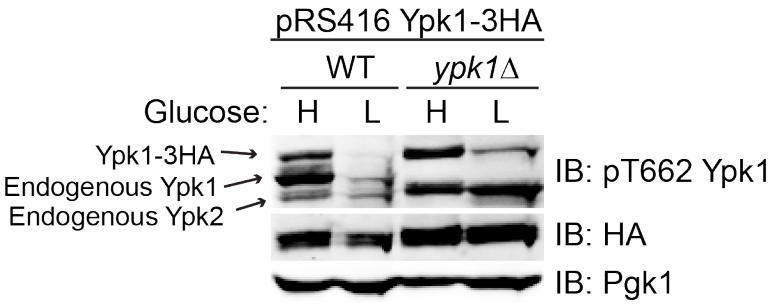


**Figure 5.3**. **TORC2 is down-regulated in glucose-limiting conditions**. BY4741 or otherwise isogenic *ypk1Δ* cells expressing Ypk1-3HA (pLB215) were grown to exponential phase in SC-Ura medium containing 2% dextrose/glucose and then a portion of the cells were shifted to prewarmed SC-Ura medium containing 0.05% dextrose/glucose. After 90 min, the cells were harvested and whole-cell extracts were prepared, resolved by SDS-PAGE and analyzed by immunoblotting with anti-phosphoT662 Ypk1, anti-HA and anti-Pgk1 antibodies.

**TORC2 coordinates with multiple signaling pathways to maintain cellular homeostasis**. Cells continuously sense their internal and external environments and alter their metabolism in order to maintain homeostasis. The TORC2 signaling network is an essential part of this homeostatic regulation. TORC2 activity is modulated in response to a variety of perturbations; these include osmotic changes, temperature fluctuations, alterations in PM sphingolipid composition and glucose availability. TORC2 responds to these perturbations by regulating the activity of its downstream effector Ypk1. I have shown that, in addition to phosphorylating Ypk1 at the turn and hydrophobic motifs, TORC2 also phosphorylates Ypk1 at four conserved residues in the C-terminus and that phosphorylation at these sites is necessary for efficient hydrophobic motif phosphorylation and full Ypk1 activation. TORC2-mediated phosphorylation of Ypk1 at multiple sites likely acts as a rheostat by which Ypk1 activity can be fine-tuned to meet the needs of the cell.

Homeostatic maintenance requires coordination between TORC2 and other signaling pathways (Figure 5.4). This coordination occurs both downstream and upstream of TORC2. Separately from the effects of its TORC2-mediated phosphorylation, Ypk1 activity is also regulated by phosphorylation at the activation loop by Pkh1 and Pkh2 (Casamayor et al., 1999). Activation loop phosphorylation is required for basal Ypk1 activity (Roelants et al., 2004) and certain stresses, such as heat shock, enhance Pkh-dependent phosphorylation of Ypk1 (Omnus et al., 2016). The phosphatase PP2A opposes Ypk1 activation loop phosphorylation (Roelants et al., 2011). Thus, by regulating basal Ypk1 activity, Pkh1/Pkh2 and PP2A indirectly impact TORC2-dependent signaling. The phosphatase(s) that counteract the TORC2-dependent phosphorylations on Ypk1 is not yet known. Identification of this phosphatase will reveal an additional layer of regulation of TORC2 signaling.

The TORC2-Ypk1 signaling axis is coordinated with the CWI pathway to promote proper actin polarization as well as cell wall maintenance and growth. First, by stimulating sphingolipid production, TORC2 ensures the efficient synthesis and trafficking of GPI-anchored cell wall proteins to the cell wall. Second, by maintaining proper lipid organization of the PM, TORC2 promotes the proper PM localization of Rom2 and Rho1 to bud tips to activate the CWI pathway (Niles and Powers, 2014; Hatakeyama et al., 2017). In addition to being activated by cell wall stress, the CWI pathway is also activated at specific points in the cell cycle to stimulate cell wall remodeling and promote polarized growth. Interestingly, TORC2 signaling has been implicated in G2/M cell cycle progression (Gaubitz et al., 2015). An analogous situation has been observed in mammalian cells; activity of the mTORC2-substrate Akt fluctuates throughout the cell cycle (Liu et al., 2014). Therefore, it seems likely that *Sc*TORC2 may coordinate growth at the PM and cell wall with cell cycle progression. Thus, it would be interesting to examine TORC2 and Ypk1 activity at different stages during cell cycle progression to determine whether TORC2 signaling is regulated in a cell cycle-coupled manner.

TORC2 regulation complements the HOG pathway in responding to hyperosmotic stress. Exposure to hypertonic conditions rapidly down-regulates TORC2-Ypk1 signaling, transiently increasing Gdp1 activity and glycerol production and closing the Fps1 channel to enhance intracellular glycerol accumulation (Muir et al., 2015). These effects then are reinforced when hypertonic conditions activate the HOG pathway, which occurs with somewhat slower kinetics (Westfall et al., 2008), because activated Hog1 elevates Gpd1 activity by upregulating *GPD1* gene expression (Albertyn et al., 1994) and maintaining the closed state of the Fps1 channel by phosphorylating and inhibiting its positive channel-opening effectors (Lee et al., 2013).

Conversely, hypotonic conditions stimulate TORC2 as well as the CWI pathway. Thus, TORC2, the CWI pathway and the HOG pathway all contribute to ensuring cell survival in response to osmotic stresses.

Upstream of TORC2, I have shown that the CWI and HOG MAPKs Slt2 and Hog1 negatively regulate TORC2 signaling. Negative feedback loops are a common mechanism for regulating signaling pathways. Sphingolipids are known to mediate a negative feedback loop in which TORC2 activity stimulates sphingolipid production and sphingolipids, in turn, down-regulate TORC2 activity (Olson et al. 2016). Slt2 and Hog1 participate in elaborate feedback loops with each other and with TORC2 to fine tune cellular responses. Slt2 likely functions in a negative feedback loop as TORC2 signaling promotes Slt2 activation and Slt2 down-regulates TORC2 signaling. Hog1-mediated down-regulation of TORC2 would, as described in the preceding paragraph, presumably help sustain the processes required for cells to respond effectively to hyperosmotic stress.

In conclusion, TORC2 integrates multiple signals including MAPK activation, PM tension and glucose availability to balance cell growth with adaptive stress responses. TORC2 coordinates with the CWI and HOG MAPK pathways to preserve the integrity of the cell wall and PM. In turn, the CWI and HOG MAPKs regulate TORC2 signaling by promoting the phosphorylation of TORC2 itself. Although more research is needed to fully elucidate the molecular mechanisms governing TORC2 activity, it is clear that TORC2 is a nodal point and essential regulator of the pathways that control cellular homeostasis.

**FIGURE 5.4**

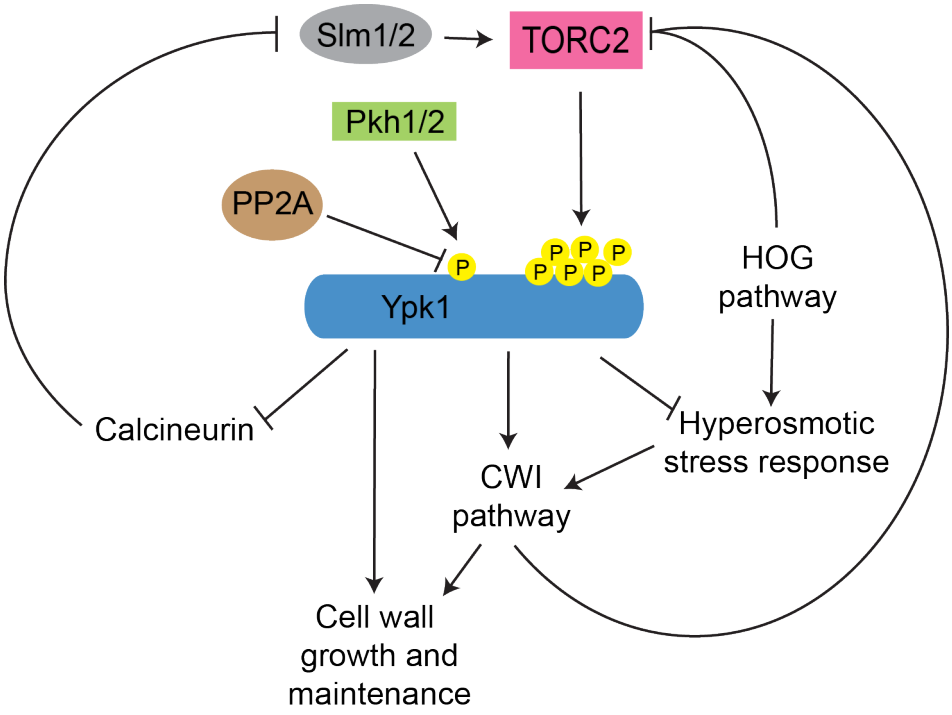


**Figure 5.4. Coordination between TORC2, calcineurin, CWI and HOG signaling.** Reciprocal regulation of TORC2 and calcineurin signaling balances anabolic growth with adaptive stress responses. TORC2 coordinates with the CWI and HOG MAPK signaling pathways to ensure the integrity of the PM and cell wall. In turn, the CWI and HOG MAPKs regulate TORC2 signaling in order to maintain homeostasis.

**REFERENCES**


Alberts, A.S., N. Bouquin, L.H. Johnston, and R. Treisman. 1998. Analysis of RhoA-binding proteins reveals an interaction domain conserved in heterotrimeric G protein beta subunits and the yeast response regulator protein Skn7. *J Biol Chem*. 273:8616-8622.

Albertyn, J., S. Hohmann, J.M. Thevelein, and B.A. Prior. 1994. *GPD1*, which encodes glycerol-3-phosphate dehydrogenase, is essential for growth under osmotic stress in Saccharomyces cerevisiae, and its expression is regulated by the high-osmolarity glycerol response pathway. *Mol Cell Biol*. 14:4135-4144.

Alvarez-Vasquez, F., K.J. Sims, L.A. Cowart, Y. Okamoto, E.O. Voit, and Y.A. Hannun. 2005. Simulation and validation of modelled sphingolipid metabolism in Saccharomyces cerevisiae. *Nature*. 433:425-430.

Alvaro, C.G., A. Aindow, and J. Thorner. 2016. Differential Phosphorylation Provides a Switch to Control How α-Arrestin Rod1 Down-regulates Mating Pheromone Response in Saccharomyces cerevisiae. *Genetics*. 203:299-317.

Aronova, S., K. Wedaman, P.A. Aronov, K. Fontes, K. Ramos, B.D. Hammock, and T. Powers. 2008. Regulation of ceramide biosynthesis by TOR complex 2. *Cell Metab*. 7:148-158.

Audhya, A., R. Loewith, A.B. Parsons, L. Gao, M. Tabuchi, H. Zhou, C. Boone, M.N. Hall, and S.D. Emr. 2004. Genome-wide lethality screen identifies new PI4,5P2 effectors that regulate the actin cytoskeleton. *EMBO J*. 23:3747-3757.

Aylett, C.H., E. Sauer, S. Imseng, D. Boehringer, M.N. Hall, N. Ban, and T. Maier. 2016. Architecture of human mTOR complex 1. *Science*. 351:48-52.

Baretić, D., A. Berndt, Y. Ohashi, C.M. Johnson, and R.L. Williams. 2016. Tor forms a dimer through an N-terminal helical solenoid with a complex topology. *Nat Commun*. 7:11016.

Bartlett, K., and K. Kim. 2014. Insight into Tor2, a budding yeast microdomain protein. *Eur J Cell Biol*. 93:87-97.

Baum, P., J. Thorner, and L. Honig. 1978. Identification of tubulin from the yeast Saccharomyces cerevisiae. *Proc Natl Acad Sci U S A*. 75:4962-4966.

Beeler, T., D. Bacikova, K. Gable, L. Hopkins, C. Johnson, H. Slife, and T. Dunn. 1998. The Saccharomyces cerevisiae TSC10/YBR265w gene encoding 3-ketosphinganine reductase is identified in a screen for temperature-sensitive suppressors of the Ca2+-sensitive csg2Delta mutant. *J Biol Chem*. 273:30688-30694.

Bender, A., and J.R. Pringle. 1992. A Ser/Thr-rich multicopy suppressor of a cdc24 bud emergence defect. *Yeast*. 8:315-323.

Berchtold, D., M. Piccolis, N. Chiaruttini, I. Riezman, H. Riezman, A. Roux, T.C. Walther, and R. Loewith. 2012. Plasma membrane stress induces relocalization of Slm proteins and activation of TORC2 to promote sphingolipid synthesis. *Nat Cell Biol*. 14:542-547.

Berchtold, D., and T.C. Walther. 2009. TORC2 plasma membrane localization is essential for cell viability and restricted to a distinct domain. *Mol Biol Cell*. 20:1565-1575.

Binda, M., M.P. Péli-Gulli, G. Bonfils, N. Panchaud, J. Urban, T.W. Sturgill, R. Loewith, and C. De Virgilio. 2009. The Vam6 GEF controls TORC1 by activating the EGO complex. *Mol Cell*. 35:563-573.

Boguski, M.S., and F. McCormick. 1993. Proteins regulating Ras and its relatives. *Nature*. 366:643-654.

Bouwman, J., J. Kiewiet, A. Lindenbergh, K. van Eunen, M. Siderius, and B.M. Bakker. 2011. Metabolic regulation rather than de novo enzyme synthesis dominates the osmo-

adaptation of yeast. *Yeast*. 28:43-53.
Breslow, D.K., S.R. Collins, B. Bodenmiller, R. Aebersold, K. Simons, A. Shevchenko, C.S. Ejsing, and J.S. Weissman. 2010. Orm family proteins mediate sphingolipid homeostasis. *Nature*. 463:1048-1053.
Brewster, J.L., and M.C. Gustin. 2014. Hog1: 20 years of discovery and impact. *Sci Signal*. 7:re7.
Brognard, J., E. Sierecki, T. Gao, and A.C. Newton. 2007. PHLPP and a second isoform, PHLPP2, differentially attenuate the amplitude of Akt signaling by regulating distinct Akt isoforms. *Mol Cell*. 25:917-931.
Brown, E.J., M.W. Albers, T.B. Shin, K. Ichikawa, C.T. Keith, W.S. Lane, and S.L. Schreiber. 1994a. A mammalian protein targeted by G1-arresting rapamycin-receptor complex. *Nature*. 369:756-758.
Brown, J.L., H. Bussey, and R.C. Stewart. 1994b. Yeast Skn7p functions in a eukaryotic two-component regulatory pathway. *EMBO J*. 13:5186-5194.
Brown, J.L., S. North, and H. Bussey. 1993. SKN7, a yeast multicopy suppressor of a mutation affecting cell wall beta-glucan assembly, encodes a product with domains homologous to prokaryotic two-component regulators and to heat shock transcription factors. *J Bacteriol*. 175:6908-6915.
Bultynck, G., Heath, V.L., Majeed, A.P., Galan, J.M., Haguenauer-Tsapis, R., and Cyert, M.S. (2006). Slm1 and Slm2 are novel substrates of the calcineurin phosphatase required for heat stress-induced endocytosis of the yeast uracil permease. . Mol Cell Biol 26: 4729–4745.
Cameron, A.J., M.D. Linch, A.T. Saurin, C. Escribano, and P.J. Parker. 2011. mTORC2 targets AGC kinases through Sin1-dependent recruitment. *Biochem J*. 439:287-297.
Carling, D. 2017. AMPK signalling in health and disease. *Curr Opin Cell Biol*. 45:31-37.
Caro, L.H., H. Tettelin, J.H. Vossen, A.F. Ram, H. van den Ende, and F.M. Klis. 1997. In silicio identification of glycosyl-phosphatidylinositol-anchored plasma-membrane and cell wall proteins of Saccharomyces cerevisiae. *Yeast*. 13:1477-1489.
Casamayor, A., P.D. Torrance, T. Kobayashi, J. Thorner, and D.R. Alessi. 1999. Functional counterparts of mammalian protein kinases PDK1 and SGK in budding yeast. *Curr Biol*. 9:186-197.
Chen, P., K.S. Lee, and D.E. Levin. 1993. A pair of putative protein kinase genes (YPK1 and YPK2) is required for cell growth in Saccharomyces cerevisiae. *Mol Gen Genet*. 236:443-447.
Chen, R.E., and J. Thorner. 2007. Function and regulation in MAPK signaling pathways: lessons learned from the yeast Saccharomyces cerevisiae. *Biochim Biophys Acta*. 1773:1311-1340.
Chiu, M.I., H. Katz, and V. Berlin. 1994. RAPT1, a mammalian homolog of yeast Tor, interacts with the FKBP12/rapamycin complex. *Proc Natl Acad Sci U S A*. 91:12574-12578.
Cliften, P., P. Sudarsanam, A. Desikan, L. Fulton, B. Fulton, J. Majors, R. Waterston, B.A. Cohen, and M. Johnston. 2003. Finding functional features in Saccharomyces genomes by phylogenetic footprinting. *Science*. 301:71-76.
Clotet, J., X. Escoté, M.A. Adrover, G. Yaakov, E. Garí, M. Aldea, E. de Nadal, and F. Posas. 2006. Phosphorylation of Hsl1 by Hog1 leads to a G2 arrest essential for cell survival at high osmolarity. *EMBO J*. 25:2338-2346.
Colicelli, J., C. Nicolette, C. Birchmeier, L. Rodgers, M. Riggs, and M. Wigler. 1991. Expression of three mammalian cDNAs that interfere with RAS function in Saccharomyces cerevisiae.

*Proc Natl Acad Sci U S A*. 88:2913-2917.
Colombo, S., D. Ronchetti, J.M. Thevelein, J. Winderickx, and E. Martegani. 2004. Activation state of the Ras2 protein and glucose-induced signaling in Saccharomyces cerevisiae. *J Biol Chem*. 279:46715-46722.
Costanzo, M., A. Baryshnikova, J. Bellay, Y. Kim, E.D. Spear, C.S. Sevier, H. Ding, J.L. Koh, K. Toufighi, S. Mostafavi, J. Prinz, R.P. St Onge, B. VanderSluis, T. Makhnevych, F.J. Vizeacoumar, S. Alizadeh, S. Bahr, R.L. Brost, Y. Chen, M. Cokol, R. Deshpande, Z. Li, Z.Y. Lin, W. Liang, M. Marback, J. Paw, B.J. San Luis, E. Shuteriqi, A.H. Tong, N. van Dyk, I.M. Wallace, J.A. Whitney, M.T. Weirauch, G. Zhong, H. Zhu, W.A. Houry, M. Brudno, S. Ragibizadeh, B. Papp, C. Pál, F.P. Roth, G. Giaever, C. Nislow, O.G. Troyanskaya, H. Bussey, G.D. Bader, A.C. Gingras, Q.D. Morris, P.M. Kim, C.A. Kaiser, C.L. Myers, B.J. Andrews, and C. Boone. 2010. The genetic landscape of a cell. *Science*. 327:425-431.
Cullen, P.J., W. Sabbagh, E. Graham, M.M. Irick, E.K. van Olden, C. Neal, J. Delrow, L. Bardwell, and G.F. Sprague. 2004. A signaling mucin at the head of the Cdc42- and MAPK-dependent filamentous growth pathway in yeast. *Genes Dev*. 18:1695-1708.
Cyert, M.S. 2003. Calcineurin signaling in Saccharomyces cerevisiae: how yeast go crazy in response to stress. *Biochem Biophys Res Commun*. 311:1143-1150.
Daquinag, A., Fadri, M., Jung, S.Y., Qin, J., and Kunz, J. (2007). The yeast PH domain proteins Slm1 and Slm2 are targets of sphingolipid signaling during the response to heat stress. Mol Cell Biol 27: 633-650.
De Groot, P.W., K.J. Hellingwerf, and F.M. Klis. 2003. Genome-wide identification of fungal GPI proteins. *Yeast*. 20:781-796.
deHart, A.K., J.D. Schnell, D.A. Allen, and L. Hicke. 2002. The conserved Pkh-Ypk kinase cascade is required for endocytosis in yeast. *J Cell Biol*. 156:241-248.
deHart, A.K., J.D. Schnell, D.A. Allen, J.Y. Tsai, and L. Hicke. 2003. Receptor internalization in yeast requires the Tor2-Rho1 signaling pathway. *Mol Biol Cell*. 14:4676-4684.
de Nadal, E., and F. Posas. 2015. Osmostress-induced gene expression--a model to understand how stress-activated protein kinases (SAPKs) regulate transcription. *FEBS J*. 282:3275-3285.
Denis, V., and M.S. Cyert. 2002. Internal Ca(2+) release in yeast is triggered by hypertonic shock and mediated by a TRP channel homologue. *J Cell Biol*. 156:29-34.
Dibble, C.C., and B.D. Manning. 2013. Signal integration by mTORC1 coordinates nutrient input with biosynthetic output. *Nat Cell Biol*. 15:555-564.
Dickson, R.C., C. Sumanasekera, and R.L. Lester. 2006. Functions and metabolism of sphingolipids in Saccharomyces cerevisiae. *Prog Lipid Res*. 45:447-465.
Divito, C.B., and S.G. Amara. 2009. Close encounters of the oily kind: regulation of transporters by lipids. *Mol Interv*. 9:252-262.
D'mello, N.P., A.M. Childress, D.S. Franklin, S.P. Kale, C. Pinswasdi, and S.M. Jazwinski. 1994. Cloning and characterization of LAG1, a longevity-assurance gene in yeast. *J Biol Chem*. 269:15451-15459.
Drogen, F., S.M. O'Rourke, V.M. Stucke, M. Jaquenoud, A.M. Neiman, and M. Peter. 2000. Phosphorylation of the MEKK Ste11p by the PAK-like kinase Ste20p is required for MAP kinase signaling in vivo. *Curr Biol*. 10:630-639.

Dunn, T.M., D.V. Lynch, L.V. Michaelson, and J.A. Napier. 2004. A post-genomic approach to understanding sphingolipid metabolism in Arabidopsis thaliana. *Ann Bot*. 93:483-497.
Ekiel, I., T. Sulea, G. Jansen, M. Kowalik, O. Minailiuc, J. Cheng, D. Harcus, M. Cygler, M. Whiteway, and C. Wu. 2009. Binding the atypical RA domain of Ste50p to the unfolded Opy2p cytoplasmic tail is essential for the high-osmolarity glycerol pathway. *Mol Biol Cell*. 20:5117-5126.
Eltschinger, S., and R. Loewith. 2016. TOR Complexes and the Maintenance of Cellular Homeostasis. *Trends Cell Biol*. 26:148-159.
Epstein, S., C.L. Kirkpatrick, G.A. Castillon, M. Muñiz, I. Riezman, F.P. David, C.B. Wollheim, and H. Riezman. 2012. Activation of the unfolded protein response pathway causes ceramide accumulation in yeast and INS-1E insulinoma cells. *J Lipid Res*. 53:412-420.
Facchinetti, V., W. Ouyang, H. Wei, N. Soto, A. Lazorchak, C. Gould, C. Lowry, A.C. Newton, Y. Mao, R.Q. Miao, W.C. Sessa, J. Qin, P. Zhang, B. Su, and E. Jacinto. 2008. The mammalian target of rapamycin complex 2 controls folding and stability of Akt and protein kinase C. *EMBO J*. 27:1932-1943.
Fassler, J.S., W.M. Gray, C.L. Malone, W. Tao, H. Lin, and R.J. Deschenes. 1997. Activated alleles of yeast SLN1 increase Mcm1-dependent reporter gene expression and diminish signaling through the Hog1 osmosensing pathway. *J Biol Chem*. 272:13365-13371.
Fassler, J.S., and A.H. West. 2010. Genetic and biochemical analysis of the SLN1 pathway in Saccharomyces cerevisiae. *Methods Enzymol*. 471:291-317.
Fernandis, A.Z., and M.R. Wenk. 2007. Membrane lipids as signaling molecules. *Curr Opin Lipidol*. 18:121-128.
Francois, J.M. 2016. Cell Surface Interference with Plasma Membrane and Transport Processes in Yeasts. *Adv Exp Med Biol*. 892:11-31.
Free, S.J. 2013. Fungal cell wall organization and biosynthesis. *Adv Genet*. 81:33-82.
Fröhlich, F., D.K. Olson, R. Christiano, R.V. Farese, and T.C. Walther. 2016. Proteomic and phosphoproteomic analyses of yeast reveal the global cellular response to sphingolipid depletion. *Proteomics*. 16:2759-2763.
Fuchs, B.B., and E. Mylonakis. 2009. Our paths might cross: the role of the fungal cell wall integrity pathway in stress response and cross talk with other stress response pathways. *Eukaryot Cell*. 8:1616-1625.
Gallego, O., M.J. Betts, J. Gvozdenovic-Jeremic, K. Maeda, C. Matetzki, C. Aguilar-Gurrieri, P. Beltran-Alvarez, S. Bonn, C. Fernández-Tornero, L.J. Jensen, M. Kuhn, J. Trott, V. Rybin, C.W. Müller, P. Bork, M. Kaksonen, R.B. Russell, and A.C. Gavin. 2010. A systematic screen for protein-lipid interactions in Saccharomyces cerevisiae. *Mol Syst Biol*. 6:430.
García-Rodríguez, L.J., R. Valle, A. Durán, and C. Roncero. 2005. Cell integrity signaling activation in response to hyperosmotic shock in yeast. *FEBS Lett*. 579:6186-6190.
Gardner, B.M., D. Pincus, K. Gotthardt, C.M. Gallagher, and P. Walter. 2013. Endoplasmic reticulum stress sensing in the unfolded protein response. *Cold Spring Harb Perspect Biol*. 5:a013169.
Gasch, A.P., P.T. Spellman, C.M. Kao, O. Carmel-Harel, M.B. Eisen, G. Storz, D. Botstein, and P.O. Brown. 2000. Genomic expression programs in the response of yeast cells to environmental changes. *Mol Biol Cell*. 11:4241-4257.
Gatta, A.T., and T.P. Levine. 2017. Piecing Together the Patchwork of Contact Sites. *Trends Cell Biol*. 27:214-229.

Gaubitz, C., T.M. Oliveira, M. Prouteau, A. Leitner, M. Karuppasamy, G. Konstantinidou, D. Rispal, S. Eltschinger, G.C. Robinson, S. Thore, R. Aebersold, C. Schaffitzel, and R. Loewith. 2015. Molecular basis of the rapamycin insensitivity of Target Of Rapamycin Complex 2. *Mol Cell*. 58:977-988.

Gaubitz, C., M. Prouteau, B. Kusmider, and R. Loewith. 2016. TORC2 structure and function. *Trends Biochem Sci*. 41:532-545.

González, A., and M.N. Hall. 2017. Nutrient sensing and TOR signaling in yeast and mammals. *EMBO J*. 36:397-408.

Green, M.R, and J. Sambrook. 2012. Molecular Cloning: A Laboratory Manual. Cold Spring Harbor Laboratory Press, Cold Spring Harbor, NY. Vol. 1, pp. 1-630.

Grodsky, N., Y. Li, D. Bouzida, R. Love, J. Jensen, B. Nodes, J. Nonomiya, and S. Grant. 2006. Structure of the catalytic domain of human protein kinase C beta II complexed with a bisindolylmaleimide inhibitor. *Biochemistry*. 45:13970-13981.

Groves, J.T., and J. Kuriyan. 2010. Molecular mechanisms in signal transduction at the membrane. *Nat Struct Mol Biol*. 17:659-665.

Guerreiro, J.F., A. Muir, S. Ramachandran, J. Thorner, and I. Sá-Correia. 2016. Sphingolipid biosynthesis upregulation by TOR complex 2-Ypk1 signaling during yeast adaptive response to acetic acid stress. *Biochem J*. 473:4311-4325.

Guillas, I., P.A. Kirchman, R. Chuard, M. Pfefferli, J.C. Jiang, S.M. Jazwinski, and A. Conzelmann. 2001. C26-CoA-dependent ceramide synthesis of Saccharomyces cerevisiae is operated by Lag1p and Lac1p. *EMBO J*. 20:2655-2665.

Hahn, J.S., and D.J. Thiele. 2002. Regulation of the Saccharomyces cerevisiae Slt2 kinase pathway by the stress-inducible Sdp1 dual specificity phosphatase. *J Biol Chem*. 277:21278-21284.

Han, J., J.D. Lee, L. Bibbs, and R.J. Ulevitch. 1994. A MAP kinase targeted by endotoxin and hyperosmolarity in mammalian cells. *Science*. 265:808-811.

Hannun, Y.A., and L.M. Obeid. 2008. Principles of bioactive lipid signalling: lessons from sphingolipids. *Nat Rev Mol Cell Biol*. 9:139-150.

Hara, K., Y. Maruki, X. Long, K. Yoshino, N. Oshiro, S. Hidayat, C. Tokunaga, J. Avruch, and K. Yonezawa. 2002. Raptor, a binding partner of target of rapamycin (TOR), mediates TOR action. *Cell*. 110:177-189.

Hardie, D.G. 2007. AMP-activated/SNF1 protein kinases: conserved guardians of cellular energy. *Nat Rev Mol Cell Biol*. 8:774-785.

Harold, F.M. 2002. Force and compliance: rethinking morphogenesis in walled cells. *Fungal Genet Biol*. 37:271-282.

Hatakeyama, R., K. Kono, and S. Yoshida. 2017. Ypk1 and Ypk2 kinases maintain Rho1 at the plasma membrane by flippase-dependent lipid remodeling after membrane stresses. *J Cell Sci*. 130:1169-1178.

Hatano, T., S. Morigasaki, H. Tatebe, K. Ikeda, and K. Shiozaki. 2015. Fission yeast Ryh1 GTPase activates TOR Complex 2 in response to glucose. *Cell Cycle*. 14:848-856.

Hauge, C., T.L. Antal, D. Hirschberg, U. Doehn, K. Thorup, L. Idrissova, K. Hansen, O.N. Jensen, T.J. Jørgensen, R.M. Biondi, and M. Frödin. 2007. Mechanism for activation of the growth factor-activated AGC kinases by turn motif phosphorylation. *EMBO J*. 26:2251-2261.

Hedbacker, K., and M. Carlson. 2008. SNF1/AMPK pathways in yeast. *Front Biosci*. 13:2408-2420.

Heitman, J., N.R. Movva, and M.N. Hall. 1991. Targets for cell cycle arrest by the immunosuppressant rapamycin in yeast. *Science*. 253:905-909.
Helliwell, S.B., I. Howald, N. Barbet, and M.N. Hall. 1998a. TOR2 is part of two related signaling pathways coordinating cell growth in Saccharomyces cerevisiae. *Genetics*. 148:99-112.
Helliwell, S.B., A. Schmidt, Y. Ohya, and M.N. Hall. 1998b. The Rho1 effector Pkc1, but not Bni1, mediates signalling from Tor2 to the actin cytoskeleton. *Curr Biol*. 8:1211-1214.
Helliwell, S.B., P. Wagner, J. Kunz, M. Deuter-Reinhard, R. Henriquez, and M.N. Hall. 1994. TOR1 and TOR2 are structurally and functionally similar but not identical phosphatidylinositol kinase homologues in yeast. *Mol Biol Cell*. 5:105-118.
Hickman, M.J., D. Spatt, and F. Winston. 2011. The Hog1 mitogen-activated protein kinase mediates a hypoxic response in Saccharomyces cerevisiae. *Genetics*. 188:325-338.
Hohmann, S. 2015. An integrated view on a eukaryotic osmoregulation system. *Curr Genet*. 61:373-382.
Holt, L.J., B.B. Tuch, J. Villén, A.D. Johnson, S.P. Gygi, and D.O. Morgan. 2009. Global analysis of Cdk1 substrate phosphorylation sites provides insights into evolution. *Science*. 325:1682-1686.
Horvath, A., C. Sütterlin, U. Manning-Krieg, N.R. Movva, and H. Riezman. 1994. Ceramide synthesis enhances transport of GPI-anchored proteins to the Golgi apparatus in yeast. *EMBO J*. 13:3687-3695.
Hsu, P.P., S.A. Kang, J. Rameseder, Y. Zhang, K.A. Ottina, D. Lim, T.R. Peterson, Y. Choi, N.S. Gray, M.B. Yaffe, J.A. Marto, and D.M. Sabatini. 2011. The mTOR-regulated phosphoproteome reveals a mechanism of mTORC1-mediated inhibition of growth factor signaling. *Science*. 332:1317-1322.
Ikai, N., N. Nakazawa, T. Hayashi, and M. Yanagida. 2011. The reverse, but coordinated, roles of Tor2 (TORC1) and Tor1 (TORC2) kinases for growth, cell cycle and separase-mediated mitosis in Schizosaccharomyces pombe. *Open Biol*. 1:110007.
Ikeda, K., S. Morigasaki, H. Tatebe, F. Tamanoi, and K. Shiozaki. 2008. Fission yeast TOR complex 2 activates the AGC-family Gad8 kinase essential for stress resistance and cell cycle control. *Cell Cycle*. 7:358-364.
Ikenoue, T., K. Inoki, Q. Yang, X. Zhou, and K.L. Guan. 2008. Essential function of TORC2 in PKC and Akt turn motif phosphorylation, maturation and signalling. *EMBO J*. 27:1919-1931.
Ikushiro, H., H. Hayashi, and H. Kagamiyama. 2004. Reactions of serine palmitoyltransferase with serine and molecular mechanisms of the actions of serine derivatives as inhibitors. *Biochemistry*. 43:1082-1092.
Inagaki, M., T. Schmelzle, K. Yamaguchi, K. Irie, M.N. Hall, and K. Matsumoto. 1999. PDK1 homologs activate the Pkc1-mitogen-activated protein kinase pathway in yeast. *Mol Cell Biol*. 19:8344-8352.
Iwamoto, K., T. Hayakawa, M. Murate, A. Makino, K. Ito, T. Fujisawa, and T. Kobayashi. 2007. Curvature-dependent recognition of ethanolamine phospholipids by duramycin and cinnamycin. *Biophys J*. 93:1608-1619.
Jacinto, E., R. Loewith, A. Schmidt, S. Lin, M.A. Rüegg, A. Hall, and M.N. Hall. 2004. Mammalian TOR complex 2 controls the actin cytoskeleton and is rapamycin insensitive. *Nat Cell Biol*. 6:1122-1128.

Jacoby, T., H. Flanagan, A. Faykin, A.G. Seto, C. Mattison, and I. Ota. 1997. Two protein-tyrosine phosphatases inactivate the osmotic stress response pathway in yeast by targeting the mitogen-activated protein kinase, Hog1. *J Biol Chem*. 272:17749-17755.

Jendretzki, A., J. Wittland, S. Wilk, A. Straede, and J.J. Heinisch. 2011. How do I begin? Sensing extracellular stress to maintain yeast cell wall integrity. *Eur J Cell Biol*. 90:740-744.

Jung, U.S., A.K. Sobering, M.J. Romeo, and D.E. Levin. 2002. Regulation of the yeast Rlm1 transcription factor by the Mpk1 cell wall integrity MAP kinase. *Mol Microbiol*. 46:781-789.

Kabeche, R., M. Madrid, J. Cansado, and J.B. Moseley. 2015. Eisosomes Regulate Phosphatidylinositol 4,5-Bisphosphate (PI(4,5)P2) Cortical Clusters and Mitogen-activated Protein (MAP) Kinase Signaling upon Osmotic Stress. *J Biol Chem*. 290:25960-25973.

Kabeche, R., A. Roguev, N.J. Krogan, and J.B. Moseley. 2014. A Pil1-Sle1-Syj1-Tax4 functional pathway links eisosomes with PI(4,5)P2 regulation. *J Cell Sci*. 127:1318-1326.

Kamada, Y., Y. Fujioka, N.N. Suzuki, F. Inagaki, S. Wullschleger, R. Loewith, M.N. Hall, and Y. Ohsumi. 2005. Tor2 directly phosphorylates the AGC kinase Ypk2 to regulate actin polarization. *Mol Cell Biol*. 25:7239-7248.

Kamada, Y., U.S. Jung, J. Piotrowski, and D.E. Levin. 1995. The protein kinase C-activated MAP kinase pathway of *Saccharomyces cerevisiae* mediates a novel aspect of the heat shock response. *Genes Dev*. 9:1559-1571.

Kamada, Y., H. Qadota, C.P. Python, Y. Anraku, Y. Ohya, and D.E. Levin. 1996. Activation of yeast protein kinase C by Rho1 GTPase. *J Biol Chem*. 271:9193-9196.

Karotki, L., J.T. Huiskonen, C.J. Stefan, N.E. Ziółkowska, R. Roth, M.A. Surma, N.J. Krogan, S.D. Emr, J. Heuser, K. Grünewald, and T.C. Walther. 2011. Eisosome proteins assemble into a membrane scaffold. *J Cell Biol*. 195: 889-902.

Kellis, M., N. Patterson, M. Endrizzi, B. Birren, and E.S. Lander. 2003. Sequencing and comparison of yeast species to identify genes and regulatory elements. *Nature*. 423:241-254.

Ketela, T., J.L. Brown, R.C. Stewart, and H. Bussey. 1998. Yeast Skn7p activity is modulated by the Sln1p-Ypd1p osmosensor and contributes to regulation of the HOG pathway. *Mol Gen Genet*. 259:372-378.

Ketela, T., R. Green, and H. Bussey. 1999. Saccharomyces cerevisiae mid2p is a potential cell wall stress sensor and upstream activator of the PKC1-MPK1 cell integrity pathway. *J Bacteriol*. 181:3330-3340.

Kim, D.H., D.D. Sarbassov, S.M. Ali, J.E. King, R.R. Latek, H. Erdjument-Bromage, P. Tempst, and D.M. Sabatini. 2002. mTOR interacts with raptor to form a nutrient-sensitive complex that signals to the cell growth machinery. *Cell*. 110:163-175.

Kinoshita, E., E. Kinoshita-Kikuta, and T. Koike. 2009. Separation and detection of large phosphoproteins using Phos-tag SDS-PAGE. *Nat Protoc*. 4:1513-1521.

Kinoshita E, Kinoshita-Kikuta E, Koike T. 2015. Advances in Phos-tag-based methodologies for separation and detection of the phosphoproteome. Biochim Biophys Acta 1854: 601– 608.

Kliegman, J.I., D. Fiedler, C.J. Ryan, Y.F. Xu, X.Y. Su, D. Thomas, M.C. Caccese, A. Cheng, M. Shales, J.D. Rabinowitz, N.J. Krogan, and K.M. Shokat. 2013. Chemical genetics of rapamycin-insensitive TORC2 in S. cerevisiae. *Cell Rep*. 5:1725-1736.

Klis, F.M., A. Boorsma, and P.W. De Groot. 2006. Cell wall construction in *Saccharomyces*

*cerevisiae*. *Yeast*. 23:185-202.
Kock, C., Y.F. Dufrêne, and J.J. Heinisch. 2015. Up against the wall: is yeast cell wall integrity ensured by mechanosensing in plasma membrane microdomains? *Appl Environ Microbiol*. 81:806-811.
Kohno, K., K. Normington, J. Sambrook, M.J. Gething, and K. Mori. 1993. The promoter region of the yeast KAR2 (BiP) gene contains a regulatory domain that responds to the presence of unfolded proteins in the endoplasmic reticulum. *Mol Cell Biol*. 13:877-890.
Komander, D., G. Kular, M. Deak, D.R. Alessi, and D.M. van Aalten. 2005. Role of T-loop phosphorylation in PDK1 activation, stability, and substrate binding. *J Biol Chem*. 280:18797-18802.
Krasley, E., K.F. Cooper, M.J. Mallory, R. Dunbrack, and R. Strich. 2006. Regulation of the oxidative stress response through Slt2p-dependent destruction of cyclin C in Saccharomyces cerevisiae. *Genetics*. 172:1477-1486.
Kunz, J., R. Henriquez, U. Schneider, M. Deuter-Reinhard, N.R. Movva, and M.N. Hall. 1993. Target of rapamycin in yeast, TOR2, is an essential phosphatidylinositol kinase homolog required for G1 progression. *Cell*. 73:585-596.
Lai, C.C., M. Boguski, D. Broek, and S. Powers. 1993. Influence of guanine nucleotides on complex formation between Ras and CDC25 proteins. *Mol Cell Biol*. 13:1345-1352.
Lamson, R.E., M.J. Winters, and P.M. Pryciak. 2002. Cdc42 regulation of kinase activity and signaling by the yeast p21-activated kinase Ste20. *Mol Cell Biol*. 22:2939-2951.
Lawrence, C.L., C.H. Botting, R. Antrobus, and P.J. Coote. 2004. Evidence of a new role for the high-osmolarity glycerol mitogen-activated protein kinase pathway in yeast: regulating adaptation to citric acid stress. *Mol Cell Biol*. 24:3307-3323.
Lebesgue, N., M. Megyeri, A. Cristobal, A. Scholten, S.G. Chuartzman, Y. Voichek, R.A. Scheltema, S. Mohammed, A.H. Futerman, M. Schuldiner, A.J. Heck, and S. Lemeer. 2017. Combining Deep Sequencing, Proteomics, Phosphoproteomics, and Functional Screens To Discover Novel Regulators of Sphingolipid Homeostasis. *J Proteome Res*. 16:571-582.
Lee, J., W. Reiter, I. Dohnal, C. Gregori, S. Beese-Sims, K. Kuchler, G. Ammerer, and D.E. Levin. 2013. MAPK Hog1 closes the S. cerevisiae glycerol channel Fps1 by phosphorylating and displacing its positive regulators. *Genes Dev*. 27:2590-2601.
Lee, S., F.I. Comer, A. Sasaki, I.X. McLeod, Y. Duong, K. Okumura, J.R. Yates, C.A. Parent, and R.A. Firtel. 2005. TOR complex 2 integrates cell movement during chemotaxis and signal relay in Dictyostelium. *Mol Biol Cell*. 16:4572-4583.
Lee, S., C.A. Parent, R. Insall, and R.A. Firtel. 1999. A novel Ras-interacting protein required for chemotaxis and cyclic adenosine monophosphate signal relay in Dictyostelium. *Mol Biol Cell*. 10:2829-2845.
Lee, Y.J., G.R. Jeschke, F.M. Roelants, J. Thorner, and B.E. Turk. 2012. Reciprocal phosphorylation of yeast glycerol-3-phosphate dehydrogenases in adaptation to distinct types of stress. *Mol Cell Biol*. 32:4705-4717.
Lev, S. 2010. Non-vesicular lipid transport by lipid-transfer proteins and beyond. *Nat Rev Mol Cell Biol*. 11:739-750.
Levin, D.E. 2011. Regulation of cell wall biogenesis in Saccharomyces cerevisiae: the cell wall integrity signaling pathway. *Genetics*. 189:1145-1175.
Li, S., S. Dean, Z. Li, J. Horecka, R.J. Deschenes, and J.S. Fassler. 2002. The eukaryotic two-

component histidine kinase Sln1p regulates OCH1 via the transcription factor, Skn7p. *Mol Biol Cell*. 13:412-424.
Liao, H.C., and M.Y. Chen. 2012. Target of rapamycin complex 2 signals to downstream effector yeast protein kinase 2 (Ypk2) through adheres-voraciously-to-target-of-rapamycin-2 protein 1 (Avo1) in *Saccharomyces cerevisiae*. *J Biol Chem*. 287:6089-6099.
Liu, P., M. Begley, W. Michowski, H. Inuzuka, M. Ginzberg, D. Gao, P. Tsou, W. Gan, A. Papa, B.M. Kim, L. Wan, A. Singh, B. Zhai, M. Yuan, Z. Wang, S.P. Gygi, T.H. Lee, K.P. Lu, A. Toker, P.P. Pandolfi, J.M. Asara, M.W. Kirschner, P. Sicinski, L. Cantley, and W. Wei. 2014. Cell-cycle-regulated activation of Akt kinase by phosphorylation at its carboxyl terminus. *Nature*. 508:541-545.
Loewith, R., and M.N. Hall. 2011. Target of rapamycin (TOR) in nutrient signaling and growth control. *Genetics*. 189:1177-1201.
Loewith, R., E. Jacinto, S. Wullschleger, A. Lorberg, J.L. Crespo, D. Bonenfant, W. Oppliger, P. Jenoe, and M.N. Hall. 2002. Two TOR complexes, only one of which is rapamycin sensitive, have distinct roles in cell growth control. *Mol Cell*. 10:457-468.
Lu, M., J. Wang, H.E. Ives, and D. Pearce. 2011. mSIN1 protein mediates SGK1 protein interaction with mTORC2 protein complex and is required for selective activation of the epithelial sodium channel. *J Biol Chem*. 286:30647-30654.
Maeda, T., M. Takekawa, and H. Saito. 1995. Activation of yeast PBS2 MAPKK by MAPKKKs or by binding of an SH3-containing osmosensor. *Science*. 269:554-558.
Maeda, T., A.Y. Tsai, and H. Saito. 1993. Mutations in a protein tyrosine phosphatase gene (PTP2) and a protein serine/threonine phosphatase gene (PTC1) cause a synthetic growth defect in Saccharomyces cerevisiae. *Mol Cell Biol*. 13:5408-5417.
Maeda, T., S.M. Wurgler-Murphy, and H. Saito. 1994. A two-component system that regulates an osmosensing MAP kinase cascade in yeast. *Nature*. 369:242-245.
Malhotra, J.D., and R.J. Kaufman. 2007. The endoplasmic reticulum and the unfolded protein response. *Semin Cell Dev Biol*. 18:716-731.
Manford, A.G., C.J. Stefan, H.L. Yuan, J.A. Macgurn, and S.D. Emr. 2012. ER-to-plasma membrane tethering proteins regulate cell signaling and ER morphology. *Dev Cell*. 23:1129-1140.
Manning, B.D., and L.C. Cantley. 2007. AKT/PKB signaling: navigating downstream. *Cell*. 129:1261-1274.
Mascaraque, V., M.L. Hernáez, M. Jiménez-Sánchez, R. Hansen, C. Gil, H. Martín, V.J. Cid, and M. Molina. 2013. Phosphoproteomic analysis of protein kinase C signaling in Saccharomyces cerevisiae reveals Slt2 mitogen-activated protein kinase (MAPK)-dependent phosphorylation of eisosome core components. *Mol Cell Proteomics*. 12:557-574.
McIsaac, R.S., S.J. Silverman, M.N. McClean, P.A. Gibney, J. Macinskas, M.J. Hickman, A.A. Petti, and D. Botstein. 2011. Fast-acting and nearly gratuitous induction of gene expression and protein depletion in Saccharomyces cerevisiae. *Mol Biol Cell*. 22:4447-4459.
Megyeri, M., H. Riezman, M. Schuldiner, and A.H. Futerman. 2016. Making Sense of the Yeast Sphingolipid Pathway. *J Mol Biol*. 428:4765-4775.

Miyake, Y., Y. Kozutsumi, S. Nakamura, T. Fujita, and T. Kawasaki. 1995. Serine palmitoyltransferase is the primary target of a sphingosine-like immunosuppressant, ISP-1/myriocin. *Biochem Biophys Res Commun*. 211:396-403.

Momoi, M., D. Tanoue, Y. Sun, H. Takematsu, Y. Suzuki, M. Suzuki, A. Suzuki, T. Fujita, and Y. Kozutsumi. 2004. SLI1 (YGR212W) is a major gene conferring resistance to the sphingolipid biosynthesis inhibitor ISP-1, and encodes an ISP-1 N-acetyltransferase in yeast. *Biochem J*. 381:321-328.

Morawska, M., and H.D. Ulrich. 2013. An expanded tool kit for the auxin-inducible degron system in budding yeast. *Yeast*. 30:341-351.

Muir, A., S. Ramachandran, F.M. Roelants, G. Timmons, and J. Thorner. 2014. TORC2-dependent protein kinase Ypk1 phosphorylates ceramide synthase to stimulate synthesis of complex sphingolipids. *Elife*. 3: e03779.1-e03779.34.

Muir, A., F.M. Roelants, G. Timmons, K.L. Leskoske, and J. Thorner. 2015. Down-regulation of TORC2-Ypk1 signaling promotes MAPK-independent survival under hyperosmotic stress. *Elife*. 4:e09336.1-e09336.13.

Mulet, J.M., D.E. Martin, R. Loewith, and M.N. Hall. 2006. Mutual antagonism of target of rapamycin and calcineurin signaling. *J Biol Chem*. 281:33000-33007.

Niles, B.J., A.C. Joslin, T. Fresques, and T. Powers. 2014. TOR complex 2-Ypk1 signaling maintains sphingolipid homeostasis by sensing and regulating ROS accumulation. *Cell Rep*. 6:541-552.

Niles, B.J., H. Mogri, A. Hill, A. Vlahakis, and T. Powers. 2012. Plasma membrane recruitment and activation of the AGC kinase Ypk1 is mediated by target of rapamycin complex 2 (TORC2) and its effector proteins Slm1 and Slm2. *Proc Natl Acad Sci U S A*. 109:1536-1541.

Niles, B.J., and T. Powers. 2014. TOR complex 2-Ypk1 signaling regulates actin polarization via reactive oxygen species. *Mol Biol Cell*. 25:3962-3972.

Nishimura, K., T. Fukagawa, H. Takisawa, T. Kakimoto, and M. Kanemaki. 2009. An auxin-based degron system for the rapid depletion of proteins in nonplant cells. *Nat Methods*. 6:917-922.

Nomura, W., and Y. Inoue. 2015. Methylglyoxal activates the target of rapamycin complex 2-protein kinase C signaling pathway in Saccharomyces cerevisiae. *Mol Cell Biol*. 35:1269-1280.

Oakhill, J.S., J.W. Scott, and B.E. Kemp. 2012. AMPK functions as an adenylate charge-regulated protein kinase. *Trends Endocrinol Metab*. 23:125-132.

Olson, D.K., F. Fröhlich, R.V. Farese, and T.C. Walther. 2016. Taming the sphinx: Mechanisms of cellular sphingolipid homeostasis. *Biochim Biophys Acta*. 1861:784-792.

Omnus, D.J., A.G. Manford, J.M. Bader, S.D. Emr, and C.J. Stefan. 2016. Phosphoinositide kinase signaling controls ER-PM cross-talk. *Mol Biol Cell*. 27:1170-1180.

Orlean, P. 2012. Architecture and biosynthesis of the Saccharomyces cerevisiae cell wall. *Genetics*. 192:775-818.

Ostrander, D.B., and J.A. Gorman. 1999. The extracellular domain of the Saccharomyces cerevisiae Sln1p membrane osmolarity sensor is necessary for kinase activity. *J Bacteriol*. 181:2527-2534.

Ozaki, K., K. Tanaka, H. Imamura, T. Hihara, T. Kameyama, H. Nonaka, H. Hirano, Y. Matsuura, and Y. Takai. 1996. Rom1p and Rom2p are GDP/GTP exchange proteins

(GEPs) for the Rho1p small GTP binding protein in Saccharomyces cerevisiae. *EMBO J*. 15:2196-2207.

Panadero, J., C. Pallotti, S. Rodríguez-Vargas, F. Randez-Gil, and J.A. Prieto. 2006. A downshift in temperature activates the high osmolarity glycerol (HOG) pathway, which determines freeze tolerance in Saccharomyces cerevisiae. *J Biol Chem*. 281:4638-4645.

Parrini, M.C., A. Bernardi, and A. Parmeggiani. 1996. Determinants of Ras proteins specifying the sensitivity to yeast Ira2p and human p120-GAP. *EMBO J*. 15:1107-1111.

Patra, K.C., and N. Hay. 2014. The pentose phosphate pathway and cancer. *Trends Biochem Sci*. 39:347-354.

Pearce, L.R., D. Komander, and D.R. Alessi. 2010. The nuts and bolts of AGC protein kinases. *Nat Rev Mol Cell Biol*. 11:9-22.

Pearce, L.R., E.M. Sommer, K. Sakamoto, S. Wullschleger, and D.R. Alessi. 2011. Protor-1 is required for efficient mTORC2-mediated activation of SGK1 in the kidney. *Biochem J*. 436:169-179.

Platta, H.W., and H. Stenmark. 2011. Endocytosis and signaling. *Curr Opin Cell Biol*. 23:393-403.

Pomorski, T., R. Lombardi, H. Riezman, P.F. Devaux, G. van Meer, and J.C. Holthuis. 2003. Drs2p-related P-type ATPases Dnf1p and Dnf2p are required for phospholipid translocation across the yeast plasma membrane and serve a role in endocytosis. *Mol Biol Cell*. 14:1240-1254.

Posas, F., and H. Saito. 1997. Osmotic activation of the HOG MAPK pathway via Ste11p MAPKKK: scaffold role of Pbs2p MAPKK. *Science*. 276:1702-1705.

Posas, F., and H. Saito. 1998. Activation of the yeast SSK2 MAP kinase kinase kinase by the SSK1 two-component response regulator. *EMBO J*. 17:1385-1394.

Posas, F., E.A. Witten, and H. Saito. 1998. Requirement of STE50 for osmostress-induced activation of the STE11 mitogen-activated protein kinase kinase kinase in the high-osmolarity glycerol response pathway. *Mol Cell Biol*. 18:5788-5796.

Posas, F., S.M. Wurgler-Murphy, T. Maeda, E.A. Witten, T.C. Thai, and H. Saito. 1996. Yeast HOG1 MAP kinase cascade is regulated by a multistep phosphorelay mechanism in the SLN1-YPD1-SSK1 "two-component" osmosensor. *Cell*. 86:865-875.

Raitt, D.C., A.L. Johnson, A.M. Erkine, K. Makino, B. Morgan, D.S. Gross, and L.H. Johnston. 2000a. The Skn7 response regulator of Saccharomyces cerevisiae interacts with Hsf1 in vivo and is required for the induction of heat shock genes by oxidative stress. *Mol Biol Cell*. 11:2335-2347.

Raitt, D.C., F. Posas, and H. Saito. 2000b. Yeast Cdc42 GTPase and Ste20 PAK-like kinase regulate Sho1-dependent activation of the Hog1 MAPK pathway. *EMBO J*. 19:4623-4631.

Rispal, D., S. Eltschinger, M. Stahl, S. Vaga, B. Bodenmiller, Y. Abraham, I. Filipuzzi, N.R. Movva, R. Aebersold, S.B. Helliwell, and R. Loewith. 2015. Target of Rapamycin Complex 2 Regulates Actin Polarization and Endocytosis via Multiple Pathways. *J Biol Chem*. 290:14963-14978.

Robinson, J.S., D.J. Klionsky, L.M. Banta, and S.D. Emr. 1988. Protein sorting in Saccharomyces cerevisiae: isolation of mutants defective in the delivery and processing of multiple vacuolar hydrolases. *Mol Cell Biol*. 8:4936-4948.

Rodríguez-Peña, J.M., S. Díez-Muñiz, C. Bermejo, C. Nombela, and J. Arroyo. 2013. Activation of the yeast cell wall integrity MAPK pathway by zymolyase depends on protease and

glucanase activities and requires the mucin-like protein Hkr1 but not Msb2. *FEBS Lett*. 587:3675-3680.

Rodríguez-Peña, J.M., R. García, C. Nombela, and J. Arroyo. 2010. The high-osmolarity glycerol (HOG) and cell wall integrity (CWI) signalling pathways interplay: a yeast dialogue between MAPK routes. *Yeast*. 27:495-502.

Roelants, F.M., A.G. Baltz, A.E. Trott, S. Fereres, and J. Thorner. 2010. A protein kinase network regulates the function of aminophospholipid flippases. *Proc Natl Acad Sci U S A*. 107:34-39.

Roelants, F.M., D.K. Breslow, A. Muir, J.S. Weissman, and J. Thorner. 2011. Protein kinase Ypk1 phosphorylates regulatory proteins Orm1 and Orm2 to control sphingolipid homeostasis in Saccharomyces cerevisiae. *Proc Natl Acad Sci U S A*. 108:19222-19227.

Roelants, F.M., K.L. Leskoske, R.T. Pedersen, A. Muir, J.M. Liu, G.C. Finnigan, and J. Thorner. 2017. TOR Complex 2-regulated protein kinase Fpk1 stimulates endocytosis via inhibition of Ark1/Prk1-related protein kinase Akl1 in Saccharomyces cerevisiae. *Mol Cell Biol*.

Roelants, F.M., B.M. Su, J. von Wulffen, S. Ramachandran, E. Sartorel, A.E. Trott, and J. Thorner. 2015. Protein kinase Gin4 negatively regulates flippase function and controls plasma membrane asymmetry. *J Cell Biol*. 208:299-311.

Roelants, F.M., P.D. Torrance, N. Bezman, and J. Thorner. 2002. Pkh1 and Pkh2 differentially phosphorylate and activate Ypk1 and Ykr2 and define protein kinase modules required for maintenance of cell wall integrity. *Mol Biol Cell*. 13:3005-3028.

Roelants, F.M., P.D. Torrance, and J. Thorner. 2004. Differential roles of PDK1- and PDK2-phosphorylation sites in the yeast AGC kinases Ypk1, Pkc1 and Sch9. *Microbiology*. 150:3289-3304.

Ron, D., and R.Y. Hampton. 2004. Membrane biogenesis and the unfolded protein response. *J Cell Biol*. 167:23-25.

Rudoni, S., S. Colombo, P. Coccetti, and E. Martegani. 2001. Role of guanine nucleotides in the regulation of the Ras/cAMP pathway in Saccharomyces cerevisiae. *Biochim Biophys Acta*. 1538:181-189.

Sabatini, D.M., H. Erdjument-Bromage, M. Lui, P. Tempst, and S.H. Snyder. 1994. RAFT1: a mammalian protein that binds to FKBP12 in a rapamycin-dependent fashion and is homologous to yeast TORs. *Cell*. 78:35-43.

Sabers, C.J., M.M. Martin, G.J. Brunn, J.M. Williams, F.J. Dumont, G. Wiederrecht, and R.T. Abraham. 1995. Isolation of a protein target of the FKBP12-rapamycin complex in mammalian cells. *J Biol Chem*. 270:815-822.

Saheki, Y., and P. De Camilli. 2017. Endoplasmic Reticulum-Plasma Membrane Contact Sites. *Annu Rev Biochem*.

Saito, H., and F. Posas. 2012. Response to hyperosmotic stress. *Genetics*. 192:289-318.

Sarbassov, D.D., S.M. Ali, D.H. Kim, D.A. Guertin, R.R. Latek, H. Erdjument-Bromage, P. Tempst, and D.M. Sabatini. 2004. Rictor, a novel binding partner of mTOR, defines a rapamycin-insensitive and raptor-independent pathway that regulates the cytoskeleton. *Curr Biol*. 14:1296-1302.

Sarbassov, D.D., S.M. Ali, and D.M. Sabatini. 2005. Growing roles for the mTOR pathway. *Curr Opin Cell Biol*. 17:596-603.

Saxton, R.A., and D.M. Sabatini. 2017. mTOR Signaling in Growth, Metabolism, and Disease. *Cell*. 168:960-976.
Schaber, J., M.A. Adrover, E. Eriksson, S. Pelet, E. Petelenz-Kurdziel, D. Klein, F. Posas, M. Goksör, M. Peter, S. Hohmann, and E. Klipp. 2010. Biophysical properties of Saccharomyces cerevisiae and their relationship with HOG pathway activation. *Eur Biophys J*. 39:1547-1556.
Schmelzle, T., S.B. Helliwell, and M.N. Hall. 2002. Yeast protein kinases and the RHO1 exchange factor TUS1 are novel components of the cell integrity pathway in yeast. *Mol Cell Biol*. 22:1329-1339.
Schmidt, A., M. Bickle, T. Beck, and M.N. Hall. 1997. The yeast phosphatidylinositol kinase homolog TOR2 activates RHO1 and RHO2 via the exchange factor ROM2. *Cell*. 88:531-542.
Schmidt, A., J. Kunz, and M.N. Hall. 1996. TOR2 is required for organization of the actin cytoskeleton in yeast. *Proc Natl Acad Sci U S A*. 93:13780-13785.
Schorling, S., B. Vallée, W.P. Barz, H. Riezman, and D. Oesterhelt. 2001. Lag1p and Lac1p are essential for the Acyl-CoA-dependent ceramide synthase reaction in Saccharomyces cerevisae. *Mol Biol Cell*. 12:3417-3427.
Schroder, W.A., M. Buck, N. Cloonan, J.F. Hancock, A. Suhrbier, T. Sculley, and G. Bushell. 2007. Human Sin1 contains Ras-binding and pleckstrin homology domains and suppresses Ras signalling. *Cell Signal*. 19:1279-1289.
Schuck, S., W.A. Prinz, K.S. Thorn, C. Voss, and P. Walter. 2009. Membrane expansion alleviates endoplasmic reticulum stress independently of the unfolded protein response. *J Cell Biol*. 187:525-536.
Sherman, F. 2002. Getting started with yeast. *Methods Enzymol*. 350:3-41.
Shimada, K., I. Filipuzzi, M. Stahl, S.B. Helliwell, C. Studer, D. Hoepfner, A. Seeber, R. Loewith, N.R. Movva, and S.M. Gasser. 2013. TORC2 signaling pathway guarantees genome stability in the face of DNA strand breaks. *Mol Cell*. 51:829-839.
Shiozaki, K., H. Tatebe, S. Murayama, and C. Kojima. 2013. Mechanisms that determine the substrate specificity of TOR kinase. In *Cell Biology of Yeasts*, M. Cyert, D.J. Lew, and K. Sawin, Organizers (Cold Spring Harbor Laboratory, Cold Spring Harbor, NY), p. 68 Abstr.
Shitamukai, A., D. Hirata, S. Sonobe, and T. Miyakawa. 2004. Evidence for antagonistic regulation of cell growth by the calcineurin and high osmolarity glycerol pathways in Saccharomyces cerevisiae. *J Biol Chem*. 279:3651-3661.
Sikorski, R.S., and P. Hieter. 1989. A system of shuttle vectors and yeast host strains designed for efficient manipulation of DNA in Saccharomyces cerevisiae. *Genetics*. 122:19-27.
Simons, K., and J.L. Sampaio. 2011. Membrane organization and lipid rafts. *Cold Spring Harb Perspect Biol*. 3:a004697.
Smits, G.J., J.C. Kapteyn, H. van den Ende, and F.M. Klis. 1999. Cell wall dynamics in yeast. *Curr Opin Microbiol*. 2:348-352.
Sriburi, R., S. Jackowski, K. Mori, and J.W. Brewer. 2004. XBP1: a link between the unfolded protein response, lipid biosynthesis, and biogenesis of the endoplasmic reticulum. *J Cell Biol*. 167:35-41.
Stathopoulos, A.M., and M.S. Cyert. 1997. Calcineurin acts through the CRZ1/TCN1-encoded transcription factor to regulate gene expression in yeast. *Genes Dev*. 11:3432-3444.

Stefan, C.J., A.G. Manford, and S.D. Emr. 2013. ER-PM connections: sites of information transfer and inter-organelle communication. *Curr Opin Cell Biol*. 25:434-442.

Sun, Y., Y. Miao, Y. Yamane, C. Zhang, K.M. Shokat, H. Takematsu, Y. Kozutsumi, and D.G. Drubin. 2012. Orm protein phosphoregulation mediates transient sphingolipid biosynthesis response to heat stress via the Pkh-Ypk and Cdc55-PP2A pathways. *Mol Biol Cell*. 23:2388-2398.

Swaney, D.L., P. Beltrao, L. Starita, A. Guo, J. Rush, S. Fields, N.J. Krogan, and J. Villén. 2013. Global analysis of phosphorylation and ubiquitylation cross-talk in protein degradation. *Nat Methods*. 10:676-682.

Tamás, M.J., M. Rep, J.M. Thevelein, and S. Hohmann. 2000. Stimulation of the yeast high osmolarity glycerol (HOG) pathway: evidence for a signal generated by a change in turgor rather than by water stress. *FEBS Lett*. 472:159-165.

Tanigawa, M., A. Kihara, M. Terashima, T. Takahara, and T. Maeda. 2012. Sphingolipids regulate the yeast high-osmolarity glycerol response pathway. *Mol Cell Biol*. 32:2861-2870.

Tanoue, D., T. Kobayashi, Y. Sun, T. Fujita, H. Takematsu, and Y. Kozutsumi. 2005. The requirement for the hydrophobic motif phosphorylation of Ypk1 in yeast differs depending on the downstream events, including endocytosis, cell growth, and resistance to a sphingolipid biosynthesis inhibitor, ISP-1. *Arch Biochem Biophys*. 437:29-41.

Tatebayashi, K., K. Yamamoto, K. Tanaka, T. Tomida, T. Maruoka, E. Kasukawa, and H. Saito. 2006. Adaptor functions of Cdc42, Ste50, and Sho1 in the yeast osmoregulatory HOG MAPK pathway. *EMBO J*. 25:3033-3044.

Tatebe, H., S. Morigasaki, S. Murayama, C.T. Zeng, and K. Shiozaki. 2010. Rab-family GTPase regulates TOR complex 2 signaling in fission yeast. *Curr Biol*. 20:1975-1982.

Tatebe, H., S. Murayama, T. Yonekura, T. Hatano, D. Richter, T. Furuya, S. Kataoka, K. Furuita, C. Kojima, and K. Shiozaki. 2017. Substrate specificity of TOR complex 2 is determined by a ubiquitin-fold domain of the Sin1 subunit. *Elife*. 6: e19594.1-e19594.20.

Tavassoli, S., J.T. Chao, B.P. Young, R.C. Cox, W.A. Prinz, A.I. de Kroon, and C.J. Loewen. 2013. Plasma membrane--endoplasmic reticulum contact sites regulate phosphatidylcholine synthesis. *EMBO Rep*. 14:434-440.

Travers, K.J., C.K. Patil, L. Wodicka, D.J. Lockhart, J.S. Weissman, and P. Walter. 2000. Functional and genomic analyses reveal an essential coordination between the unfolded protein response and ER-associated degradation. *Cell*. 101:249-258.

Truckses, D.M., J.E. Bloomekatz, and J. Thorner. 2006. The RA domain of Ste50 adaptor protein is required for delivery of Ste11 to the plasma membrane in the filamentous growth signaling pathway of the yeast Saccharomyces cerevisiae. *Mol Cell Biol*. 26:912-928.

Truman, A.W., S.H. Millson, J.M. Nuttall, M. Mollapour, C. Prodromou, and P.W. Piper. 2007. In the yeast heat shock response, Hsf1-directed induction of Hsp90 facilitates the activation of the Slt2 (Mpk1) mitogen-activated protein kinase required for cell integrity. *Eukaryot Cell*. 6:744-752.

Umemura, M., M. Fujita, T. Yoko-O, A. Fukamizu, and Y. Jigami. 2007. Saccharomyces cerevisiae CWH43 is involved in the remodeling of the lipid moiety of GPI anchors to ceramides. *Mol Biol Cell*. 18:4304-4316.

Urban, J., A. Soulard, A. Huber, S. Lippman, D. Mukhopadhyay, O. Deloche, V. Wanke, D. Anrather, G. Ammerer, H. Riezman, J.R. Broach, C. De Virgilio, M.N. Hall, and R. Loewith. 2007. Sch9 is a major target of TORC1 in Saccharomyces cerevisiae. *Mol Cell*.

26:663-674.
Vallejo, M.C., and P. Mayinger. 2015. Delayed Turnover of Unphosphorylated Ssk1 during Carbon Stress Activates the Yeast Hog1 Map Kinase Pathway. *PLoS One*. 10:e0137199.
van Meer, G., D.R. Voelker, and G.W. Feigenson. 2008. Membrane lipids: where they are and how they behave. *Nat Rev Mol Cell Biol*. 9:112-124.
Vlahakis, A., M. Graef, J. Nunnari, and T. Powers. 2014. TOR complex 2-Ypk1 signaling is an essential positive regulator of the general amino acid control response and autophagy. *Proc Natl Acad Sci U S A*. 111:10586-10591.
Vlahakis, A., N. Lopez Muniozguren, and T. Powers. 2016. Calcium channel regulator Mid1 links TORC2-mediated changes in mitochondrial respiration to autophagy. *J Cell Biol*. 215:779-788.
Volmer, R., and D. Ron. 2015. Lipid-dependent regulation of the unfolded protein response. *Curr Opin Cell Biol*. 33:67-73.
Walter, P., and D. Ron. 2011. The unfolded protein response: from stress pathway to homeostatic regulation. *Science*. 334:1081-1086.
Walther, T.C., J.H. Brickner, P.S. Aguilar, S. Bernales, C. Pantoja, and P. Walter. 2006. Eisosomes mark static sites of endocytosis. *Nature*. 439:998-1003.
Warmka, J., J. Hanneman, J. Lee, D. Amin, and I. Ota. 2001. Ptc1, a type 2C Ser/Thr phosphatase, inactivates the HOG pathway by dephosphorylating the mitogen-activated protein kinase Hog1. *Mol Cell Biol*. 21:51-60.
Watanabe, Y., G. Takaesu, M. Hagiwara, K. Irie, and K. Matsumoto. 1997. Characterization of a serum response factor-like protein in Saccharomyces cerevisiae, Rlm1, which has transcriptional activity regulated by the Mpk1 (Slt2) mitogen-activated protein kinase pathway. *Mol Cell Biol*. 17:2615-2623.
Wedaman, K.P., A. Reinke, S. Anderson, J. Yates, J.M. McCaffery, and T. Powers. 2003. Tor kinases are in distinct membrane-associated protein complexes in Saccharomyces cerevisiae. *Mol Biol Cell*. 14:1204-1220.
Westfall, P.J., D.R. Ballon, and J. Thorner. 2004. When the stress of your environment makes you go HOG wild. *Science*. 306:1511-1512.
Westfall, P.J., J.C. Patterson, R.E. Chen, and J. Thorner. 2008. Stress resistance and signal fidelity independent of nuclear MAPK function. *Proc Natl Acad Sci U S A*. 105:12212-12217.
Whiteman, E.L., H. Cho, and M.J. Birnbaum. 2002. Role of Akt/protein kinase B in metabolism. *Trends Endocrinol Metab*. 13:444-451.
Winkler, A., C. Arkind, C.P. Mattison, A. Burkholder, K. Knoche, and I. Ota. 2002. Heat stress activates the yeast high-osmolarity glycerol mitogen-activated protein kinase pathway, and protein tyrosine phosphatases are essential under heat stress. *Eukaryot Cell*. 1:163-173.
Wu, C., E. Leberer, D.Y. Thomas, and M. Whiteway. 1999. Functional characterization of the interaction of Ste50p with Ste11p MAPKKK in Saccharomyces cerevisiae. *Mol Biol Cell*. 10:2425-2440.
Wu, N., B. Zheng, A. Shaywitz, Y. Dagon, C. Tower, G. Bellinger, C.H. Shen, J. Wen, J. Asara, T.E. McGraw, B.B. Kahn, and L.C. Cantley. 2013. AMPK-dependent degradation of TXNIP upon energy stress leads to enhanced glucose uptake via GLUT1. *Mol Cell*. 49:1167-1175.
Wullschleger, S., R. Loewith, W. Oppliger, and M.N. Hall. 2005. Molecular organization of target

of rapamycin complex 2. *J Biol Chem*. 280:30697-30704.
Yaakov, G., A. Duch, M. García-Rubio, J. Clotet, J. Jimenez, A. Aguilera, and F. Posas. 2009. The stress-activated protein kinase Hog1 mediates S phase delay in response to osmostress. *Mol Biol Cell*. 20:3572-3582.
Yamamoto, K., K. Tatebayashi, K. Tanaka, and H. Saito. 2010. Dynamic control of yeast MAP kinase network by induced association and dissociation between the Ste50 scaffold and the Opy2 membrane anchor. *Mol Cell*. 40:87-98.
Yancey, P.H., M.E. Clark, S.C. Hand, R.D. Bowlus, and G.N. Somero. 1982. Living with water stress: evolution of osmolyte systems. *Science*. 217:1214-1222.
Yang, H., D.G. Rudge, J.D. Koos, B. Vaidialingam, H.J. Yang, and N.P. Pavletich. 2013. mTOR kinase structure, mechanism and regulation. *Nature*. 497:217-223.
Yang, J., P. Cron, V.M. Good, V. Thompson, B.A. Hemmings, and D. Barford. 2002a. Crystal structure of an activated Akt/protein kinase B ternary complex with GSK3-peptide and AMP-PNP. *Nat Struct Biol*. 9:940-944.
Yang, J., P. Cron, V. Thompson, V.M. Good, D. Hess, B.A. Hemmings, and D. Barford. 2002b. Molecular mechanism for the regulation of protein kinase B/Akt by hydrophobic motif phosphorylation. *Mol Cell*. 9:1227-1240.
Yang, Q., K. Inoki, T. Ikenoue, and K.L. Guan. 2006. Identification of Sin1 as an essential TORC2 component required for complex formation and kinase activity. *Genes Dev*. 20:2820-2832.
Yeung, B.K. 2011. Natural product drug discovery: the successful optimization of ISP-1 and halichondrin B. *Curr Opin Chem Biol*. 15:523-528.
Young, C., J. Mapes, J. Hanneman, S. Al-Zarban, and I. Ota. 2002. Role of Ptc2 type 2C Ser/Thr phosphatase in yeast high-osmolarity glycerol pathway inactivation. *Eukaryot Cell*. 1:1032-1040.
Yu, J.W., J.M. Mendrola, A. Audhya, S. Singh, D. Keleti, D.B. DeWald, D. Murray, S.D. Emr, and M.A. Lemmon. 2004. Genome-wide analysis of membrane targeting by S. cerevisiae pleckstrin homology domains. *Mol Cell*. 13:677-688.
Zarzov, P., C. Mazzoni, and C. Mann. 1996. The SLT2(MPK1) MAP kinase is activated during periods of polarized cell growth in yeast. *EMBO J*. 15:83-91.
Zhao, B., R. Lehr, A.M. Smallwood, T.F. Ho, K. Maley, T. Randall, M.S. Head, K.K. Koretke, and C.G. Schnackenberg. 2007. Crystal structure of the kinase domain of serum and glucocorticoid-regulated kinase 1 in complex with AMP PNP. *Protein Sci*. 16:2761-2769.
Zhong, W., D.J. Murphy, and N.H. Georgopapadakou. 1999. Inhibition of yeast inositol phosphorylceramide synthase by aureobasidin A measured by a fluorometric assay. *FEBS Lett*. 463:241-244.